UNIVERSITÀ DEL PIEMONTE ORIENTALE

PhD in Medical Sciences and Biotechnologies

XXX cycle

Department of Health Sciences (DISS)

SSD: MED/08

ROLE OF HMGB1 (High Mobility Group Box-1) IN MALIGNANT MESOTHELIOMA
PATHOGENESIS, PROGNOSIS AND AS PREDICTIVE BIOMARKER.

PhD thesis by:

RRAPAJ ELTJONA

Coordinator of PhD programme: Prof. Marisa Gariglio

Supervisor: Prof. Renzo Boldorini

Academic Year 2016/2017

Dedication

This thesis is dedicated to the memory of my grandfather Isuf Xhyheri, a smart man, who inspired and supported me to pursue a career in research.

Eltjona Rrapaj, MSc

TABLE OF CONTENTS:

1. SUMMARY……4

2. INTRODUCTION……...7

3. AIM OF THE STUDY……..45

4. MATERIALS AND METHODS……47

5. RESULTS……59

6. DISCUSSION……..85

7. REFERENCES……89

1. SUMMARY (*Italian*)

Il mesotelioma pleurico maligno (MPM) è un tumore aggressivo di origine mesoteliale che viene spesso diagnosticato in uno stadio avanzato. Anche per questo motivo il mesotelioma spesso presenta resistenza alla maggior parte dei trattamenti terapeutici e una prognosi infausta, esiste pertanto la necessità di sviluppare nuovi biomarcatori per la diagnosi precoce e di identificare nuovi target per trattamenti preventivi e terapeutici. Studi recenti dimostrano che la proteina High-mobility group box-1 (HMGB1) svolge un ruolo fondamentale nella carcinogenesi dell'MPM. HMGB1 è una proteina strutturale della cromatina, espressa ubiquitariamente nei nuclei delle cellule dei mammiferi. Quando trasportata nello spazio extracellulare, tra le altre funzioni, può agire sia come oncosoppressore che come proteina oncogena. Nel mesotelioma pleurico maligno, livelli sierici elevati di HMGB1 sono stati correlati a una prognosi infausta. Al contrario, il significato dell'espressione di HMGB1 nei tessuti di mesotelioma pleurico maligno deve ancora essere definito.

La discrepanza tra l'incidenza crescente di MPM e la mancanza di successo di nuove strategie terapeutiche più efficaci può essere in parte correlata a sistemi in vitro e in vivo inadeguati che imitano la tumorigenesi del MPM. Recenti scoperte hanno dimostrato che il mesotelioma maligno è un tumore policlonale e la sua formazione e crescita è influenzata dal microambiente infiammatorio. Valutare il mesotelioma come un organo completo risulta cruciale per comprenderne la biologia e sviluppare nuove strategie terapeutiche. Il nostro obiettivo è sviluppare modelli tridimensionali di mesotelioma in vitro. Gli organoidi umani derivati da paziente potranno rivelarsi di grande utilità per esaminare la sensibilità ai trattamenti farmacologici e per studiare la diafonia tra tumore e cellule immunitarie. In quest'ottica, sferoidi ottenuti da mesotelioma murino e xenotrapianti derivati da paziente (PDX) rappresentano modelli alternativi e utili per conseguire il medesimo obiettivo.

Campioni di tessuto neoplastico ottenuti mediante biopsia da 170 pazienti con MPM sono stati valutati mediante immunoistochimica e Reverse Transcription-Polymerase Chain Reaction (RT-PCR) per valutare la proteina HMGB1 e l'espressione genica. Il livello di espressione della proteina HMGB1 è stato valutato utilizzando un metodo semi-quantitativo, che somma l'intensità (0-3) e la percentuale (da 0 a 4) delle cellule con colorazione positiva, nei nuclei, nel citoplasma e in entrambi. Il punteggio finale è stato classificato come alta (> 3) o bassa (< 3) espressione proteica. I livelli di espressione genica sono stati calcolati con il metodo ΔΔCt. Livelli di espressione elevati di HMGB1 totale ($p = 0,0011$) e citoplasmatico ($p = 0,0462$), correlavano con una peggiore sopravvivenza malattia specifica (DSS) nell'intera coorte e nei sottogruppi clinico-patologici. Non è stata tuttavia osservata nessuna correlazione significativa tra espressione del gene HMGB1 e DSS.

Nella seconda parte del nostro studio, biopsie di mesotelioma umano sono state utilizzate per la generazione di organoidi seguendo procedure sperimentali precedentemente pubblicate. Gli stessi

frammenti tumorali sono stati trapiantati in topi immunodeficienti (NOD scid gamma, NSG). Gli organoidi ottenuti da biopsie umane presentano dimensioni ridotte (200 µm di diametro) e possono essere propagati fino a tre passaggi in vitro. La caratterizzazione morfologica degli organoidi mostrava una struttura definita con polarità interno-esterno. Gli organoidi erano inoltre positivi per i marcatori tipici del mesotelioma. Abbiamo ottenuto tre PDX; l'immunofenotipizzazione ha mostrato come i tumori propagati nei topi siano simili al tumore originale.

Questi risultati indicano che HMGB1 può essere utile come biomarcatore prognostico nel mesotelioma pleurico quando valutato mediante colorazione immunoistochimica nel tessuto neoplastico. Tuttavia, poiché è espresso anche in cellule mesoteliali normali e reattive, la valutazione dell'espressione di HMGB1 in campioni istologici di mesotelioma sembra non presentare utilità a fini diagnostici.

Siamo inoltre riusciti a generare e caratterizzare organoidi e modelli PDX di mesotelioma, ci aspettiamo che questi modelli ci aiutino a capire meglio la patogenesi del mesotelioma.

SUMMARY (*English*)

Malignant pleural mesothelioma (MPM) is an aggressive tumour of mesothelial origin, often diagnosed in an advanced stage, which contributes to its very poor prognosis and resistance to most of the therapeutic treatments. Therefore, the development of new biomarkers for early diagnosis and of novel targets for preventive and therapeutic treatments are needed. Recent studies show that High Mobility Group Box 1 protein (HMGB1) plays a critical role in the carcinogenesis of MPM. High-mobility group box-1 (HMGB1) is a chromatin structural protein, ubiquitously expressed in the nuclei of mammalian cells. When transported extracellularly, it, among other functions, could act as tumor suppressor and oncogenic protein. In malignant pleural mesothelioma (MPM), high serum levels of High-mobility group box-1 (HMGB1) have been related to a poor prognosis. Conversely the significance of HMGB1 expression in malignant pleural mesothelioma (MPM) tissues is still unclear.

The discrepancy between the rising incidence of MPM and the lack of success of new more effective therapeutic strategies may be related in part to inadequate *in vitro* and *in vivo* systems that mimic MPM tumorigenesis. Recent findings showed that malignant mesothelioma is a polyclonal tumor and its formation and outgrowth is determined by the inflammatory microenvironment. Evaluating mesothelioma as a complete organ becomes crucial to understand its biology and to develop new therapies. Our aim is to develop 3D in vitro models of mesothelioma. Patient-derived human organoids are useful to screen for drug sensitivity and to study the crosstalk between tumor and immune cells. Murine mesothelioma spheroids and patient derived xenografts (PDX) are alternative models that help us to pursue the same goal.

Biopsy samples from 170 patients with MPM were assessed by immunohistochemistry and Reverse Transcription-Polymerase Chain Reaction (RT-PCR) to evaluate HMGB1 protein and gene expression. The expression level of HMGB1 protein was scored using a semi-quantitative system, that sums the intensity (0-3) and the percentage (from 0-4) of positively stained cells, in nuclei, cytoplasm and in both. The final score was considered as high (>3) or low (<3) expression. Gene expression levels were calculated with ΔΔCt method. High expression levels of HMGB1 as total (P = 0,0011) and cytoplasmic score (P = 0,0462), were related with a worse disease-specific survival (DSS) in the entire cohort and in the clinicopathologic subgroups. No significant correlation was found between HMGB1 gene expression and DSS.

Human mesothelioma biopsies were used for organoid generation following published protocols. The same tumor fragments were transplanted in immune deficient mice (NOD scid gamma, NSG mice). Organoids obtained from human biopsies are small in size (200 μm in diameter) and can be propagated up to three generations. The morphological characterization of organoids showed a defined structure with inside-outside polarity; organoids were positive for mesothelioma markers. We obtained three PDX; immunophenotyping showed that the tumors propagated in mice are similar to the original tumor.

These findings indicate that HMGB1 may be a useful prognostic biomarker in MPM when detected by immunohistochemistry. Conversely, since it is expressed also in normal and reactive mesothelial cells, HMGB1 cannot be considered a diagnostic biomarker, in histologic samples of mesothelioma.

We have the ability to generate and characterize organoids and PDX models of mesothelioma. We expect these models will help us to better understand the mesothelioma pathogenesis.

2. INTRODUCTION

An overview of Malignant Pleural Mesothelioma

Malignant mesothelioma (MM) is a slow-growing solid tumor originating from the mesothelial cells lining the pleural and peritoneal cavities, or less commonly the pericardium, tunica vaginalis testis and ovarian epithelium[1]. It is uncommon for MM cases to suffer metastasis in its early stage.[2]

The most frequent site of the disease presentation is the pleural surface (>70%),[3] since asbestos, after inhalation in the lungs, reaches the pleura via the lymphatic system. The occurrence of MPM is related mainly with asbestos exposure; [4] when the exposure is high, further dissemination of asbestos to the peritoneum may occur. [5] Moreover, other potential carcinogenic agents, including infection by Simian Virus 40, radiation exposure, [6] germline BRCA1-associated protein 1 (BAP1) mutations [7] as well as exposure to other fibers with similar physical properties to asbestos should be considered. In the asbestos-associated MPM cases, the disease develops after a long latency period, interval between the first exposure to carcinogens and the development of the pathology, which ranges on average 30–60 years.[8] The prognosis of malignant pleural mesothelioma is very poor with a median survival in no treated patients of 6–12 months. [1] Unfortunately, MPM is resistant to chemotherapy, and the efficacy of the most commonly used chemotherapy is very limited: the combination of pemetrexed and cisplatin led to an overall survival benefit of about 11 weeks.[9]

The incidence of MPM has a growing tendency worldwide, mainly due to the lag time after exposure to asbestos and the banning of handling and importing this product in the late twentieth century (**Table 1**). [10] Several studies recently conducted demonstrated that the disease incidence is likely to peak between 2015 and 2030.[11, 12] In US the incidence of mesothelioma reached 3,200 cases/year in 2003 and it has remained stable since, despite the stringent regulations introduced between 1970s and 1980 to limit asbestos exposure. [12]

in Italy its incidence is 2,94/100.000 for men and 1,06/100.000 for women. In the areas in which asbestos production factories are frequent like Casale Monferrato in Piedmont region, the incidence is estimated to be about 43.7/100.000 for men and 27/100.000 for woman (Centro di Riferimento per l'Epidemiologia e la Prevenzione Oncologica in Piemonte).

According to the predominance of the histomorphologic growth pattern, MPM is divided into four histologic subtypes: epithelial (50-70%), sarcomatoid (10-15%), biphasic (30%) and desmoplastic, a quite rare variant of the tumour [11, 13] associated with different prognosis (**Figure 1**). The epithelioid subtype is the less aggressive and most responsive to treatments, with a better prognosis than the non-epithelioid.[14] The sarcomatoid subtype is associated with the worst prognosis. [15] The epithelioid MPM presented a proliferation of oval or polygonal tumor cells, often lacking nuclear scission, being lined by vascular structures formed by cuboidal cells. Whereas, the sarcomatoid subtype is characterized by the proliferation

of spindle cells which presents oval prominent nuclei and small amount of double-staining cytoplasm. In some others mesothelioma cases the morphology is fibrosarcoma-like. The biphasic subtype is the combination of both characteristics as stated above. In all of the histotypes, the malignant cells are frequently bi- or multi- nucleated, organized in clumps. MPM occurs in any part of the parietal pleura and the visceral pleura, while about 80% occurs in the visceral pleura and 20% occurs in the parietal pleura. [16]

Country	Annual incidence per million	Male-Female ratio	Predicted peak
Australia	29	4:1	2014-2021
United Kingdom	29	4.9:1	2011-2015
USA	10	4.6:1	2000-2005
Italy	24	2.6:1	2015-2024
Japan	8	3.5:1	2027

Table 1: Current incidence and predicted peak for malignant mesothelioma in various countries. [259]

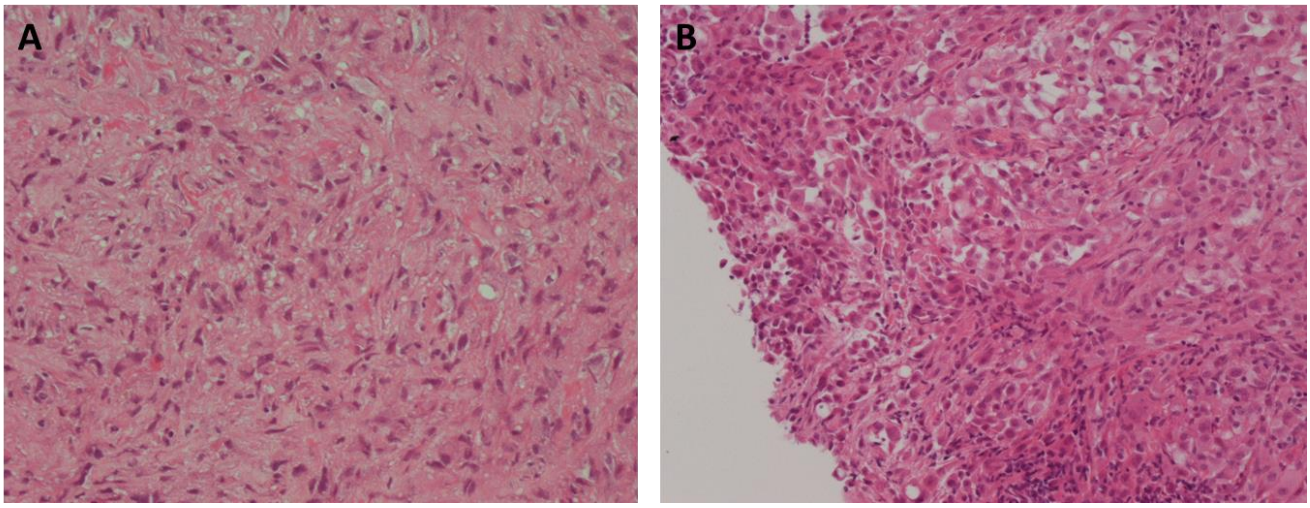

Figure 1. Example of histologic subtypes of MPM cases obtained from Pathologic Anatomy of Novara Hospital: A) Sarcomatoid, B) Epithelioid. Magnification 200X

Etiology and pathogenesis

Mesothelioma is officially recognized as an occupational cancer and as a signal disease for occupational asbestos exposure. [11] The rare cases of MPM in children and young adults suggest that other factors different from asbestos exposure may be involved in the etiology of this tumor. [17] Furthermore, it has been reported that some individuals develop mesothelioma following exposure to small amounts of asbestos,

whereas others exposed to heavy amounts do not. Additional well-established risk factors for MM include exposure to the naturally occurring asbestos-like mineral fibers, such as germline BRCA1-associated protein 1 (BAP1) mutations, erionite, SV40 exposure and chest irradiation.[18]

Asbestos

Before 1950, malignant mesotheliomas were extremely rare neoplasms.[19] So, the first mesothelioma case was reported in 1947 and its diagnosis relied on the current diagnostic criteria. However, the increasing use of asbestos after the second world war led to the description of a causal relationship between asbestos exposure and MPM development.[4] In the 1980s, when people became aware to the risks of asbestos exposure, its use was widely abandoned in the western world. But the long latency period between exposure to asbestos and mesothelioma development,[20] meant that the mortality rates from mesothelioma have continued to rise.

Asbestos, from Greek means "inextinguishable", is a natural silicate mineral with different carcinogenicities.[1,21] Asbestos refers to a family of six mineral fibers that were used commercially in the '70s, and are classified into two major subgroups: the serpentine group, consisting of chrysotile (white asbestos), and the amphiboles. The amphibole is a group of rod-like fibers, and includes crocidolite (blue asbestos), the most oncogenic type of asbestos, amosite (brown asbestos), anthophyllite, actinolite and tremolite.[17] The most common and economically important form of asbestos in the Western World is represented by chrysotile.

The main asbestos mineral groups differ from each other also for their structure: the serpentine fibers are long and curly, whereas the amphibole fibers are straight, needle-like and friable. This distinction is important as the serpentine shape is more easily cleared from the respiratory tract. Furthermore, epidemiologic data suggests that the amphiboles are associated with the highest risk of mesothelioma,[22] and that the serpentine fibers has the lowest. WHO confirmed that the different shapes of asbestos fibers seem to have different abilities to induce mesothelioma.[23]

The mechanisms at the basis of asbestos carcinogenesis are being clarified. Long and thin asbestos fibers are inhaled deeply into the lung, penetrate the pleural space and induce a chronic inflammatory response at sites of fiber deposition in the pleura that over time may lead to malignant cell transformation (Figure 2). Three main contributing mechanisms have been proposed.

1- Different studies reported that asbestos fibers are able to generate reactive oxygen species (ROS) and reactive nitrogen species, which subsequently can cause DNA damage and strand breaks into the normal mesothelial cells and macrophages at the sites of fibers deposition. Furthermore, macrophages phagocytose asbestos fibers but are unable to digest them, and produce also abundant reactive oxygen species.[24,25] At the other hand, asbestos fibers are also engulfed by mesothelial cells, and into the cells can physically interfere with the mitotic process of the cell cycle

by disrupting mitotic spindles. This can produce abnormalities into chromosomal structures and aneuploidy of the mesothelial cells.

2- Asbestos fibers absorb a variety of proteins and chemicals, which could lead to the accumulation of harmful molecules including carcinogens. [26] Furthermore, asbestos fibers bind important cellular and functional proteins and their functional and structural deficiency may also be damaging for normal mesothelial cells.

3- Lastly, asbestos-exposed mesothelial cells and macrophages release a variety of cytokines and growth factors able to induce inflammation and tumor promotion. Those include tumor necrosis factor-α, interleukin-1β, high-mobility group box 1 (HMGB1). [27, 28] The mechanisms that describes this malignant transformation process was revealed by Yang et al.[27] Asbestos caused the necrotic death of primary human mesothelial cells (HM) exposed to it, and release HMGB-1 in the extra cellular space, which cause a chronic inflammatory response. This event elicits macrophage accumulation and the secretion of TNF-alpha, which activates the NF-κB pathway. This lead to increased survival of asbestos-damaged mesothelial cells. Thus, the aberrantly activated signaling network among mesothelial cells, inflammatory cells, fibroblasts and other stromal cells may create a pool of mesothelial cells, which harbor asbestos-induced genetic damages potentially developing into cancer cells and together forming a tumor microenvironment that supports and nourishes them.[1]

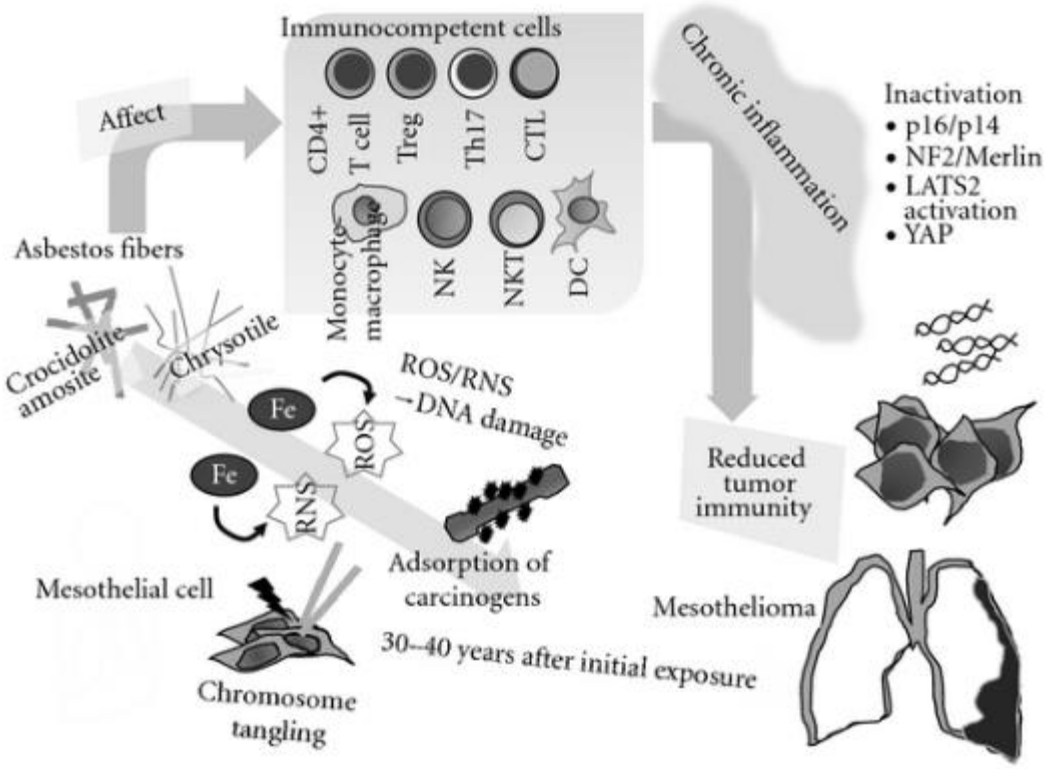

Figure 2: Schematic model showing mechanisms of asbestos-induced carcinogenesis and genomic/epigenetic changes found in mesothelioma cells, carcinogenic activities of asbestos fibers, and the relationship of the immunological effects of asbestos in regard to chronic inflammation and reduced tumor immunity.[199]

.

Erionite

Erionite is a fibrous form of the zeolite group of minerals, which is less widespread, but several times more carcinogenic than asbestos in causing mesothelioma.[29] Wagner and colleagues showed that mice injected with erionite develop MM in almost all cases, instead mice injected with asbestos fibers has MM in a lower percentage of cases (48%).

Urban development may disturb natural outcrops of asbestos and erionite, thus leading to more occurrences of exposure. [1,29,30] One example, during the past 2 decades, was the case of erionite exposure in North Dakota where over 300 miles of roads, playgrounds and driveways have been paved, mostly with gravel-containing erionite. More erionite-exposure is also suspected in nearby States. Furthermore, in a recent work Carbone linked erionite with endemic cases of mesothelioma. The mortality rate was 6,5% in some Turkish villages of Cappadocia where erionite is natural component of the stones of this region.[30] In the North and South Dakota roads, the air concentrations of erionite were equal or exceeded of those found in the Cappadocia villages indicating that here erionite remains a serious environment pollution. Similar problems occurred in New Caledonia, where the use of antigorite (a type of serpentine) as road gravel led to mesothelioma epidemy. [31]

Genetic predisposition and BAP-1 gene

In 2001, in a study conducted in some Turkish villages was reported that the development of mesothelioma has been correlated with genetic susceptibility transmitted in an autosomal dominant manner. [32] Another study has found that family members genetically susceptible to MM, when raised outside the villages, not exposed to carcinogenic minerals did not develop MM; in addition, when high-risk MM family members married into families with no history of MM, MM appeared in the descendants. [33]

Initially, these findings were received with skepticism. [34] Only recently, a study conducted by Carbone et al, which was focused on two American families with high incidence of developing mesothelioma and without previous asbestos exposure, identified germline mutations in BAP1 (BRCA-1 associated protein 1) gene. [35] BAP-1 is a tumor suppressor gene located on chromosome 3p21.3 and causes the "BAP1 cancer syndrome", characterized by the presence of benign atypical melanocytic lesions, known as melanocytic BAP1-mutated atypical intradermal tumors (MBAITs) a very high incidence of both pleural and peritoneal MMs as well as uveal melanomas (UVMs). [35] Individuals that carried germline BAP1 mutations also have an elevated risk of developing several other malignancies, such as cutaneous melanoma, clear cell renal cell carcinoma, intrahepatic cholangiocarcinoma, basal cell carcinoma, etc.

SV40 and mesothelioma

Simian virus 40 (SV40) is a DNA monkey virus that was found in contaminated polio vaccines produced from 1955 to 1978. [36] The most likely route of SV40 transmission into humans were correlated with the contaminated forms of polio vaccines injected in millions of people worldwide in this period. SV40 is a double circle DNA virus and its oncogenic activity rests on the production of 2 proteins; the large T antigen (TAG) and small t antigen (tag), encodes respectively by early and late coding regions. The ability to induce tumor transformation in the host cells is linked to the large T antigen able to inactivate essential tumor suppressor genes, like p53 and pRb. These genes encode key proteins to the cell cycle checkpoints, and the loss of these proteins leads to uncontrolled cell proliferation. [37] However, its ability to cause tumor in humans is not clear since several conflicting data have been reported. Different preclinical studies reported that animals injected with SV40 in the pleural tissue developed MM within 6 months in 100 % of cases sustaining its probable carcinogenic role, [38] at least in animal studies. Another study conducted in hamsters indicates that SV40 alone was not able to cause mesothelioma, but infected animals exposed to lower amounts of asbestos can develop tumors in 90% of cases.[36] At the other hand, it was recently shown that T antigen participates in generation of TAG-p53-pRb-p300 complex, which regulates the transcription of the insulin-like growth factor I (IGF-1) gene. An increase of IGF-1 production leads to enhanced cell growth.[39] It is still not completely clear the direct carcinogenic effects of SV40 in MM in humans; however, it the role of SV40 as a co-carcinogenic player in association with asbestos in the development of MM is widely accepted. [40]

Radiation

The pathogenesis of MPM is also linked with radiation exposure, even though these cases are rarely observed. [41] Ionizing radiation is recognized as a carcinogen and is at the basis of development of different tumors including hematologic malignancies and solid tumors. Different evidences were reported from case reports studies and indicates the development of MM in humans previously treated with therapeutic radiation. [41] Several large-scale retrospective cohort studies investigated the occurrence of MM after exposure to therapeutic radiation for treatment of several different types of cancer. De Bruin et al found that among patients survived by Hodgkin lymphoma, the risk for developing malignant mesothelioma was almost 30-fold for patients treated with irradiation, as compared to the general population. [42] Moreover, studies in rats demonstrate that radiation is a causative co-factor of MM in combination with asbestos exposure.

In summary, the association between asbestos, erionite, SV40 infection, genetic predisposition and radiation exposure suggests a multifactorial origin for malignant mesothelioma and each factor plays a crucial role in necrosis, inflammation and genetic damage.

Diagnosis

Diagnosis of malignant mesothelioma requires the combination of careful evaluation of clinical features, examination, radiology, acquisition of pathology and accurate history of asbestos exposure. [43] Patients typically presents symptoms as shortness of breath, pain and weight loss that occur over a period of many years. It is also of great importance to be informed about the patient occupational history in a detailed way. During physical examination, unilateral effusions are often observed.

The diagnostic standard work-up includes the following steps:

- Chest X-ray
- Computed tomography (CT) scan of chest and upper abdomen
- Thoracentesis, with examination of the pleural effusion
- General laboratory blood tests

Radiology

Radiological imaging is essential to determine the diagnosis, staging and management of mesothelioma. The main imaging diagnostic techniques used to evaluate the disease are based on: X-ray, CT, magnetic resonance imaging (MRI) and the positron tomography (PET). [43]

X-ray, is the most practical method able to detect pleural thickening, pleural nodules or pleural effusion. Because of the lack of specificity, the X-ray can't provide a complete diagnosis for MPM.

Computer Tomography (TAC) TAC is commonly used in the preferred examination, which allow the visualization of whole pleural surface, the diaphragm and the status of lymph nodes. [44] This method can detect different degrees of pleural effusion, a nodular or thickening of the pleura, calcification, and

potential thoracic invasion. However, TAC cannot determine the tumor staging and distinguish between diffuse pleural thickening from MPM. This method presents difficulty in detecting the tumor staging. The TAC scanning may help fine needle aspiration/biopsy of pleural mass.

Magnetic resonance Imaging (MRI) MRI is not used as a routine examination of malignant mesothelioma but can do a better assessment of the individual for surgical treatment. So, MRI could allow the preoperative evaluation of the mediastinal structures, chest wall and diaphragm involvement. MRI scanning determines tumour size, the tumor area and distinguish the normal part. The imaging features and the sensitivity of MRI are similar to the chest CT. MRI also is the imaging modality of choice in those in whom intravenous iodinated contrast is contraindicated. [45]

Positron emission tomography (PET) PET/CT imaging has been used for MPM diagnosis by 18F-fluorodeoxyglucose (18FDG). PET/CT have the ability to monitor the concentration of 18F-fluorodeoxyglucose (18FDG) at different levels in lesions by a semiquantitative measure (standardized uptake value, SUV) of the metabolic activity of a lesion. It was observed that SUV is higher in mesothelioma than in other benign pleural diseases, [45] underlying its role at distinguishing benign from malignant disease. PET could be also an adjunctive tool to determine the MPM staging, and play an important role in curative evaluation, and estimating of prognosis. [46] So, there are evidences that changes in the fluorodeoxyglucose (FDG) uptake within the tumour might indicate response to treatment suggesting its role in monitoring the tumor response to different treatment alternatives. Despite the unique features of PET/CT, there are still some deficiencies such as the high expense and the false positive. [47]

Thoracoscopy to obtain adequate tissue biopsy

When the occupational data of patient indicates a significant asbestos exposure, or the radiology is suggestive of mesothelioma, we need to determine a definitive diagnosis of MPM. In those patients with a pleural effusion, sampling of the fluid for cytological examination is the first step in confirming the diagnosis. But unfortunately, pleural fluid cytology is positive for malignant cells in about a third of cases. Furthermore, many pleural effusions present cytologic atypia, papillary structures, cells with frequent cytoplasmic vacuoles and focal necrosis; features which are shared between reactive mesothelial hyperplasia and malignant mesothelioma. [48, 49, 50] Thus, if we are able to determine a definitive diagnosis of mesothelioma by clinical, radiological and cytological results then this could be accepted. However, it is uncommon for the definitive diagnosis to be made on pleural fluid cytology alone. Therefore, the thoracoscopic pleural biopsy for tissue diagnosis are recommended. Thoracoscopy, as a real-time imaging technique, has become the most reliable method for obtaining of tissue specimens and the diagnosis of MPM for its comprehensive observation. This method also enables clinicians to improve tumor staging, particularly in the mediastinal region, and allow pleural fluid evacuation (pleurodesis). [50] This can be performed as a pleuroscopy or as video-assisted thoracic surgery (VATS). [51] However Kao *et al* found that it

is difficult to make a definite diagnosis through the pleural biopsy alone. [52] And the accuracy of diagnosis could be improved when immunohistochemical examination is considered. In the vast majority of cases, it is necessary to have adequate tissue biopsies and to investigate a panel of tumoral markers by the mean of immunohistochemistry.

Cytokeratin (CK) has important significance in the diagnosis of mesothelioma, and a study has also shown that 92% of sarcomatoid mesothelioma is positive for CK. [53, 54] The related immunohistochemical markers of MPM also include calretinin (CR), D2-40, CK5/6, WT-1, VIM, CD105 and so on. The sensitivity of CR in the diagnosis of epithelioid mesothelioma is 94-100%, making it a screening index of MPM. CK5/6 is located on the plasmalemma, and mostly expressed in epithelioid mesothelioma. Vimentin (VIM) is mainly expressed in stromal cells and tumor derived cells; it also can be expressed in MPM, especially in the sarcomatoid mesothelioma and the poorly mixed mesothelioma, which can be used for differential diagnosis with metastatic adenocarcinoma of lung. [53, 54] Thus, according to the embryologic histogenesis of mesothelial tissue, MPM shows epithelial and mesothelial markers such as cytocheratin 5/6, calretinin, thrombomodulin, mesothelin and the Wilms Tumor 1 (WT-1). The presence of at least two of positive markers in the context of a clinical and histological suspicion, is sufficient to confirm the diagnosis of MPM.[55] A combination of the imaging techniques may be necessary for determining the best approach to the patient.

Staging system

Most of these staging systems had limitations, being based on small numbers of patients. The most recent system was developed in 1995; it was presented by the International Mesothelioma Interest Group (IMIG) and is approved by the Union for International Cancer Control (UICC) (**Table 2**). [56]

Stage	TNM	Comments
Ia	T1a N0 M0	Primary tumour limited to ipsilateral parietal pleura
Ib	T1b N0 M0	As stage Ia plus focal involvement of visceral pleura
II	T2 N0 M0	As stage Ia or Ib plus confluent involvement of diaphragm or visceral pleura or involvement of the lung
III	Any T3 M0	Locally advanced tumour
	Any N1 M0	Ipsilateral, bronchopulmonary or hilar lymph node involvement
	Any N2 M0	Subcarinal or ipsilateral mediastinal lymph node involvement
IV	Any T4	Locally advanced, technically unresectable tumour
	Any N3	Contralateral mediastinal, internal mammary, and ipsilateral or contralateral supraclavicular lymph node involvement
	Any M1	Distant metastases

Reproduced with permission from the American College of Chest Physicians.

Table 2. TNM staging according to the International Mesothelioma Interest Group (IMIG)/Union for International Cancer Control (UICC). [56]

Prognostic factors and survival time

Patients with malignant pleural mesothelioma have a poor prognosis, with estimated median survival ranging between 4 to 12 months. [57] The Cancer and Leukaemia Group B, and the European Organization for Research and Treatment of Cancer have analyzed a large number of patients enrolled in treatment trials for mesothelioma and have established the main prognostic factors. According to this analysis, the non-epithelioid subtype, chest pain, poor performance status at the time of diagnosis (PS), male gender, age older than 75 and high tumor stage are the main predictors of a negative prognosis. [58] Most of the patients who survive more than 2 years have epithelioid histology and death from mesothelioma could be consequence of respiratory failure.

Other prognostic factors which are mainly used for purposes of clinical research are high leucocytes counts, platelets greater than 400 000 per µL, low hemoglobin content, thrombocytosis and high LDH level. Potential serum markers, such as soluble mesothelin or osteopontin, are now being studied but cannot currently be used for valid prognostication. [57]

Therapy/Treatment

MPM is highly aggressive and if left untreated the median survival time of the patients is very poor. [59] So, treating MPM patients remains a challenge. Current approaches consist in treating the MPM cases by chemotherapy, or multimodal treatment. The most promising strategy up to date is the multimodality therapy including resection of visible tumor as much as possible, combined with radiotherapy, chemotherapy and immunotherapy. [60] This strategy has been adopted because also the most complete surgical resection is associated with residual microscopic malignant tumor, and the subsequent local adjuvant treatment is able to kill residual tumor cells. Unfortunately, the treatment efficacy is very limited because of the late diagnosis. All of the current established therapies improve only the quality of life and prolong survival time of the patients. [61] The treatment options depend on the performance status, pulmonary function, stage, and age of the patient.

Surgery/Surgical treatment

The potential aims of surgery in MPM patients is to remove tumor with therapeutic intent and to relieve symptoms. [62] So far, the most commonly used operation approaches are extrapleural pneumonectomy (EPP) and pleurectomy/decortication (P/D). [63] EPP performs the complete resection of the affected visceral pleura and parietal pleura, the lungs, the diaphragm, and even part of the pericardium. The trauma caused by EPP is quite large, and the perioperative mortality is used to be as high as 32%. But, the recent developments of the surgical methods and screening techniques reduce the mortality in perioperative period to about 4%. P/D requires the complete resection of the visceral and parietal pleura, and the retention of the lung. The trauma caused by P/D is relatively small, and the perioperative mortality rate is about 1.5-5.4%. This method has some limitations: the complete eradication of tumor by P/D has not been performed, especially when the tumor invaded other parts. [64] EPP is not able to extend the patients survival compared with P/D and increase the postoperative complications for the MPM patients at the early stage. [65] Nowdays, pleurectomy P/D is the preferred surgery and the most frequent because extrapleural pneumectomy (EPP) has higher morbidity without showing significant survival advantages.

If progressive disease is observed after neoadjuvant chemotherapy, surgery is not recommended. EEP is only recommended in the context of controlled clinical trials performed by specialized teams of investigators. [66] So, for staging procedures, large biopsies samples can be obtained using VATS or thoracoscopy. In this way, the subsequent pathological, molecular and immunohistochemistry assessment/evaluation will follow. During this methodology, the pleural effusions can be drained and, if required, a decortication or pleurodesis can be carried out.

Radiotherapy

Mesothelioma is resistant to radiotherapy, so its effect is unsatisfactory. It is also difficult to prepare the effective radiation dose, due to the ability of MPM to spread along the pleura, surrounding the lungs and other vital organs adjacent to the site of primary tumor, which may represent one of the reasons for its unsatisfactory therapeutic effect. [67] Some of the severe adverse effects of radiation therapy include pneumonitis, myocarditis, and myelopathy due to spinal cord toxicity. Nowadays, it seems that the development of three-dimensional imaging techniques has solved this problem to some extent. [67] Radiotherapy has a certain effect in relieving the symptoms, especially easing the pain. [68] Therefore, the radiation therapy is mostly used for palliative purposes or in combination with surgery. Further clinical researches at large-scale are needed, because there is still no sufficient evidence about the radiation therapy of MPM.

Chemotherapy

Chemotherapy aims at killing the tumor cells in uncontrolled proliferation, in order to extend patient survival and improve the quality of life. [69] The chemotherapeutic treatment can be used alone or in combination with surgical treatment. Chemotherapy is the preferred treatment because of the late stage diagnosis of MPM cases. A study conducted by Vogelzang et al, 2003, reported the research results from a phase III clinical trial in a large cohort (456 patients) of MPM patients comparing the pemetrexed and cisplatin treatment with cisplatin alone. Response rates were significantly better in the pemetrexed/cisplatin arm than in the cisplatin alone arm (41.3% vs. 16.7%), and median survival time was significantly increased as well (median survival 12.1 months versus 9.3 months. [70] Afterwards, in 2004, pemetrexed (PEM) was approved by the US Food and Drug Administration (FDA) and the European Union (EU) to be used for MPM treatment. Thus, the combination of cisplatin (CDDP) and PEM become the first-line chemotherapeutic treatment for MPM. [71] Chemotherapy for MPM can be used alone or combined with surgical treatment. Treatment with vitamin B12 and folic acid could also reduce toxicity without altering survival benefit.

Recently some experts proposed in a phase II clinical study the combination of PEM and carboplatin plus bevacizumab as the first-line chemotherapeutic regimen of MPM, but further validation about the role of bevacizumab is needed. [72] Thus, the main treatment for pleural effusion remains intrathoracic chemotherapy.

Molecular genetics and molecular therapies

Germline and somatic BAP1 mutations

Recently, mounting evidence has shown that germline mutations in BAP1, a tumor suppressor gene located on chromosome 3p21.3, are the cause of the "BAP1 cancer syndrome" (**Figure 3.a**). [73] This cancer syndrome is accompanied by the presence of benign atypical melanocytic lesions, [74, 75] known as melanocytic BAP1-

mutated atypical intradermal tumors (MBAITs), [73] a very high incidence of both pleural and peritoneal MMs as well as uveal melanomas (UVMs). Furthermore, it has been recently shown that the all carriers of BAP1 germline mutations have developed one or more malignancy by age 55.[76] In addition to germline mutations, the majority (63.6%) of sporadic MMs contain somatic BAP1 mutations/inactivation. [77] Recent next generation sequencing (NGS) studies of the MPM genome revealed that in MPM biopsies various inactivating mutations occur rarely and randomly, with the exception of BAP1 that was found mutated in a high percentage (about 58%) of MPMs. [78] These data pointing at BAP1 as the putative driver mutation for a significant number of MMs.

BAP1 is a member of the ubiquitin C-terminal hydrolase (UCH) subfamily of deubiquitinating enzymes (DUBs).[79] BAP1 functions as a tumor suppressor because has the ability to perform the deubiquitination of histone H2A, and to remodel the chromatin, leading to transcriptional activation of genes that regulate cell growth. [80] Epigenetic regulation of tumor suppressor genes through chromatin condensation and decondensation has emerged as an important mechanism that leads to tumorigenesis. The balance between the acetylated and deacetylated forms of histone proteins is regulated by histone acetyltransferases (HATs) and histone deacetylases (HDACs). HATs increase acetylation promoting greater chromatin accessibility for gene expression, whereas HDAC inhibitors alter the packaging of the DNA around histones, impacting the expression of various genes. Different preclinical studies were conducted by testing in vitro- effect of various HDAC inhibitors, such as valproic acid, trichostatin A, LBH-589, and suberoylanilide hydroxamic acid (vorinostat). *In vitro* data studying the role of HDAC inhibitors in MM showed increased apoptosis in MM cell lines after treatment with inhibitors, either alone or in combination with conventional chemotherapy. [81- 86] Furthermore, the combination of valproic acid and chemotherapy completely suppress the tumor generated in a mouse xenograft model of MM. [86]

Vorinostat has been approved by FDA for the treatment of cutaneous T-cell lymphoma. But a Phase III trial (VANTAGE 014) study including 660 pre-treated advanced MPM patients used Vorinostat as a second-line or third-line therapy and reported that this treatment modality did not improve overall survival. Therefore, Vorinostat was not recommended as a therapy in MPM patients. [87]

Loss of the tumor suppressor gene NF2, encoding Merlin

Mounting evidence has shown that NF2 plays an important role in MM pathogenesis (**Figure 3.a**). Recent data indicates that asbestos-treated NF2+/− mice accelerate MM tumor formation compared to the wild-types. [88] The NF2 gene is located on chromosome 22q12 and encodes merlin, a tumor suppressor protein. [89] Merlin can interact with various proteins, and in this way modulates multiple signal transduction cascades, including mTOR, focal adhesion kinase (FAK) and Hippo signaling pathways (**Figure 3**). In MM cells, loss of merlin causes activation of mTOR signaling, [90] therefore in merlin-silenced tumors there is an upregulation of mitogenic signaling and increased cell proliferation. As expected, merlin-negative MM cells

were more sensitive to the mTOR inhibitor rapamycin, compared to merlin-positive cells. [90] Therefore, in the large fraction of MMs that carry NF2 mutations, mTOR could be a therapeutic target and provide the rationale for testing mTOR inhibitors in MM. Unfortunately, the oral mTOR inhibitor everolimus (RAD001) had limited clinical activity when tested in a phase II trial S0722 (NCT 00770120) as second- and third-line treatment agent in unselected pre-treated MPM patients. [91] It was concluded that additional studies of single-agent everolimus in advanced MPM were not warranted. [91] The inhibition of mTOR can generate a compensatory mechanism of resistance, that consist in upregulation of PI3KCA and the restoration of the downstream AKT signaling pathway. [92] To address this mechanism of mTOR resistance, a selective dual inhibitor (GDC-0980) of class I PI3K and mTOR was tested. This inhibitor demonstrated broad activity in various xenograft cancer models, including MPM, [93] but also pulmonary toxicity. However, despite these disappointing results, the role of PI3K/AKT/mTOR survival pathway in MM is being further evaluated in clinical trials (NCT01655225, NCT01991938).

Deficiency in the CDKN2A /ARF locus

Previous genetic analysis performed into MM biopsies has revealed that cyclin-dependent kinase inhibitor 2A (CDKN2A)/alternative reading frame (ARF) and neurofibromatosis type 2 (NF2) were the most commonly mutated tumor suppressor genes in MM. [94, 95] The CDKN2A/ARF is a tumor suppressor gene located at chromosome 9p21.3. [96] CDKN2A encodes p16INK4a, whereas ARF encodes p14ARF. p16INK4a inhibits the cyclin-dependent kinase (CDK)-mediate hyperphosphorylation that leads to retinoblastoma protein (pRb) inactivation. So, loss of p16INK4a results in inactivation of pRb and, consequently, failure of cell cycle arrest. The p14ARF protein promotes degradation of the human ortholog of mouse double minute 2 (MDM2), leading to stabilization of p53. A particularly high frequency of homozygous deletion of CDKN2A/ARF has been detected in mesothelioma samples, causing loss of function of both p53 and pRb tumor suppressors, with a consequent breakdown of cell cycle control mechanisms (**Figure 3.a**). Otherwise, only a limited number of MM biopsies contain TP53 mutations, the tumor suppressor gene that encodes p53. Different *in vivo* studies indicate that the inactivation of both CDKN2A and ARF gene cooperates to accelerate asbestos-induced tumorigenesis in mice. [97] However, since genetic defects in p16INK4a/p14ARF are very common, and lead to loss of function of both p53 and Rb, the defective p53 pathways is a potential target for MM gene therapy. [98] Direct restoration of p16INK4a using gene therapy has also been tested and it has shown some promising activity in preclinical models but is still far from clinical development. [99, 100]

Receptor Tyrosine Kinase Inhibitors

In MM was often observed an activation/upregulation of several receptor tyrosine kinases that constitute a large family of receptors and regulate the cell cycle (**Figure 3.b**). [101] Activation of these receptors lead to the

transduction of abnormal cell growth signaling pathways, which is at the basis of cancer initiation and progression. Inhibition of RTKs or of their ligands with specific antibodies or small molecules has been proven to be an effective and safe targeted approach in several malignancies. [102]

Inhibition of angiogenesis was shown to produce antitumor responses and decrease pleural effusion. [103] Mesothelioma secretes pro-angiogenic factors, platelet-derived growth factor (PDGF) and vascular endothelial growth factor (VEGF), both of which are also associated with cell proliferation and pleural effusion. In pleural effusions of MPM patients were detected high levels of VEGF, associated with a worse patient survival. [104] Bevacizumab is an anti-VEGF humanized monoclonal antibody approved for use in several cancers. [105] Results obtained from three independent phase II clinical trials showed that addition of bevacizumab to the standard of care failed to increase survival of MM patients. [106–108]

However, recently, results from a randomized phase III trial (IFCT-GFPC-0701 MAPS) indicate that patients treated with bevacizumab and the standard of care (pemetrexed + cisplatin) experienced a significant longer median survival (18.82 months vs. 16.07 months, p = 0.0127) (2015 ASCO Meeting, Abstract #7500). These results might translate into addition of bevacizumab as part of the first line treatment for MPM.

There are different studies that reported the high expression of EGFR into MM specimens, thus several inhibitors of this pathway were tested in clinical trials. The results obtained by using erlotinib and gefitinib, inhibitors of EGFR were very disappointing. [109, 110] Negative results were obtained also using erlotinib in combination with bevacizumab after platinum-based chemotherapy. [111] In MM tissue and cell lines an overexpression of several fibroblast growth factors (FGFs) and FGF receptors (FGFRs) were observed. Furthermore, a correlation between high expression of these factors and tumor aggressiveness was also detected. [112, 113] Moreover, inhibition of FGFR1 represses MM cell growth and migration in vitro and in vivo and potentiates the effect of chemotherapeutic drug or ionizing irradiation.[114] Thus, inhibition of FGF signals seems to be promising and may permit further evaluation of FGFR targeting strategies.

Other activated pathways in MM are also hepatocyte growth factor (HGF) and the receptor c-Met which are important for tumor invasion and metastasis. It has been demonstrated that inhibition of this pathway suppresses tumor infiltration into neighboring tissues. [115] So, an inhibitor of c-Met kinase is under investigation for clinical efficacy. Other preclinical studies that inhibit HGF/c-Met pathways were conducted for MM. [116] It is worthwhile to note that in several of the mentioned clinical trials, a small percentage of patients (usually ~1–5%), did experience partial benefits from the therapy with RTK inhibitors, highlighting the need to identify predictive biomarkers to select likely responders (**Figure 3.b**).

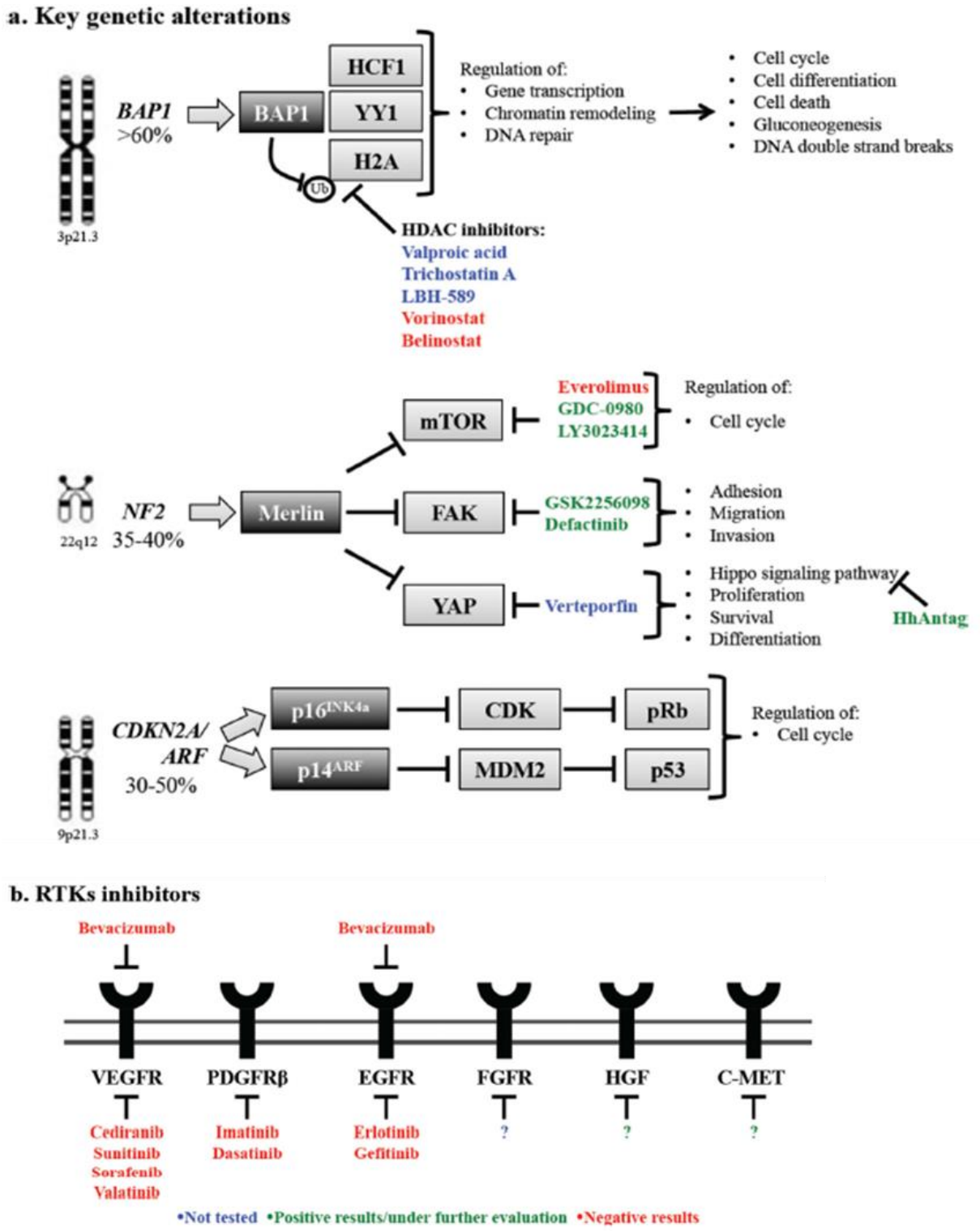

Figure 3: Key genetic alterations in MPM and potential strategies for therapeutic intervention. [10]

Immunotherapy and immune checkpoint inhibitors

It is known that an immune response is induced by mesothelioma, but it is weak (Robinson *et al,* 2000). [117] This knowledge has prompted a number of investigators to study different ways to consolidate that response. The intrapleural instillation of cytokines is limited by the short half-life of most cytokines,

necessitating repeated injections or continuous infusion via a pleural catheter. Intrapleural interferon-gamma twice weekly for 2 months was reported to induce response rate of 56% in early stage disease. [118] A continuous intrapleural infusion of interleukin-2 induced a partial response in four of 21 patients and an overall survival of 16 months. [119] In both cases, side effects were minimal and consisted primarily of fever and constitutional symptoms. Studies in animals suggest that interferons have an antiproliferative effect on mesothelioma cells and enhance the cytotoxic effect of cisplatin. The results from these studies led to the development of a Phase II trial of cisplatin-doxorubicin and interferon alpha-2 in advanced malignant mesothelioma. The overall response rate was 29% and the median survival was 9.3 months with one year survival of 45% and two year of 34%. [120] However, severe myelosuppression was seen in 60% of patients limiting the application of this treatment. One of the newest hallmark of cancer proposed recently was among others, the evasion of immune destruction, [121] by expressing endogenous immune checkpoints that normally terminate immune responses after antigen activation. This state of tumor-induced immunological anergy is associated to up-regulation in tumor-infiltrating T cells of immune checkpoint molecules, such as cytotoxic T-lymphocyte-associated protein 4 (CTLA-4), and programmed cell death protein 1 (PD-1). [122] Alternatively tumors can block immune activation by upregulating PD-1 ligands. Like many other tumors, MM express high levels of the immunosuppressive PD-1 ligand 1 (PD-L1). [123, 124] Monoclonal antibodies against CTLA4 (tremelimumab, ipilimumab), PD-1 (nivolumab, pembrolizumab), and PD-L1 (avelumab, MPDL3280A) can reactivate the immune response against cancer cells, and have shown promising clinical results in melanoma and some other cancer types. [122] The CTLA4 inhibitor, tremelimumab, at a dose of 15 mg/kg once every 12 weeks, showed clinical activity in 38% of advanced MM patients in a phase II study. [125] An intensified regiment showed a good safety profile, and clinical and immunological activity in patients with advanced MM, with more than 40% of the patients achieving disease control with a median duration of response of almost 11 months. [126] Other clinical trials with PD-1 inhibitor pembrolizumab (NCT02399371) and PD-L1 inhibitor avelumab (NCT01772004) are currently ongoing.

HMGB1

High-mobility group box 1 protein (HMGB1) is a chromatin-binding factor that bends DNA and promotes access to transcriptional protein assemblies on specific DNA targets.[127, 128] This protein was isolated and characterized in calf thymus in 1973, and its name derives from its electrophoretic mobility on polyacrylamide gels. HMGB1 has two HMG-box domains (N-terminal A and central B) able to bind DNA and an acidic C terminal tail (**Figure 4.a**). HMGB1 is a highly conserved nuclear protein, present in almost all metazoans and plants. [129] In most cells, HMGB1 acts as a DNA chaperone to help maintain nuclear homeostasis. Later, it was discovered that HMGB1 is also expressed on cell surface membranes, cytosol, and mitochondria, and could be released into the extracellular space. So, in addition to its nuclear function,

HMGB1 has also many biological functions outside the cell playing a significant role as extracellular signaling molecule during inflammation, cell differentiation, cell migration, and tumor metastasis. [127] HMGB1 is passively released from necrotic cells and is actively secreted by inflammatory cells, binding to several receptors such as the receptor for advanced glycation end products (RAGE), Toll-like receptors (TLR)-2, TLR-4, TLR-9, and, as a negative signaling molecule, CD24. The interaction between HMGB1 and its functional receptors mediates the response to infection and injury, thereby promoting inflammation (**Figure 4.b**). [127, 128, 129, 130, 131, 132]. As such HMGB1 is the prototypic Damage Associated Molecular Pattern Molecule, or DAMP, associated with both acute inflammatory responses and driving much of the biology of chronic inflammation and wound repair.[133, 134] HMGB1 plays a significant role in many diseases, especially inflammatory diseases and cancer. [135-139] Recent evidences indicate that HMGB1 dysfunction is associated with each of the central hallmarks of cancer and contributes to cancer development and therapy.

Nuclear Function of HMGB1

HMGB1 proteins are constitutively expressed in the nucleus of cells due to the presence of two lysine-rich nuclear localization sequences (NLSs) located in the A box and in the B box (**Figure 4.a**). Hyperacetylation of NLSs endorses the translocation of HMGB1 from the nucleus to the cytosol, and its consequent release. The studies, which have measured the affinity of HMGB1 with different DNA structures, indicated that HMGB1 is able to binds preferentially different DNA structures such as supercoiled, single-stranded, B- and Z-DNA, DNA mini-circles, and triplex DNA. [139, 140] This ability is promoted from its HMG boxes that allow HMGB1 to bind DNA without sequence-specificity and to act as a DNA chaperone. Thus, HMGB1 is the structural protein of chromatin which regulates nuclear homeostasis and genome stability in several ways (**Figure 4**).

1) Nucleosome structure and dynamics. Chromatin contains nucleosome units which consist in a short length of DNA wrapped around a core of histone proteins. HMGB1 binds to nucleosomes at the dyad axis, induces the sliding of nucleosome, relaxes nucleosome structure, and due to its ability of DNA-bending, makes chromatin more accessible. [141]

2) Gene transcription. HMGB1 has been found to interact with and enhance the binding affinity of many sequence- specific transcriptional factors to their cognate DNA, such as p53, [142] p73, [143] the retinoblastoma protein, [144] members of the Rel/NF-κB family [145] and estrogen receptors. This could increase their activity as transcriptional factors implicated in cancer development. Mounting evidence has shown that HMGB1 interacts with p53 and provides the optimal DNA structure for p53 binding through its bending/binding effects. [146] p53 family members are important because participate in the regulation of cell cycle progression functioning as tumor suppressors.

3) **DNA repair.** HMGB1 also plays a critical role in DNA repair by being part of a nuclear protein complex involved in the cytotoxic response to DNA modified by incorporation of anticancer nucleoside analogues. In addition, loss of HMGB1 increases DNA damage and decreases DNA repair efficiency in response to

chemotherapy, irradiation, and oxidative stress. HMGB1 directly binds to a variety of bulky DNA lesions and allows it to participate in DNA repair pathways including nucleotide excision repair, base excision repair, mismatch repair, and double strand break repair via nonhomologous end-joining. [147]

Cytosolic HMGB1

Different studies have investigated the levels and distribution of HMGB1 between the nucleus and cytoplasm in different cells and tissues. Localization of HMGB1 in the cytoplasm has been confirmed in living fibroblasts, thymocytes and several different tissues (e.g., liver, kidney, brain, heart, and lung). [148, 149] Currently, we know that HMGB1 normally is located in the nucleus and translocate from the nucleus to the cytosol, including mitochondria and lysosome, following various stressors (e.g., cytokine, chemokine, heat, hypoxia, H2O2, and oncogene). Although the function of cytosolic HMGB1 still remains poorly studied, we demonstrated that the main function of HMGB1 in cytoplasm is to function as a positive regulator of autophagy. Autophagic stimuli promote the translocation of HMGB1 to the cytosol. Cytosolic HMGB1 binds to Beclin-1 inducing autophagy for degrading damaged organelles and unused proteins. [150] HMGB1 also interacts with many apparently unrelated proteins by recognizing short amino acid sequence motifs. [151] For example, the motifs PXXPXP and WXXW (where X can be any amino acid) can interact with box A and box B of HMGB1, respectively. [151] Thus, HMGB1 may be involved in many cell processes by promoting protein protein interactions.

Another potential function for cytosolic HMGB1 is involvement in the unconventional secretory pathway, found based on mass spectrometry-mediated binding partner analysis in 2010. [152]

HMGB1 release

In addition to its role inside the cell, HMGB1 also functions as a damage-associated molecular pattern (DAMP) when passively released from dead, dying, or injured cells. It is also actively secreted from immune cells or cancer cells in response to exogenous and endogenous stimuli such as endotoxin, CpG DNA, double-stranded RNA (dsRNA), tumor necrosis factor (TNF)-α, interleukin (IL)-1, interferons (IFN)-γ, hydrogen peroxide, adenosine triphosphate (ATP), and hypoxia. In addition, macrophage engulfment of apoptotic cells may induce significant active HMGB1 release, suggesting a direct interplay between dying cells and immune cells, which also induces HMGB1 release. [153] Depending on the inducing stimulus, the mechanism of HMGB1 secretion and release could be different.

Extracellular HMGB1

Besides its nuclear and cytosolic function, HMGB1 performs a significant extracellular role in inflammation, immunity, cell growth, cell proliferation, and cell death. HMGB1 can be actively secreted by immune cells or

passively released by dead, dying, or injured cells. Once released, extracellular HMGB1 binds to several cell surface receptors to activate the downstream signaling pathway (e.g., NF-κB, IFN regulatory factor-3 (IRF3), and phosphatidylinositol 3-kinase [PI3K]) to produce a functional response, such as activation of innate immune cells, induction of proinflammatory cytokines and type I IFNs, stimulation of cell adhesion and migration, inhibition of phagocytosis, promotion of cell proliferation and angiogenesis, and induction of autophagy. [154, 155] In addition, extracellular HMGB1 functions as an immune adjuvant to trigger a robust response to activation or suppression of T cells, dendritic cells, and endothelial cells. Activated immune cells (e.g., macrophages, monocytes, and dendritic cells) and endothelial cells also secrete HMGB1, which in turn generates a positive feedback loop that causes the release of supplemental cytokines and chemokines following engagement of multiple receptors. Thus, HMGB1 has the ability to sustain a long-term inflammatory state under stress. Interestingly, extracellular HMGB1 has antibacterial, cell growth, and mitotic activity. These extracellular HMGB1 activities are not only mediated by receptors, but also by its redox state and structure.[156]

Native HMGB1 proteins from eukaryotic sources have the same (though less pronounced) biological activity *in vitro* compared to recombinant HMGB1 proteins from prokaryotic sources. [157] The extracellular HMGB1 plays its function by binding to several receptors such as the receptor for advanced glycation end products (RAGE), Toll-like receptors (TLRs, such as TLR2, TLR4, and TLR9), Mac-1, syndecan-1 (CD138), phosphacan protein-tyrosine phosphatase (PPTP)- ζ/β, CD24, chemokine (C-X-C motif) ligand 4 (CXCL4), T cell immunoglobulin mucin-3 (TIM-3), and possibly others. Of these receptors, CD24 and TIM-3 act as negative receptors and inhibit immune activity of HMGB1 in macrophages and tumor-associated dendritic cells (TADCs), respectively. [158, 159] Apart from a direct receptor interaction, HMGB1 may form heterocomplexes with other immune co-activators such as IL-1, CXCL12, DNA, nucleosome, or LPS that generate synergistic responses in inflammation and immunity. The first receptor demonstrated to bind HMGB1 was RAGE.[160] Later, it was discovered that HMGB1 signaling through RAGE mediates chemotaxis and migration, proliferation and differentiation of immune and cancer cells, and upregulation of cell surface receptors. In addition, RAGE provides a functional platform for crosstalk with other HMGB1 receptors. For example, interplay between RAGE and TLR9 is important for critical for HMGB1-DNA complex, which activates the immune responses in dendritic cells (DCs). [161] The interplay between Mac-1 and RAGE is required for HMGB1-mediated adhesive and migratory neutrophil functions. [162] whereas, the interplay between syndecan-1, PPTP-ζ/β, and RAGE is required for neurite outgrowth mediated by HMGB1.

Apart from RAGE, HMGB1 binding of TLR2 and TLR4 also results in NF-κB activation. TLR4 may be more important for HMGB1-induced macrophage activation and proinflammatory cytokine release. [163] Experimental data obtained by using TLR4-deficient animals suggest that TLR4 plays a critical role in sterile inflammation. [164] These animal models are significantly protected from ischemia-reperfusion injury to the liver, kidney, and heart.

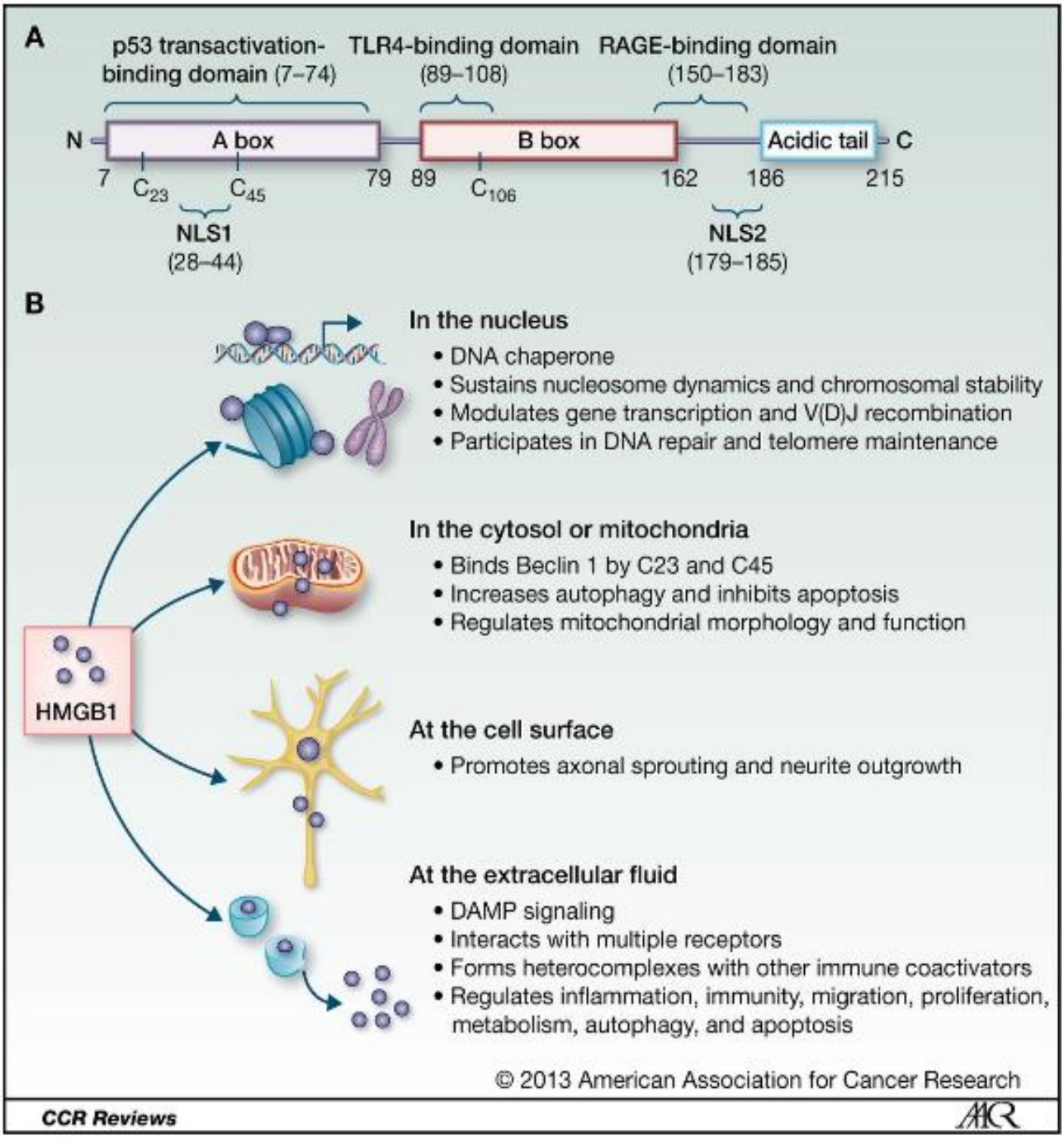

Figure 4. Structure and function of HMGB1

(A) HMGB1 is structurally composed of three different domains: two homologous DNA binding domains (box A and box B) and a negatively charged C-terminal domain. Two nuclear localization signals (NLS1 and NLS2) control nuclear transport of HMGB1. In addition, HMGB1 contains three redox-sensitive cysteine residues (C23, C45 and C106), which are important for HMGB1 activity. (B) HMGB1 has multiple roles inside and outside the cell. [266]

HMGB1 Redox States

Recent studies underline the importance of redox modification in the regulation of HMGB1 translocation, release, and activity in disease.[164] Three cysteines are encoded within the HMGB1, two vicinal cysteines in

box A (C23 and C45) and a single one in box B (C106). Replacement of Cys23 and/or 45 with serine did not affect the nuclear distribution of the mutant proteins. Whereas, C106S and triple cysteine mutations impaired the nuclear localization of HMGB1, allowing entry of some of the protein into the cytosol. Moreover, increased endogenous and exogenous ROS promotes HMGB1 translocation and release. [165] The redox status of HMGB1 promotes to distinguish between its cytokine and chemokine activity.[166] Initial studies suggest that reduced C106 is necessary for the binding of HMGB1 to TLR4 and promotes cytokine release and inflammation. A recent study suggests that a disulfide bond between C23 and C45 is also required for HMGB1 cytokine activity. Mutations of C45 or C23 abolish the cytokine activity of HMGB1. In contrast, all-cysteine-reduced HMGB1 does not have TLR4-dependent cytokine activity, but binds to CXCL4 to induce inflammatory cell recruitment and chemotaxis by the CXCL12 receptor. [167] ROS oxidizes the HMGB1 at C106 released from apoptotic cells, thereby neutralizing its cytokine-inducing activity and promoting tolerance in DCs. Finally, all-cysteine oxidized HMGB1 impairs HMGB1's cytokine or chemotactic activity.[168] Thus, redox modifications are crucial for HMGB1 functionality as a mediator during infection and sterile inflammation.

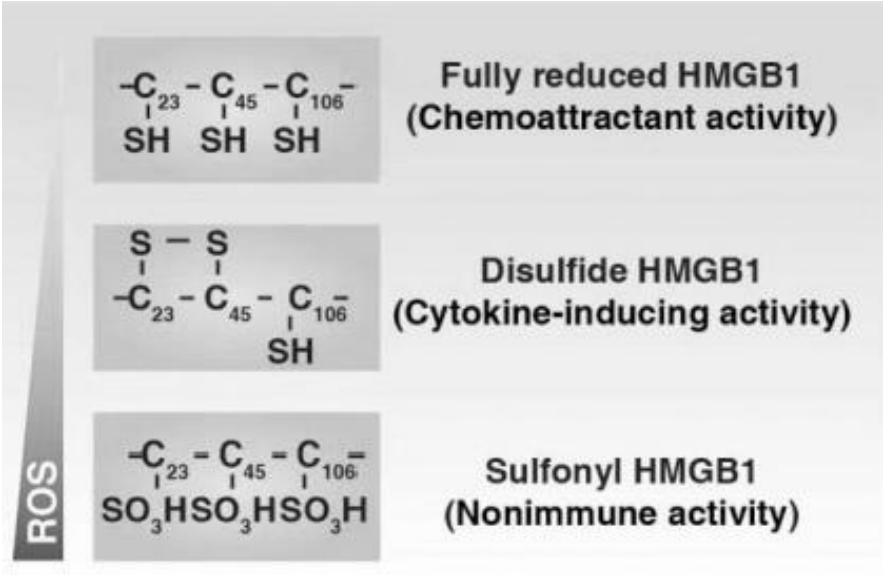

Figure 5: The redox status of HMGB1 regulates its cytokine-inducing and chemokine activities.[200]

HMGB1's Roles in Tumorigenesis

Mounting evidences has shown that disfunction of HMGB1 is associated with tumorigenesis and contributes to cancer development and therapy (**Figure 6**).[169] For this purpose, it will be important to understand HMGB1 regulation and its function in the mechanism of cancer biology. Furthermore, the understanding of its role in tumorigenesis will influences the strategies of a HMGB1 targeted therapy for prevention and treatment.

The inflammatory tumor microenvironment (TME) is able to support the neoplastic transformation, tumor growth, invasion, and metastasis. The development of the inflammatory tumor microenvironment is associated with the tumor-infiltrating leukocytes and the cytokine-related signaling pathways. Infiltrating

leucocytes, as well as the cancer cells themselves, have the ability to secrete HMGB1 under hypoxia, injury, inflammatory stimuli, or environmental factors.[170] In turn, extracellular HMGB1 can activate proinflammatory signaling pathways, such as the NF-κB and inflammasome pathways, to induce proinflammatory cytokine release. This loop will accelerate inflammatory responses and induce tumor formation, and metastasis.
Another of the most common cancer phenotypes is a high energy request by cancer cells to allow a rapid, invasive and metastatic growth of tumor. While normal cells produce ATP through a combination of oxidative and glycolytic metabolism, cancer cells effectively stimulate and reprogram their metabolism to better fit the energy demand. HMGB1 has been implicated in tumor energy metabolism. [171,172,173] Recombinant exogenous HMGB1 or endogenous HMGB1 derived from necrotic tumor cell lysates are likely to rise ATP production and pancreatic tumor cell proliferation, providing a direct link between inflammation and energy metabolism with the TME. [171] Recently it was shown that extracellular HMGB1 increases mitochondrial RAGE expression and translocation, which in turn increases mitochondrial complex I activity and ATP production. [174] Most cancer deaths are caused by tumor invasion and metastasis rather than the primary tumor itself. In the clinic, expression of RAGE is strictly associated with cancer invasiveness and metastasis activity such as gastric cancer [175] and colorectal cancer.[176] Different *in vivo* and *in vitro* studies showed that impairment of RAGE–HMGB1 interaction inhibit tumor growth and metastasis by activation of mitogen-activated protein kinases and the NF-kB pathway. The NF-kB activation results in the expression of matrix metalloproteinases (MMP), such as MMP2 and MMP9,[177, 178] which degrade extracellular matrix proteins and play an important role in tumor invasion and metastasis.[177] Thus, HMGB1–RAGE signaling pathway plays a major role in tumor invasion and metastasis.
The immunity surveillance of cancer is considered to be an important defense process against carcinogenesis. HMGB1, as a multifunctional cytokine, has been characterized with both immunosuppressive and immune-activation properties, which depends on receptors, targeted cells, and redox state. [179] So, HMGB1 has the ability to induce apoptosis in macrophage-derived DCs, which diminish host anti-cancer immunity. [180] In addition, HMGB1, derived from tumor cells, suppresses naturally-acquired CD8+ T cell-dependent antitumor immunity, partly by enhancing tumor-associated Treg to produce IL-10.[181] Recent findings suggest that endogenous intracellular HMGB1, as a RB- associated protein, suppresses breast tumorigenesis, acting as a tumor suppressor gene (**Figure 6)**.[182] RB is a well-known tumor suppressor protein that is dysfunctional in many cancers. HMGB1 enhances RB-mediated transcription repression such as E2F and cyclin A1, and causes RB-dependent G1 arrest and apoptosis induction. In addition, overexpression of HMGB1 inhibits RB positive breast cancer growth in vitro and prevents tumorigenicity in subcutaneous tumor models in vivo. [182] In addition, HMGB1 is also an important regulator of autophagy and its lost inhibits autophagy and increases apoptosis. Several studies have indicated that defective autophagy-associated genes (e.g., Beclin1, ATG5, UVRAG, Bif-1) in mice increase genome instability, inflammation, oxidative stress, and mitochondrial injury, which contribute to tumorigenesis. [183-185] So, these findings underscore that HMGB1 inhibition lead to

autophagy deficiency, cause genomic instability, inflammation and induce tumorigenesis. Thus, suppression of autophagy promotes tumorigenesis and increases the effectiveness of anticancer therapy.

HMGB1's Protective Roles in Anticancer Therapy

Immunogenic cell death (ICD), contributes to immune-mediated elimination of tumors during chemotherapy (e.g., anthracyclines) or radiotherapy. [186-189] ICD is characterized by the release of dying cancer cells or cell surface exposure of DAMPs (e.g., calreticulin, heat shock proteins, ATP, and HMGB1). These events are useful for the maturation, antigen uptake, and presentation of DCs and works as high-powered immunological adjuvants to active cytotoxic T lymphocyte response. Several *in vivo* and *in vitro* studies indicate that blocking the HMGB1- TLR4 pathway inhibits ICD and the anticancer immune responses upon chemotherapy. [189] (**Figure 6**). However, HMGB1 released from necrotic cancer cells treated with chemotherapy amplifies regrowth and metastasis of residual cancer cells in a RAGE-dependent way. [190] Thus, blocking HMGB1-RAGE signaling rise the effectiveness of chemotherapy.[191] These studies suggest that TLR4 in DC is important for HMGB1-mediated ICD and tumor clearance, whereas RAGE in cancer cells is critical for HMGB1-mediated survival after chemotherapy. Although both apoptotic and necrotic cells have the ability to release HMGB1, only the HMGB1 released from apoptotic cells is tolerogenic. [190] Thus, determining the role of extracellular HMGB1 in a context specific way in chemotherapy and immunotherapy, including ICD, and the mechanisms involved will be important to optimize the therapeutic outcomes.

The negative roles of HMGB1 in Anticancer Therapy

It has been demonstrated that suppression of HMGB1 expression by RNAi increased the anticancer activity of cytotoxic agents, whereas overexpression of HMGB1 expression by gene transfection increased drug resistance. [192, 193] HMGB1 expression regulates chemotherapeutic response and resistance by interfering with autophagy and the apoptotic pathway (**Figure 6**). HMGB1 has the ability to increase the pro-survival autophagy in a Beclin 1- dependent way in chemotherapy, whereas HMGB1 inhibits both intrinsic and extrinsic programmed cell death/apoptosis in a caspase-dependent way in cancer cells. The crosstalk between apoptosis and autophagy regulates cell death and determines cell fate in anticancer therapy. Upregulation of apoptosis inhibits autophagy, whereas upregulation of autophagy inhibits apoptosis during chemotherapy. HMGB1 and p53 are capable of physical interaction (**Figure 6)**, [194] and the interplay between HMGB1 and p53 regulates apoptosis and autophagy in clone cancer cells after treatment with DNA-damaging anticancer drugs.[193] DNA damage promotes interactions between p53 and HMGB1 in the nucleus and cytoplasm. Loss of p53 increases cytosolic HMGB1, leading to increased binding to Beclin 1, thereby promoting autophagy and decreasing apoptosis; In contrast, loss of HMGB1 increases cytosolic p53

and apoptosis and decreases autophagy. [193] These findings provide new insights into the HMGB1-p53 signaling and cancer cell response to DNA damage.

HMGB1-Targeting Therapeutic Agents

Apart from genetic inhibition or overexpression of HMGB1 expression in cancer cells, several HMGB1-targeting agents have been used in experimental cancer research. These agents including sRAGE, HMGB1 neutralizing antibody, A box protein, platinating agent, ethyl pyruvate, quercetin, and glycyrrhizin. sRAGE acts as a decoy to prevent RAGE signaling and has been used successfully in blocking the HMGB1-RAGE signaling pathway in animal tumor models. HMGB1 neutralizing antibody and A box protein can block activity of extracellular HMGB1 in tumor therapy.[195] Interestingly, platinating agents such as cisplatin and oxaliplatin have the ability to retain HMGB1 within the nucleus by conformational changes in the double helix to which HMGB1 binds quite stably. [196] Ethyl pyruvate, the first HMGB1 inhibitor used in animal models of sepsis by inhibition of NF-κB pathway, inhibits liver tumor growth. [197] In addition, glycyrrhizin and quercetin, potential HMGB1 inhibitors by directly binding to HMGB1 or inhibition of PI3K, improve the effectiveness of anticancer agents in several different tumor models. [195] Further investigation is needed to evaluate these therapies and their possible role in clinical practice.

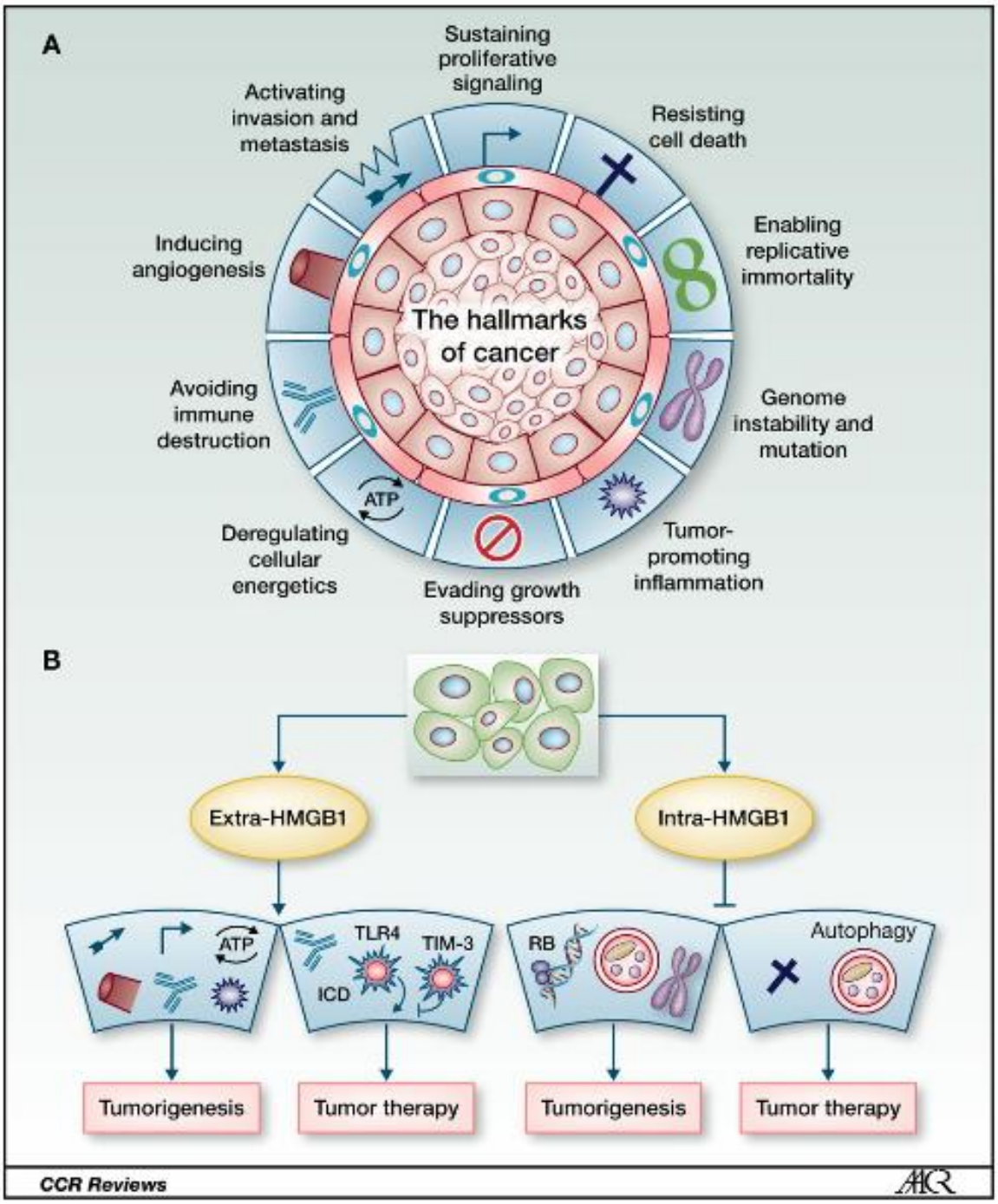

Figure 6. The dual roles of HMGB1 in cancer

(A) The hallmarks of cancer comprise ten biological capabilities acquired during the multistep development of human tumors. Deregulation of HMGB1 is associated with the hallmarks of cancer. Figure modified from Hanahan and Weinberg (4). (B) HMGB1 acts as an anti- or pro-tumor protein in tumor development and therapy. [266]

HMGB1 and Malignant mesothelioma

The deposition of asbestos in tissue induce inflammation and contributes to asbestos carcinogenesis. [198] The inflammatory infiltrate into tissue areas containing asbestos deposits consists largely of phagocytic macrophages that internalize asbestos and release numerous cytokines and mutagenic ROS.

A key mechanism by which asbestos causes the transformation of mesothelial cells has recently been elucidated: working with primary human mesothelial (HM) cells, Yang et al discovered that asbestos induces necrotic cell death with resultant release of HMGB-1 in the extra cellular space. [27] Extracellular HMGB1 binds several pro-inflammatory molecules and triggers the inflammatory responses that distinguish this type of cell death from apoptosis. These findings provide mechanistic links between asbestos-induced cell death, chronic inflammation, and mesothelioma. Secreted HMGB1 stimulates RAGE, TLR2 and TLR4 (the three main HMGB1 receptors) expressed on neighboring macrophages and induces the release of several inflammatory cytokines, including TNF-α and IL-1β. In addition, HMGB1 enhances the activity of NF-κB, leading to the survival of HM cells that have accumulated genetic damage because of asbestos exposure (**Figure 7**). [27] This process promotes tumor formation, progression, and metastasis. Thus, as shown in figure 7 it has been hypothesized that HMGB1 functions as a "master switch" initiating a series of inflammatory responses leading to malignant transformation of asbestos- or erionite damaged HM**.** Furthermore, another study unveils that HMGB1 is highly expressed and secreted by malignant mesothelioma cells, establishing an autocrine circuit that supports their malignant phenotype.[170] These findings suggest an important role of HMGB1 in development and progression of mesothelioma, at least in preclinical studies. In addition, patients with peritoneal and pleural mesothelioma showed higher serum levels of HMGB1 compared with the controls, suggesting that this protein may be a useful diagnostic and prognostic biomarker of malignant mesothelioma. [277, 278]

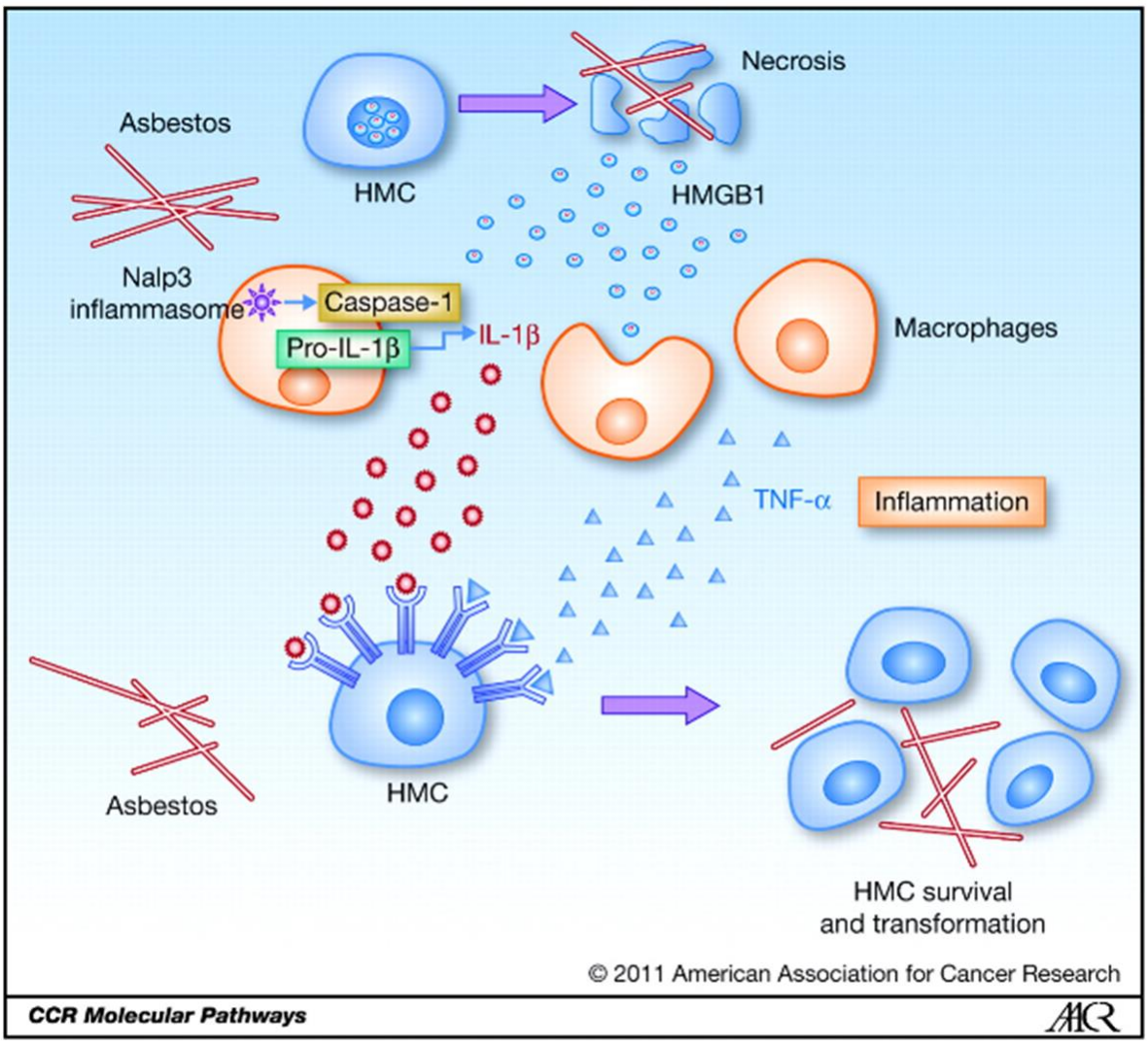

Figure 7. Working hypothesis for mesothelioma carcinogenesis. Asbestos causes necrotic HMC death, leading to the release of HMGB1 into the extracellular space. As a typical DAMP and a key mediator of inflammation, HMGB can induce activation of Nalp3 inflammasome and subsequent IL-1β secretion, as well as eliciting macrophage accumulation and triggering the inflammatory response and TNF-α secretion, which increases the survival of asbestos-damaged HMCs. This allows key genetic alterations to accumulate within HMCs that sustain asbestos-induced DNA damage, leading to the initiation of mesothelioma. [198]

Targeting asbestos induced inflammation to prevent or treat mesothelioma

Chronic inflammation has been associated with an increased risk of developing numerous cancers. Accordingly, daily treatment with aspirin for 5 or more years reduced tumor burden in several common malignancies. [201] Animal experiments support a beneficial role for anti-inflammatory therapies in mesothelioma; [202] thus, prolonged aspirin treatment might help reduce the incidence of mesothelioma and other asbestos-related malignancies among high-risk cohorts that have either a lengthy history of exposure and/or genetic predisposition. Based on recent findings, it is tempting to speculate that HMGB1 and the Nalp3 inflammasome act as critical initiators of chronic inflammation in asbestos- and erionite exposed

individuals, with the secretion of IL-1β and TNF-α acting as the key downstream driving force. HMGB1, Nalp3, TNF-α and IL-1β can therefore all serve as potential targets for inhibitors of asbestos-induced inflammation leading to mesothelioma. As several solid tumors in addition to mesothelioma display elevated levels of HMGB1, including melanoma, prostate, pancreatic, breast and gastrointestinal cancers, therapies that seek to block HMGB1 signaling would likely prove effective in other cancer types in addition to mesothelioma. Treatment with an IL-1 receptor antagonist can protect mice from developing fibrosis upon exposure to silica; [203] and in murine models of silica- induced pulmonary fibrosis, infusion with the human recombinant soluble TNF receptor rsTNFR-β or TNF- α antibodies [204] was effective not only in preventing the development of pulmonary fibrosis but also in the treatment of established fibrosis. There are specific-FDA approved reagents that inhibits these molecules which are at the basis of chronic inflammation. Anakinra, an IL-1 receptor antagonist, is used in therapies for patients with autoimmune diseases and gout. Remicade (Infliximab), a chimeric human-mouse anti-TNF- α, and Enbrel (Etanercept), a soluble TNF receptor fusion protein, have both been used to treat patients with rheumatoid arthritis. Glyburide, the most widely used sulfonylurea drug for type 2 diabetes in the US, inhibits the Nalp3 inflammasome. [205] Specific molecules that target the activity of HMGB1 are anti-HMGB1 and anti-RAGE antibodies, recombinant HMG Box A, and ethyl pyruvate, an inhibitor of HMGB1 secretion (**Figure 8**).

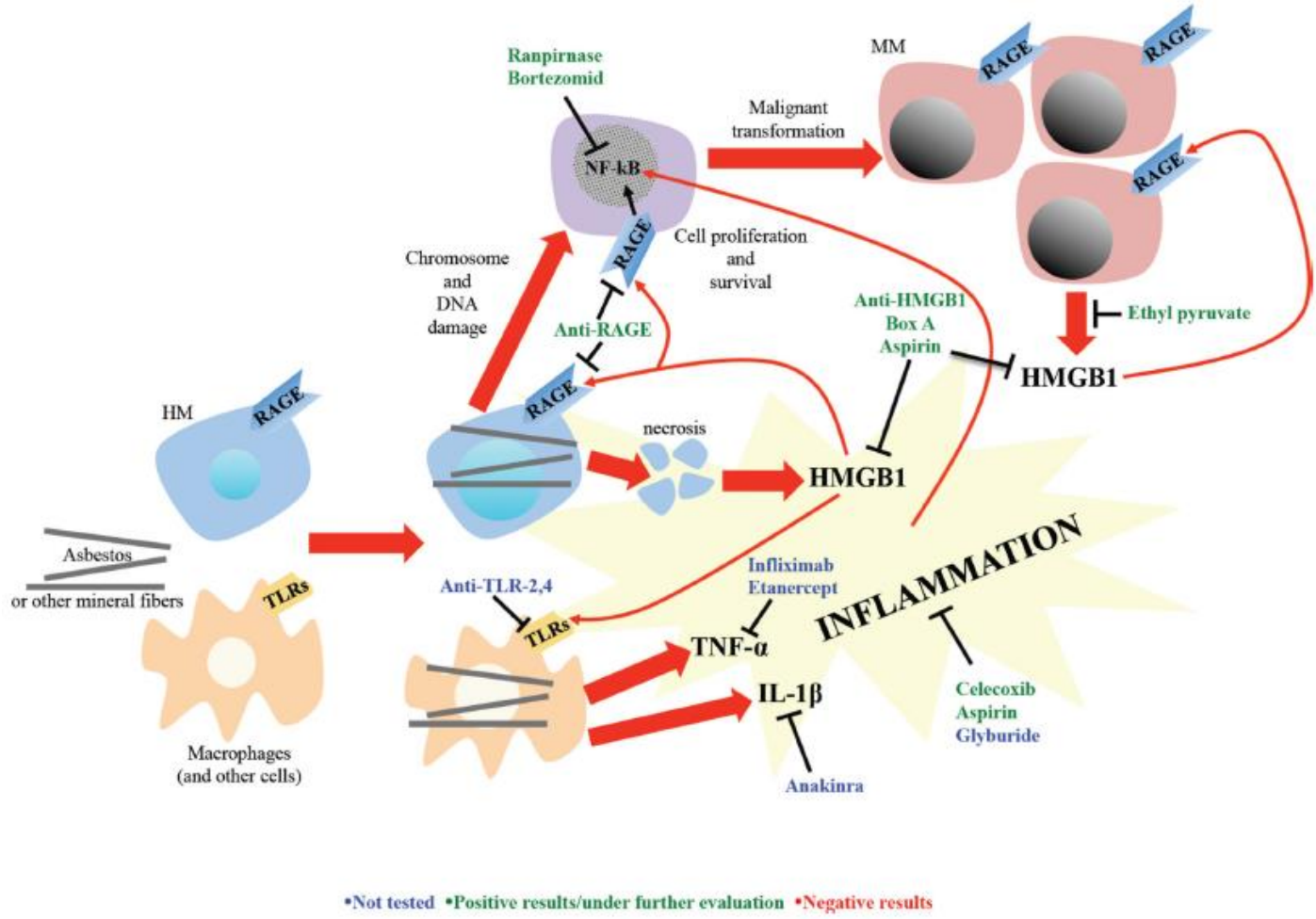

Figure 8. Targeting asbestos induce inflammation to prevent or treat mesothelioma. [10]

***In vivo* and *in vitro* cancer models for studying mesothelioma**

MM is resistant to the conventional forms of treatment, and adequate scientific and clinical assessment of this disease has been severely limited by the lack of representative cell lines and animal models and by the limited number of patients treated in a single institution. Thus, the establishment of representative in vitro cell lines and animal models is important for the development of potentially effective forms of diagnosis and therapy and for the study of basic biology.

***In vivo* cancer models**

Syngeneic tumor models

Syngeneic studies use immunocompetent wild type mice or rats, typically inbred strains, for engraftment of a tumor cell from the same strain (**Figure 9**). Allograft mouse tumor systems, otherwise known as syngeneic models, are tumor models whose genetic background is similar, if not identical, to the host animal.[206] Because

they retain complete immune systems, these models can be particularly appropriate for studies of interplay between the tumor and immunity, and for immunologically-based targeted therapies. Lack of rejection of the transplant by the host's immune system allows researchers to monitor the tissues for changes, such as growth or shrinkage, metastasis, and survival rate. Therapeutic interventions can be performed and the results are assessed to understand the treatment potentials. A mouse tumor growing in mice of the strain in which the tumor originated, offer several advantages [207] that includes:

a. Relatively low cost and high reproducibility.

b. Grow in immunocompetent hosts.

c. Wide variety of tumor types.

d. Generally non-immunogenic.

e. Long history of use and strong baseline of drug response data.

f. Hosts are readily available.

g. Studies are easily conducted with statistically meaningful numbers of mice per group.

Whereas, the main disadvantages of syngeneic tumor models are that the tumor cells are of rodent species, and therefore express the mouse/rat homologues of the desired molecular targets. Another limit is that the tumors tend to grow fast.

In spite of this, syngeneic models are proving to be an excellent model to test compound focusing on immuno-oncology targets for the treatment of cancer.

Syngeneic models and Immuno-oncology

The immune system has the greatest potential for the specific destruction of tumors with no toxicity to normal tissue and for long-term memory that can prevent cancer recurrence. The immuno-oncology research has provided solid evidence that tumors are recognized by the immune system and their development can be stopped or controlled in long term through a process known as immuno-surveillance. [208]

In many cancers, malignant progression is accompanied by profound immune suppression that interferes with an effective anti-tumor response and tumor elimination. Initially, most of the escape from immuno-surveillance was ascribed to changes in the tumor cells themselves (loss of tumor antigens, loss of human leukocyte antigen molecules, loss of sensitivity to complement, or T-cell or natural killer (NK) cell lysis), making them a poor target of an immune attack. However, it has become clear that the suppression comes from the ability of tumors to subvert normal immune regulation to their advantage. The tumor microenvironment can prevent the expansion of tumor antigen-specific helper and cytotoxic T-cells and instead promote the production of pro-inflammatory cytokines and other factors, leading to the accumulation of suppressive cell populations that inhibit instead of promote immunity.[209]

Studies of the tumor microenvironment are providing information about immuno-surveillance of tumors from early premalignant lesions to more advanced dysplastic lesions to cancer. At each step, tumor-derived

and immune system-derived components have a unique composition that will have distinct effects on immunotherapy. Because these premalignant microenvironments are less developed and immunosuppressant is less entrenched, it should be easier to modulate towards the elimination of abnormal cells.[209]

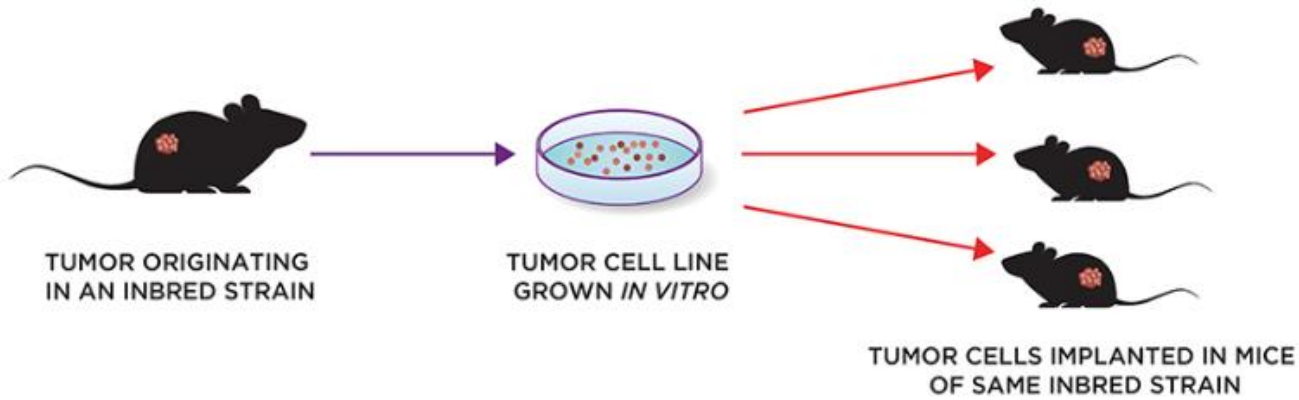

Figure 9: Syngeneic mouse model

Syngeneic model of mesothelioma

Malignant mesothelioma (MM) is an aggressive tumor of the serosal cavities which is associated with previous asbestos exposure and is generally found to be resistant to conventional forms of therapy. Adequate scientific and clinical assessment of this disease has been severely limited by the relatively low incidence of mesothelioma and the lack of representative cell lines and animal models. For this reason, as also in other cancer models, it is necessary to develop adequate in vitro and in vivo models of tumorigenesis and cancer. Previously, by Davis et al, 1991 were developed an asbestos-induced murine model of MM both as an in vivo-passaged malignancy and as in vitro-established cell lines. [210] Such a model system would be invaluable for use in the study of various cellular, molecular and genetic aspects of the disease, and for the pre-clinical evaluation of potential therapeutic agents. BALB/c and CBA mice were injected intraperitoneally with crocidolite asbestos. Months after exposure, 35% of the mice developed mesothelioma (5 BALB/c, 9 CBA), as determined by standard cytological and histological parameters. From these primary tumors, 12 continuously growing cell lines (5 BALB/c, 7 CBA) were established in culture. These cell lines have been confirmed as mesothelioma by cytological and ultrastructural (electron microscopy) analyses. They have been in culture for 7 to 24 months and all cell lines produced tumors when injected into syngeneic mice.

Xenograft cancer models

One of the most widely used models is the human tumor xenograft. Here, human tumor cells are transplanted, either under the skin or into the organ type in which the tumor originated, into

immunocompromised mice that do not reject human cells. For example, the xenograft will be readily accepted by athymic nude mice, severely compromised immuno-deficient (SCID) mice, or other immuno-compromised mice. [211] The development of human tumor xenograft models was a big step in moving toward more clinically relevant tumor models.[212, 213]

The advantages of using human tumor xenografts are:

I. Malignant cells are human.

II. Reproducibility of many of the models.

III. Long history and a strong baseline of drug response data.

IV. Readily available hosts.

V. Statistically valid numbers of mice can be used in studies.

VI. Availability of a wide variety of tumor lines.

Some disadvantages of using these models:

i. Syngeneic models are less costly to run.

ii. Stromal component of the tumors is rodent.

iii. Most of the tumor lines were developed using early technology.

iv. Tumors are regularly grown in a non-natural site (subcutaneous).

However, the major disadvantage is the lack of immune response inherent in these models. Because tumors can promote anti-tumor responses, such as tumor infiltrating lymphocytes, macrophages and myeloid-derived immuno-suppressor cells (MDSCs), these models may not accurately represent disease progression and therapeutic response observed in otherwise immune-competent individuals. [214, 215] As a result of these inherent weaknesses, alternative models have been utilized, emphasizing a need for improvements to current models.

Patient Derived Xenograft (PDX) models

Another option, in addition to traditional cell line-derived xenograft models, involves the direct transfer of tumor fragments from individual patients at the time of surgical resection into immunodeficient mice. Tumor graft models (otherwise referred to as patient-derived xenografts, PDX) are based on the transfer of primary tumors directly from the patient into an immuno-deficient mouse (**Figure 10**). [216] Models resulting from this approach utilize human tumor and recapitulate many tumor/ microenvironment interactions, retain important genetic features and heterogeneity, and often develop distant metastases.

Because PDX mice are derived from human tumors, they offer a tool for developing anticancer therapies and personalized medicine and can also be used to study metastasis and tumor genetic evolution. In spite of these advantages, several factors have contributed to hinder the use of PDX mice. The first is cost, tumor grafts can only be maintained in mice, and their passage requires a more specialized skill set than does the simple maintenance of cultured cell lines. Moreover, PDX models can suffer from long latency periods after

engraftment and variable engraftment rates. Tumor graft latency, measured as the time between implantation and the development of a progressively growing xenograft tumor, can range from 2 to 12 months. [217] Engraftment rates typically vary depending on the tumor type. Higher engraftment rates are associated with more clinically aggressive tumors.[218] Correlations between poor prognosis and engraftment rate were so marked that it has been suggested to be predictive of the disease course. Finally, there is the problem of broad availability and the number of PDX models that have been reported. Newer strategies to build orthotopic models include implanting human bone marrow–derived mesenchymal stem cells resulting in greater vascularity and maintenance of hormonal status.

Several classes of immunodeficient mice have been utilized as biologic platforms upon which to grow xenograft tumors. Athymic nude mice (T-cell deficient) have proven useful for the establishment of tumors both from patients' tumor samples and from established from human cancer cell lines. Reduced cost, widespread availability, and the absence of fur have offered investigators convenient access to these useful in vivo tumor model systems of human cancers. However, a relatively intact humoral immunity in nude mice likely results in reduced efficiency of tumor formation relative to mice with severe combined immunodeficiencies (SCID mice-lack functional T- and B-cells), particularly in cases of low cell inoculum.[279] Further still, NOD/SCID mice harboring additional deficiencies in natural killer cells (NOD/SCID Il2rg−/−) have permitted tumor establishment from even fewer numbers of tumor cells than previously seen in NOD/SCID and nude mice.[218, 220] Additional cell selection almost certainly occurs against xenografts in nude mice relative to SCID mice, further reducing tumor heterogeneity and the biologic complexity present in original human tumor. Nevertheless, both athymic nude and NOD/SCID mice continue to be used widely for molecular and translational studies of human cancers.

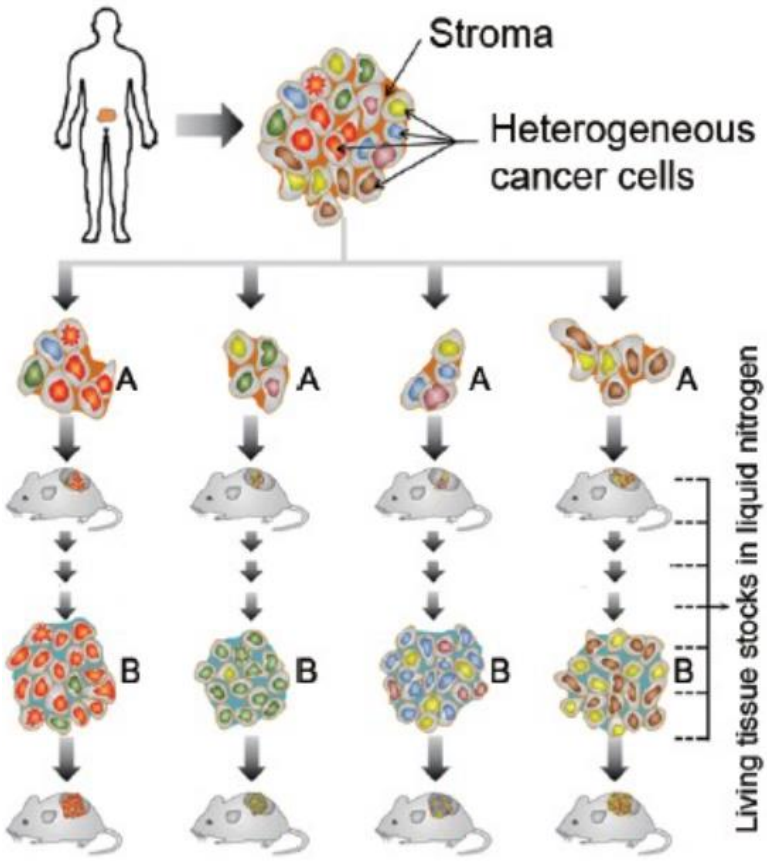

Figure 10: Diagram showing the development of Patient derived Xenograft model. [219]

In vitro cancer models

P**rimary tumor cell lines**

Multidrug resistant tumors relapse frequently despite different therapeutic strategies. After investment of billions of dollars for drug development and clinical trials every year due to lack of objective clinical response or toxicities, only few drugs have so far been approved by FDA for clinical use. [221,222] Though cancer therapeutics has undergone considerable development, we need a robust platform for pre-clinical testing so that efficacy identified in the pre-clinical studies can be translated to clinical trials and beyond. Preclinical studies with cancer cell lines have played an important role in our understanding of tumor biology and high throughput screening for drug development. However, accumulation of genetic aberrations of cancer cell lines that occurs with increasing passage numbers has limited their clinical correlation. [223, 224] Genetically altered cancer cell lines under in vitro condition do not truly represent clinical scenarios. [225] Moreover, there is a wide range of variability in patient response towards the same drugs used on tumors that are identical in their genetic aberration. Thus, it may be difficult to comprehend the genetic and epigenetic diversities of millions of patients from small number of cancer cell lines.[226, 227] These disparities in clinical responses and patient dependent tumor variability are the driving force behind personalized medicine and provide the

impetus to develop methods of generating and culturing primary tumor cells from patients that will enable effective bench to bed side translation. [228-230]

Isolation and culture of solid tumor cells under in vitro environment similar to the microenvironment of the original tumor is a challenge and requires specialized techniques.[231, 232] Successful isolation of tumor cells with suitable technologies is critically dependent upon an appropriate method to disrupt the extracellular matrix, which consists of a complex mixture of cohesive factors among constitutive proteins. [233, 234] Generally, these cohesive materials contain various compositions of connective tissues, glycoproteins, and tissue specific proteins. Additional cell culture complications include i) non-tumor cells contaminating the culture and disrupting tumor cell growth, ii) few viable cells due to resection from a necrotic area, and iii) normal stromal cells outcompeting sluggish cancer cells in long term-cultures. Cultured tumor cells need to be supplemented with various factors found in vivo. Essential supplements such as mitogenic and comitogenic growth factors are important to sustain cell viability, genotype and phenotype of the tumor cells in vitro. [233-235] Various pre-coated culture dishes are very effective at providing physiological environment for tumor cell growth by pursuing various biochemical studies.[236, 237] Technological advancements, sorting of tumor cells from heterogeneous mixtures, clonal propagation and validation of tumorgenicity have provided essential tools for primary tumor cell line development. In the era of personalized therapy, researchers need a repertoire of patient derived primary tumor cells that can generate high-fidelity data for translating in vitro findings to in vivo models and ultimately to clinical settings. This will provide more refined database compared to tissue bank.

In vitro 3D tumor spheroids

Conventional 2D cell cultures are not capable of mimicking the complexity and heterogeneity of clinical tumors as in vivo tumors grow in a three-dimensional (3D) conformation with a specific organization and architecture that a 2D monolayer cell culture cannot reproduce. Consequently, numerous signals that govern different cellular processes are lost when cells are grown in 2D plastic substrata. [238] Three-dimensional (3D) growth of immortalized established cell lines or primary cell cultures is regarded as a more stringent and representative model on which to perform in vitro drug screening. [239] As reported in detail by Kimlin et al, [240] 3D cell cultures possess several in vivo features of tumors such as cell-cell interaction, [241] hypoxia,[242] drug penetration, response and resistance,[242] and production/deposition of extracellular matrix. [240] All of these factors shift growth dependence away from the phenotype of unrestrained proliferation which is dominant in standard 2D cultures. Furthermore, the study of cancer cell dynamics in a 3D context allows us to recapitulate the architecture of living tissue and to better investigate the pathobiology of human cancers. [243, 244] It is now common opinion that in vitro 3D cultures could fill the gap between conventional 2D in vitro testing and animal models, [245] and many researchers

recommend the use of 3D cell cultures in drug screening programs as support for conventional 2D monolayer studies and before activating animal protocols. [246, 247]

Several types of 3D culture models have been developed. These are generally subdivided into liquid-based and scaffold-based 3D-models.[239] Scaffold platforms for 3D culture are made of synthetic or naturally-derived polymers that provide a support for cell growth and mimic extracellular matrix conditions. Currently available scaffolds often show difficulties in obtaining a controlled matrix that can support the cellular physiologic growth and interaction profile found in vivo. Tumor spheroids are one of the most common and versatile scaffold-free methods for 3D cell culture. Spheroids are either self-assembling or are forced to grow as cell clusters starting from single cell suspensions. Compared to cells cultured on a flat surface, they more closely mimic the complex scenario of tissues and organs where each cell interacts with nearby cells through the formation of desmosomes and dermal junctions. Depending on the researcher's needs and on the method used, it is possible to obtain spheroids of any dimension. In particular, large spheroids (starting from about 500 μ m in diameter) are characterized by an external proliferating zone, an internal quiescent zone caused by limited distribution of oxygen, nutrients and metabolites, and a necrotic core resembling the cellular heterogeneity of solid in vivo tumors.

Organoids

Costs of new anti-cancer drugs have surged over the past years due to, among others, the increasing complexity of clinical trials and regulatory requirements. [248] Meanwhile, the likelihood that a drug will reach market approval after entering phase 1 clinical testing has remained the same, and is significantly lower for anti-cancer drugs compared with drugs in other disease areas (**Figure 11**). [248]

While there are several factors that contribute to the low success rate from bench to bedside, one stands out: the translatability of pre-clinical cancer models to the patient. The difficulties of using model systems to predict drug efficacy in patients hamper not only general drug development pipelines, but also the advancement of companion diagnostics that can select subgroups of patients for treatment with molecularly targeted agents. 3D tumor organoid cultures are a novel pre-clinical model system in oncology that allows ex vivo propagation of tumors from individual patients and could facilitate the drug discovery process. Ex vivo culture of tumor cells from patients has been hampered in the past by low culture success and a limited proliferative capacity. The ability to perform long-term culture of primary colorectal cancer (CRC) cells came from the fundamental discovery that healthy mouse intestinal stem cells could be propagated in vitro long term using Wnt, R-spondin1, epidermal growth factor (EGF), and Noggin. [249, 250, 251] Healthy intestinal stem cells formed crypt-villus-like structures in Matrigel and were able to generate all cell lineages of the gut upon withdrawal of particular medium components. Importantly, these cultures retained their normal genome over time. Irrespective of its previous use to describe organogenesis experiments, the term ‘‘organoids’’ was used, mainly because of the crypt-like architecture in vitro, and the

distinct resemblance to the in vivo situation. [249, 250, 251] Matrigel and a cocktail of essential stem cell growth factors, which were used to culture healthy mouse intestinal tissue, supplemented with a transforming growth factor b receptor inhibitor (A83-01) and p38MAPK inhibitor (SB202190), served as the basis for growth medium of healthy human intestine/colon, and eventually also for CRC organoids.[251] Subsequently, similar culture protocols were developed for healthy and malignant tissue of the pancreas, stomach, prostate, and liver. The ability to culture patient-derived healthy and diseased cells was immediately recognized as a major breakthrough and holds potential for the transformation of biomedical research into more patient-focused approaches. Since the development of organoid culture protocols, several key papers have been published in which organoids have been used as a tool to broaden our basic understanding of cancer. [252, 253] These and subsequent studies help to determine whether organoid cultures have the potential to improve drug development and clinical practice.

Van de Wetering et al [254] were the first to describe a collection of well-characterized patient-derived organoids. They report the successful culture of 20 matched healthy and tumor organoids derived from treatment-naive surgical resections with a 90% success rate. [254] In summary, organoid cultures can be established from a range of different tumor types, which paves the way for more successful drug development and precision medicine.

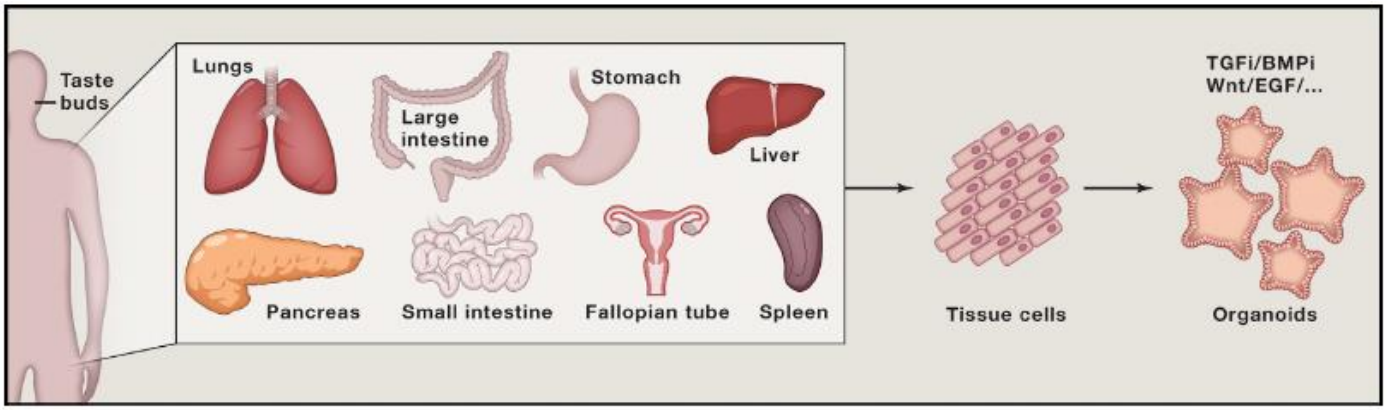

Figure 11: Schematic of the Various Regions of the Body that Can Be Cultured as Patient Derived Organoids.[249]

3. AIMS OF THE STUDY

Aim 1:

Patients with MPM have poor prognosis, with a median survival ranging from 8 to 12 months. The European Organization for Research and Treatment of Cancer has established that the main predictors of a negative prognosis. However, unlike other solid tumors, there are not yet specific tissue biomarkers with a prognostic significance useful in clinical practice.

High Mobility Group Box 1 (HMGB1) is a highly conserved nuclear protein, which has been implicated into several important biological processes and has an important role into tumor progression and prognosis of several cancers. Well-powered studies evaluating the prognostic significance of HMGB1 in tissue samples of MPM are, to the best of our knowledge, still lacking. In this work, we evaluate both protein expression and mRNA levels of HMGB1 by means of immunohistochemistry and RT-PCR from a large series of histologic samples of MPM, to investigate its potential role as a novel prognostic biomarker. We have also collected patients clinicopathological data from Oncology Unit of Novara Hospital in order to perform statistical analysis which assess the potential correlation between HMGB1 expression and clinicopathological patients' data.

Aim 2:

MM is resistant to the conventional forms of treatment, and adequate scientific and clinical assessment of this disease has been severely limited by the lack of representative cell lines and animal models and by the limited number of patients treated in a single institution. Thus, the establishment of representative in vitro cell lines and animal models is important for the development of potentially effective forms of diagnosis and therapy and for the study of basic biology.

So, in this study, we set up representative *in vitro* and *in vivo* models of mesothelioma as valid experimental study systems.

Aim 2a: We will use murine mesothelioma cell lines (AB1, AB12 and AB22) obtained by tumor masses which were developed into BALB/c mice induced by asbestos intraperitoneally injection and were previously showed to be tumorigenic and retain the mesothelioma features. To complete their characterization, we provide the elucidating of phenotypical and molecular features of AB cell lines and tumor masses derived thereof in BALB/c mice. Furthermore, we use these murine cell lines to set up a syngeneic model system of mesothelioma providing a full immunological tumor response and an experimental system for preclinical studies. However, this system limit us to better understand the spectrum of genetic, epigenetic changes and the role of tumor microenvironment in tumorigenesis of mesothelioma. Recently, xenografts and 3D in vitro systems using human tumor fragments/biopsy have become popular because they accurately recapitulate the features of original patient tumors and the complex factors that promote tumor progression and metastasis.

Aim 2b: In the present study, we will obtain primary mesothelioma cells; we will develop 3D in vitro models of mesothelioma in order to create a collection of patient-derived human organoids, to screen for drug sensitivity and to study the crosstalk between tumor and immune cells. Human Mesothelioma spheroids and patient derived xenograft (PDX) are alternative models that help us to pursue the same goal. More importantly, generation of these patient-derived 3D models can serve as a platform to test the role of BoxA (antagonist of HMGB1) in tumour shrinkage, providing highly translational results.

4. MATERIALS AND METHODS

MPM samples for clinical studies

In this study we used two different clusters of MPM tumor samples:

Firstly, we collected Formalin-Fixed Paraffin Embedded MPM samples from the Thoracic Unit and Pathological Anatomy of the University Hospital of Novara on which we performed the evaluation of HMGB1 protein and gene expression (Novara samples).

In the second case, 16 biopsies or tumor fragments were obtained from Thoracic Surgery Units of Novara Hospital, and San Raffaele Hospital and were collected for translational medicine studies. We used fresh patient-derived tumors in order to generate *in vitro* and *in vivo* mesothelioma models in accordance with protocols approved by the Institutional Review Board of each center and upon patients informed consent.

Samples collection and preparation

In this study we included biopsy samples from 170 patients with definite diagnosis of MPM admitted to the Hospital of Novara between April 2005 and December 2014. All the samples were collected by means of video-assisted thoracoscopy performed at the Thoracic Unit of Novara Hospital. The patients with adequate biopsy tissue and available clinical data were included. Moreover, for comparison, 8 biopsies of normal mesothelium sampled at the time of bullectomy in patients with pneumothorax, and 6 of reactive mesothelium (pleura samples from patients with pleuritis) were also considered for examination. Informed consent was obtained from all patients before surgery, and this investigation was approved by the Research Ethics Committee of 'Maggiore della Carità' Hospital of Novara. The assessment of the clinical records of each patient permit us to collect the following data:

Demographic data of the patient; MPM diagnosis date; surgery or biopsy date; therapy; status (Dead/Alive); follow up: from the date of diagnosis to April 2017 for alive patients, and from the date of diagnosis to the date of death for dead patients.

All the tumor samples were classified according to the WHO classification of pleural tumors,[255] clinically and pathologically staged based on the TNM staging system.[256] The patients' performance status (PS) at the time of diagnosis was graded using the Eastern Cooperative Oncology Group (ECOG) scale, and the patients with a PS of 0–2 underwent therapeutic protocols indicated by the referring oncologist. All tumour samples from MPM patients were collected before treatment.

Following the collection, tumor and control samples were immediately fixed in neutral buffered formalin for 24 h; once fixed tissue is processed using gentle agitation usually on a tissue processor at Pathologic Anatomy Unit, and embedded in paraffin. From each Formalin Fixed Paraffin-Embedded block we prepared H&E stained slides for histological evaluation and immunohistochemistry staining of diagnostic markers. The diagnosis of MPM was based on standard histologic and immunohistochemistry criteria, including positivity

to calretinin, vimentin, cytokeratin 5 and 6, Wilms Tumor 1 and negativity to carcinoembryonic antigen, thyroid transcription factor 1, and BerEP4.

Looking through the ARMONIA database of the Pathology Department of "Maggiore della Carità" Hospital we got these data:

• haematoxylin/eosin-stained slides of the pleural biopsies and corresponding formalin fixed, paraffin-embedded blocks for each patient case

- histotype: epithelioid, sarcomatoid and biphasic.
- the immunophenotyping of each sample for the routine diagnostic markers

Hematoxylin/eosin-stained slides of the pleural biopsies/tumor fragments of each case were reviewed by a pathologist (RB) in order to:

• confirm the diagnosis and the histotype;

• to select the area with 50% of tumour cells (minimum required for gene expression analysis);

• identify the best sample, in term of cellularity, in case we have more than one biopsy or surgery piece.

Immunohistochemistry

Immunohistochemistry analysis was performed in 170 FFPE MPM biopsies, using standard protocols. Each specimen was sliced with microtome in 3-μm-thick sections and placed on a microscope polarized slide. The sections were baked for 1 h at 65 °C and were deparaffinized with xylene and rehydrated using washes of graded ethanol to water. Antigen retrieval was performed in heated citrate buffer for 30 minutes at 650 Watt in microwave. HMGB1 immunostaining process was carried out on a DAKO Autostainer (Dako, Carpinteria, CA). The endogenous peroxidase activity of tissue sections was blocked by incubation with 3% H_2O_2 for 5 minutes. The incubation with primary antibody was performed for 60 minutes at room temperature, using a rabbit polyclonal HMGB1 antibody (diluted at 1:500, clone ab18256, Abcam, Cambridge, UK). Subsequently, the reaction was revealed with Envision Dual Rabbit/mouse detection system purchased by Dako (Carpinteria, CA). The slides were counterstained with hematoxylin. Normal liver parenchyma and reactive lymph nodes were selected as positive controls.

Evaluation of staining

The expression of HMGB1 in MPMs was scored using the semi-quantitative system derived from Soumaoro et al[257] for both the percentage of positive cells and the intensity of staining. The extent of staining was scored as 0 (<1%), 1 (1-25%), 2 (26%-50%), 3 (51%-74%), and 4 (≥75%), according to the percentage of the positive staining. Then we evaluated the intensity of the staining and grouped them into the following four categories: no staining (score = 0), weak staining detectable above background (score = 1), moderate staining (score = 2), and intense staining (score = 3). The final index was obtained by the sum of the intensity and percentage scores for each subgroup ranging from 0 to 7.

The localization of HMGB1 immunostaining was evaluated according to the system proposed by Koo e collaborators[258] for the evaluation of p16 immunohistochemistry expression. In particular, we considered the nuclear (N), the cytoplasmic staining (C) and the total staining (mean N+C) of the tumor cells, and then we applied the semi-quantitative scoring system described above. For the purpose of statistical evaluation, samples with a final staining score >3 were considered as high expression of HMGB1, whereas samples with a final score 0-3 were considered as low expression. Each sample was independently scored by two pathologists (RB, LB). If an inconsistency occurred, slides were reviewed jointly by two pathologists to reach a consensus.

HMGB1 expression analysis

RNA extraction and reverse transcription

The tumor area, previously selected by an expert pathologist, was manually macrodissected from FFPE tissue blocks, and 5-μm-thick sections were collected in a 1,5mL tube for the RNA extraction process. After deparaffinization with xylene, RNA was isolated by using the RecoverAll Total Nucleic Acid Isolation Kit (Life Technologies, USA) following the manufacturer instructions, and resuspended in 30 µl of elution buffer. RNA yields were checked by mean of a Nanodrop.

A total of 100 ng of mRNA per sample were reverse transcribed to cDNA by TaKaRa PrimeScript™ RT reagent Kit (Takara Bio, USA) using 200 pmol of random examers for each reaction.

Quantitative Real-time PCR

Quantitative real-time polymerase chain reaction (qRT-PCR) was performed in triplicate with 2 **µl** of cDNA, 1x TaqMan® Gene Expression Master Mix and 1x of TaqMan® Gene Expression assay HMGB1, ID: Hs01037385_s1 (Applied Biosystems, USA) in a final reaction volume of 10 µl.

Samples were amplified by the ABI 7500 real-time PCR machine (Applied Biosystems, USA) under the following thermal profile: initial incubation at 95°C for 20 seconds, 40 cycles of denaturation at 95°C for 15 seconds followed by annealing and extension at 60 °C for 30 seconds. Assay results were normalized to rRNA Eucaryotic 18S rRNA Endogenous Control (Life Technologies, USA) and gene expression quantification was performed by $\Delta\Delta C_t$ method[31] using the Sequence Detection System 7500 (Applied Biosystems; software v2.0.4), comparing tumor samples with a pool of normal pleura obtained from pneumothorax samples.

Statistical analysis

Patients characteristics were described in terms of number and percentage, median and range. Disease-specific survival (DSS) was defined as the time from diagnosis to death or until April 2017, date of last follow-up for alive patients. Survival analyses were undertaken using the Kaplan-Meier method and curves were compared by the log-rank test. The association between IHC staining score or mRNA levels and the clinicopathologic characteristics of the patients was analyzed respectively by chi-square test. The correlation

between *HMGB1* gene expression and HMGB1 protein expression by IHC was analyzed by Pearson test. All the statistical analysis were performed using STATA 11 (Stata Corp LLC, Texas, USA) and software Prism (GraphPad, version 7.03, La Jolla, CA). The level of significance was set at P=0.05.

Cell lines, culture conditions and manipulations. Murine malignant mesothelioma (MM) AB1, AB12 and AB22 cells were obtained from Cell Bank Australia, and their establishment and partially characterization were performed by Davis MR et al. These cell lines were obtained following this experimental protocol: intraperitoneal injections of about 2,5 mg of crocidolite asbestos suspended in 500 µl RPMI in female Balb/c mice were performed for generation of tumor masses. When ascites became evident, animals were killed. Samples of ascites and solid tumors were used for cytological/histological examination, and remaining ascites were processed for culturing primary murine cells. These lines have been shown to be mesothelial in origin, to be tumorigenic in syngeneic mice and to have many features in parallel with human MM cell lines.

The AB cell lines are cultured in RPMI 1640 (Life Technologies) supplemented with 5% (AB1 and AB12) or 10% (AB22) v/v fetal bovine serum (Life Technologies), 2 mM L-glutamine and 100 U/ml penicillin/streptomycin. We injected intraperitoneally each cell line in BALB/c mice to obtain tumors. The masses were explanted and mechanically disaggregated; the obtaining cells were cultured as above. The established cells were named AB1-B/c, AB12-B/c and AB22-B/c.

MM cells were infected with a 3rd generation lentiviral vector expressing the luciferase gene (pLenti PGK V5-LUC Neo (w623-2) Addgene) (**Figure 12**). The selection of cells with geneticin were performed and maintained in culture as above. The murine luciferase-expressing cells, derived directly from the original strains AB1, AB12, and AB12 were named respectively: AB1-LUC, AB12-LUC and AB22-LUC. Cells generated from the masses in BALB/c mice were named AB1-B/c-LUC, AB12-B/c-LUC and AB22-B/c-LUC. (**Figure 12)**

Mice. Animal experiments have been revised and approved by the Animal Care and Use Committees (IACUC) of both Ospedale S. Raffaele and Istituto di Ricerche Farmacologiche “Mario Negri”. All experiments were done in conformity with the approved guidelines.

The Animal Care Facilities of the Institutes, which meet international standards, were used for animal housing. In both institutions, certified veterinarians monitor and supervise the animal welfare and health, the experimental protocols and revised regularly the procedures.

***In* vivo BioLuminescence optical Imaging (BLI)**

We injected intraperitoneally 7 x 104 AB1-B/c-LUC cells on mice and monitored tumour growth using an IVIS SpectrumCT System (Perkin Elmer).The system is equipped with a low noise, back-thinned, back-illuminated CCD camera cooled at -90 C (quantum efficiency in the visible range above 85%). The mices received intraperitoneally injections of 6 g of luciferin/kg body weight about 20 minutes before image

acquisition. During image acquisition, the animals were kept at 37 °C and under gaseous anesthesia (2–3% isoflurane and 1 lt/min O_2). After luciferin injection, dynamic BLI was performed from 0 to 30 minutes by acquiring an image every 2 minutes (exposure time = auto, binning = 8, f = 1 and a field of view equal to 13 cm (field C)) in order to detect the highest BLI signal. BLI image analysis was performed by measuring the total light flux (photons/seconds) in a Region of Interest (ROI) placed over the animal abdomen. Images were acquired and analyzed using Living Image 4.4 (Perkin Elmer).

Ultrasound scans

First we anesthetized the mices by gaseous isoflurane. We use a Vevo 2100 equipment (FUJIFILM VisualSonics Inc.) especially designed for the examination throught ultrasound of small experimental animals to examine the tumor masses. Ultrasound images in B-mode (Brightness mode) were performed using a Vevo 2100 linear array transducer with a center frequency of 40 MHz (MicroScan MS 550D; 22–55 MHz; FUJIFILM VisualSonics Inc).

Clear field microscopy

The Cell lines maintained in culture (AB1, AB12 and AB22) in cell dishes were visualized with a Zeiss Observer Z1 microscope.

Electron microscopy

Cells were grown on coverslips and previously prepared to be mounted on a Leica Ultracut UCT ultramicrotome. Ultrathin (70-90nm) sections were collected on copper grids and stained with uranyl acetate and Sato's lead citrate before imaging with a ZEISS Leo AB 912 Omega transmission microscope. Images were acquired by a 2k x 2k bottom-mounted slowscan Proscan camera controlled by the EsivisionPro 3.2 software.

Histopathology and Immunohistochemistry

The samples that will be processed for histopathological examination were fixed in formalin at 10% for at least 24-48 hours and paraffin embedded (Embedding Center Leica EG1160). 4-µm-sections were routinely stained with Hematoxylin-Eosin (HE) and evaluated under a light microscope (Leica DM 2500). The images were captured with a digital camera (Leica DFC310 FX). For immunohistochemistry 4-µm serial sections from each sample were immunostained with the primary antibody anti-CD31, specific for endothelial cells to monitor the vascularization into the tumor masses. After the incubation with appropriate biotinylated secondary antibody (goat antirabbit VC-BA-1000-MM15 or rabbit anti-goat VC-BA-5000-MM15, Vector Laboratories, USA) will occur. Sections were labelled by the avidin-biotin-peroxidase (ABC) procedure using the VECTASTAIN® Elite ABC-Peroxidase Kit Standard, VC-PK-6100-KI01 kit (Vector Laboratories). The immunoreaction was visualized with 3,3'-diaminobenzidine (Peroxidase DAB Substrate Kit, VC-SK-4100-KI01, Vector Laboratories) substrate and sections were counterstained with Mayer's haematoxylin.

Generation of primary human mesothelioma cells. MPM tumor specimen (sample ID: MN11) was obtained by means of extrapleural pneumectomy at Unit of Thoracic Surgery, Novara Hospital. The tumor fragments

were manipulated in a sterile, ventilated hood according to primary cell establishment protocol.[24] One fragment of original tumor sample was processed for Hematoxylin and eosin stain and Immunohistochemistry in order to obtain a definitive diagnosis and histologic classification at Pathologic Anatomy Unit; whereas another fragment was stored in culture medium at 4°C for a few hours (2-5 hours after resection) for further *in vitro* manipulation. The tumor specimens were placed into a cell culture plate to be processed into a sterile, ventilated hood. Additional non-tumor tissue may be removed at this time and sections of tumor were excised. Tumor specimen was cut into small pieces using sterile sharp bladdes and curved forceps until we obtained 1–2 mm^3 tumor fragments. Then, the fragments were mashed through a 100 µm *cell strainer* with the plunger of a syringe, taking care to thoroughly rinse the strainer with culture medium to minimize cell loss. The cell suspension was collected into 50 ml- sterile falcon, and the further cell disaggregation is stimulated by pipetting cell suspension up and down different times using a 10 ml pipette. The disaggregated cells of 'MN11' were cultured in RPMI-1640 medium supplemented with 10% fetal bovine serum and 1 × penicillin/Streptomycin (Gibco BRL Life Technologies), hydrocortisone 400 µg/l, 20 mM HEPES, and 10–5 M 2-mercaptoethanol (10 micromolar, 0.35 microliter in 500 ml). The cells were incubated at 37°C in 5% CO_2 with a balance of air at 37°C. After 5-6 days, the medium was replaced to remove nonadherent cells; thereafter the medium was replaced twice weekly and cells were passaged when they reached confluency in a monolayer (21 days after). The established cell line was subcultured for over 50 passages, approximately more than one year from initial culturing. The cell cultures were routinely checked for mycoplasma using detection kit, and resulted mycoplasma-free.

Furthermore, we collected MN11 cell pellets, fixed in formalin and embedded in agar/paraffin; and cut specimens slides. The H&E and IHC characterization was performed comparing their immunophenotype with the original tumor.

***In vitro* tumor-sphere formation.** The primary mesothelioma cells 'MN11', previously established, and maintained in culture in culture dish were harvested using trypsin 1x. The resulting pellet were therefore washed with PBS and resuspended in tumorsphere medium. The cell suspension was mixed vigorously, to have an homogeneous cell-suspension and were counted into the Bukner chamber. Afterwards, the cells were seeded in petri dish (non-adherent conditions) at about 10^4 cells/mL of medium. The culture was incubated to 37 °C, 5% CO2 for one week. At the 4°day post-seeding we can observe the generation of nonadherent spheres into a phase-contrast microscope. The medium is not changed or added until the detection of tumorspheres, so as to not disturb them.

Generation of Patient Derived Xenograft from mesothelioma biopsies

13 resected biopsies/tumor fragments of Malignant Pleural mesothelioma were collected after extrapleural pneuctomeny at the Unit of Thoracic Surgery at Hospital of Novara for the period 2014-2015. Fragments for each tumor samples was processed for the standards pathologic evaluation in order to obtain a definitive diagnosis. The samples were frozen in 10% DMSO/90% FCS and stored at -135 °C for future use. These

stocks should maintain their capacity to grow both in vitro and in vivo. The human MPM samples from surgical specimens should be acquired under the strict supervision of staff pathologist(s) to maintain patient care and to ensure adequate tissue diagnosis. The MPM specimens were used for performing direct xenograft establishment into Immunodeficient mice NSG (NOD/SCID Il2rg − / −). Immunodeficient mice NSG aged 6 to 8 weeks should be housed under specific pathogen-free conditions to prevent sickness and infectious outbreak. Tumor fragments (0.7-1.0 cm) were implanted subcutaneously, in the flank of mouse, in a heterotopic site that permit us to monitor accurately and measure the tumor size. The tumor implantation will be performed as described into the protocol. [279] After tumor implantation, mice should be monitored daily for signs of illness and surgical wounds assessed for infection. To maintain and expand tumor derived from a specific xenograft 'line', we routinely propagate heterotopic tumors.
Direct transfer of human tumours into immunodeficient mice requires institutional review board as well as Institutional Animal Care and Use Committee (IACUC) approval and must be conducted in accordance with institutional and national regulations.

Generation of Mesothelioma Organoids

MPM biopsies were processed for organoid generation into very clean conditions following the protocol (**Figure 13**) below based on the protocol previously developed by Drost et al: [280]

Tumour samples (biopsy or tumour fragments) are kept moist in the 150 cm^2 petri dish by the addition of small quantities of medium or HBSS (250-500 µl). Try to add enough medium to keep the tumor moist, but not so much that it floats- with too much medium, the tumor can slide around when you are trying to cut it.

The tumor is diced /minced using scalpels and disposable blades into small pieces (1-5 mm^3). The small tissue fragments were collected and mashed into a cell strainer of 100 µm or 70 µm; the cell strainer was rinsed different times with PBS and culture medium. We use this type of cell strainer in order to separate the cell aggregate from the fibrotic material. Monitor the cell suspension and cell aggregates every 20 minutes during the mechanical disaggregation, by observing a drop of cell suspension on a sterile plate by microscope. After the mechanical disaggregation process, the cell suspension was centrifuged at 2000 rpm for 3 minutes. Hemolysis can be performed if lots of red blood cells are visible in the cellular pellet by incubating the pellet in hemolysis solution. The supernatant was aspirated and the pellet were resuspended in 10 ml of adDMEM/F12 +/+/+ 1% FBS. Then the tube was centrifuged at 1500 rpm for 3-5 min. The cell pellet was washed once in medium and antibiotics. For culturing organoids, we always use Costar 24-well ultra-low attachment bottom plate (Corning 3473) and Matrigel (Corning® Matrigel® Growth Factor Reduced (GFR) Basement Membrane Matrix, Phenol Red-Free, 10mL (Product #356231)). Matrigel is stored at -20°C as frozen 1-mL aliquots. When needed, we thawed Matrigel aliquots at 4°C usually overnight (it takes 4-5 hours to melt completely). Once thawed, store Matrigel at 4°C. During this

procedure, we work in sterile conditions, under the hood and we transport the Matrigel bottle with an ice box, because it will be further used for cell embedding. We put the tube (15 ml Falcon Tube) with the cellular pellet, which were previously collected and isolated from patient biopsy, in the ice box to avoid solidification of Matrigel in the tube before plating.

After washing/filtering, cells must be embedded in Matrigel. The cell density is an important factor: Highly dense cells tend to suffer, but also a very low number of cells do not support efficient organoid growth according to our experience. Unfortunately, counting is impossible because in the precipitate you will always have single cells, clumps and/or bigger structures. So, we tried to plate the same amount of cells per well.

We use 200 µl of matrigel to enclose organoids and plates them into one well of a 24 well plate, paying attention not to accumulate cells on the border of the well because our bright images will be compromised by the shadow of the wall of the well. On average, one mesothelioma biopsy will yield 1-2 well of a 24-well culture plate. Work quickly and on ice (4°C conditions) to ensure that the Matrigel does not solidify before plating. To ensure efficient plating, do not dilute the Matrigel too much. The average final percentage of matrigel should be ~75%. The culture plate with just-seeded cell aggregates enclosed in matrigel were placed in the incubator (5% CO2, at 37 °C) for 30 min – 1h to allow the solidification of the Matrigel.

The Organoids culture medium was prewarmed in a 37 °C water bath for ~10 min before adding it to the organoids. After the solidification of Matrigel, at about 500-800 ul of Medium per well was added on top of the Matrigel, for each well. Avoid pipetting the medium directly on Matrigel as this might damage the cushion/layer of Matrigel. Instead, place the tip on the wall of the well and slowly deposit the medium. The plate was placed into the CO2 incubator (5% CO2, 37 °C).

We refresh the medium with 10 µM Y-27632 dihydrochloride every 2–3 days. From 7 d after initial plating, medium without Y-27632 dihydrochloride should be used. When removing the exhausted culture medium, we should pay attention to Matrigel: if Matrigel is a compact gel, we just have to aspirate and add new medium slowly; otherwise we should be very careful not to aspirate the floating pieces of Matrigel containing potentially precious organoids. We monitor the organoid growth daily and acquire photo by inverted microscope every 2 days post-seeding. Usually, it takes 2-3 weeks for organoids to reach good sizes and to be passaged. In any case, every 3 weeks Matrigel should be changed as it started to collapse or dissolve. Depending on the original tissue material, the first passage of organoid- seeding could be critical for the purification of Organoids from the cellular debris and contamination with fibroblasts.

Passaging of organoids

If we need to split organoids for subculture/expand them or to recover/collect organoids for RNA extraction, fixation/inclusion for histology, immunoprecipitation, etc, an adequate method for harvesting them should be chosen. In our experience, we used Harvesting solution of Trevigen Culturex and followed the manufacturer protocol, described as follow:

1. Gently remove 250-300 µl of Organoids culture medium from each well without disturbing the matrigel. Add 1ml of cold HBSS and collect organoids (~16-21 d after starting the culture) by scraping the matrigel and pipetting up and down using cold 1000µl tips. Transfer organoids from the same sample into one 15-ml tube.
2. 2- Pipette up and down 15-20 times and add 5-7 ml of ice-cold HBSS by topping up to 12-13 ml of final volume.
3. Incubate in 4 °C for 1 h in order to dissolve any residual matrigel.
4. Centrifuge the tube at 1500 rpm for 5 min at 4 °C.
5. Aspirate and discard the supernatant.
6. Add cold-ice HBSS.
7. Dissociate the organoids mechanically by pipetting up and down with P1000 cold tips for at least 10 times.
8. Repeat once the washing passage.
9. Remove the supernatant without disturbing the pellet and resuspend the pellet in matrigel; replate the matrigel and cell suspension in 2-4 wells. Resuspend the pellet in 400- 800 µl of Matrigel and place 200 µl of Matrigel into one well of a 24-well plate, thus splitting each organoid culture at a 1:2 – 1:4 ratio (the variability of ratio splitting is due to the quantity of organoids obtained and growth after day 0 of plating).
10. Place the plate into the CO2 incubator (5% CO2, 37 °C) for 15 min to allow the Matrigel to solidify.
11. Gently pipette 500 µl of prewarmed (37 °C) organoid culture medium into each well and place into a CO2 incubator (5% CO2, 37 °C).
12. Replace the medium every 2–3 d. It is not necessary to add Y-27632 dihydrochloride to the medium at this stage of the culture. Y-27632 dihydrochloride is only required in the culture medium when organoids have been recently passaged using enzymatic dissociation like treatment with trypsine or tryple.

Collection of Formalin-fixed and embedding of tumour organoids in agar/paraffin for IHC

1. Gently remove 250-300 µl of Organoids culture medium from each well without disturbing the matrigel. Add 1ml of cold HBSS and collect organoids (~16-21 d after starting the culture) by scraping the matrigel and pipetting up and down using cold 1000µl tips. Transfer organoids from the same sample into one 15-ml tube.

2. Pipette up and down 15-20 times and add 5-7 ml of ice-cold HBSS by topping up to 12-13 ml of final volume.

3. Incubate in 4 °C for 1 h in order to dissolve any residual matrigel.

4. Centrifuge the tube at 1500 rpm for 5 min at 4 °C.

5. Aspirate and discard the supernatant.

6. Add cold-ice HBSS.

7. Repeat once the washing passage.

8. Remove the supernatant and add 6-7 ml of formalin. Resuspend the pellet in formalin. Incubate for 90 minutes at room temperature.

9. Centrifuge the tube at 2000 rpm for 5 minutes and wash once with PBS.

10. Remove the supernatant and add 10 ml of 80% ethanol with eosin. The eosin (red dye) is added in order to allow the detection of pellet during the embedding process and when cutting the blocks. Resuspend the pellet in ethanol and store at 4 °C indefinitely but we prefer to embed them in paraffin within a month.

11. Prepare the agar solution for embedding process. The 3 % agarose solution in PBS is prepared and kept warm in microwave.

12. Then, centrifuge the tube at 2000 rpm for 10 minutes. Remove the supernatant. We add 200-300 µl of warm agarose solution and gently flick the bottom of the tube to resuspend the organoids fully in agarose solution. The tube is vigorously tapped on the bench surface to bring all the material to the bottom. We can centrifuge rapidly for 1-2 minutes at 2000 rpm in order to collect all the solution to the bottom of the tube.

13. Incubate the tube for 15-20 minutes at -20°C to harden. The pellet is removed and placed in an IHC cassette. The cassettes are then placed in 80% ethanol overnight.

14. The Unit of Pathology of Novara Hospital do the regular processing of pellets and their embedding process in paraffin.

15. We cut 3- µm slices for processing in immunohistochemistry for mesothelioma markers staining and 5 µm slices for hematoxylin and eosin staining.

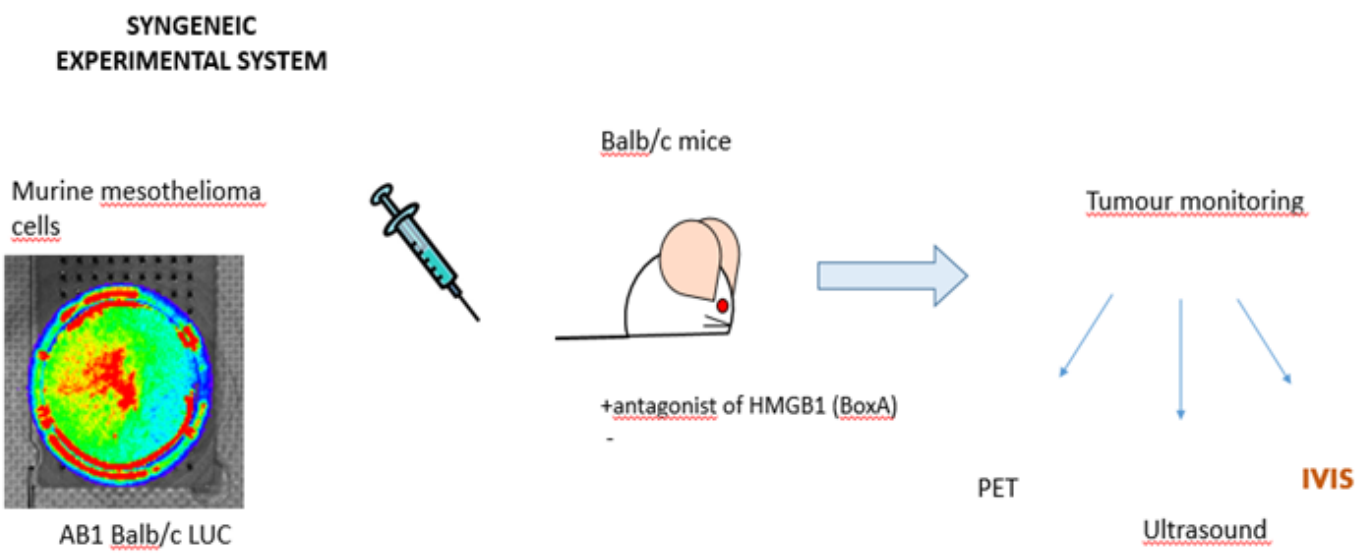

Figure 12: Generation of a syngeneic experimental system of mesothelioma.

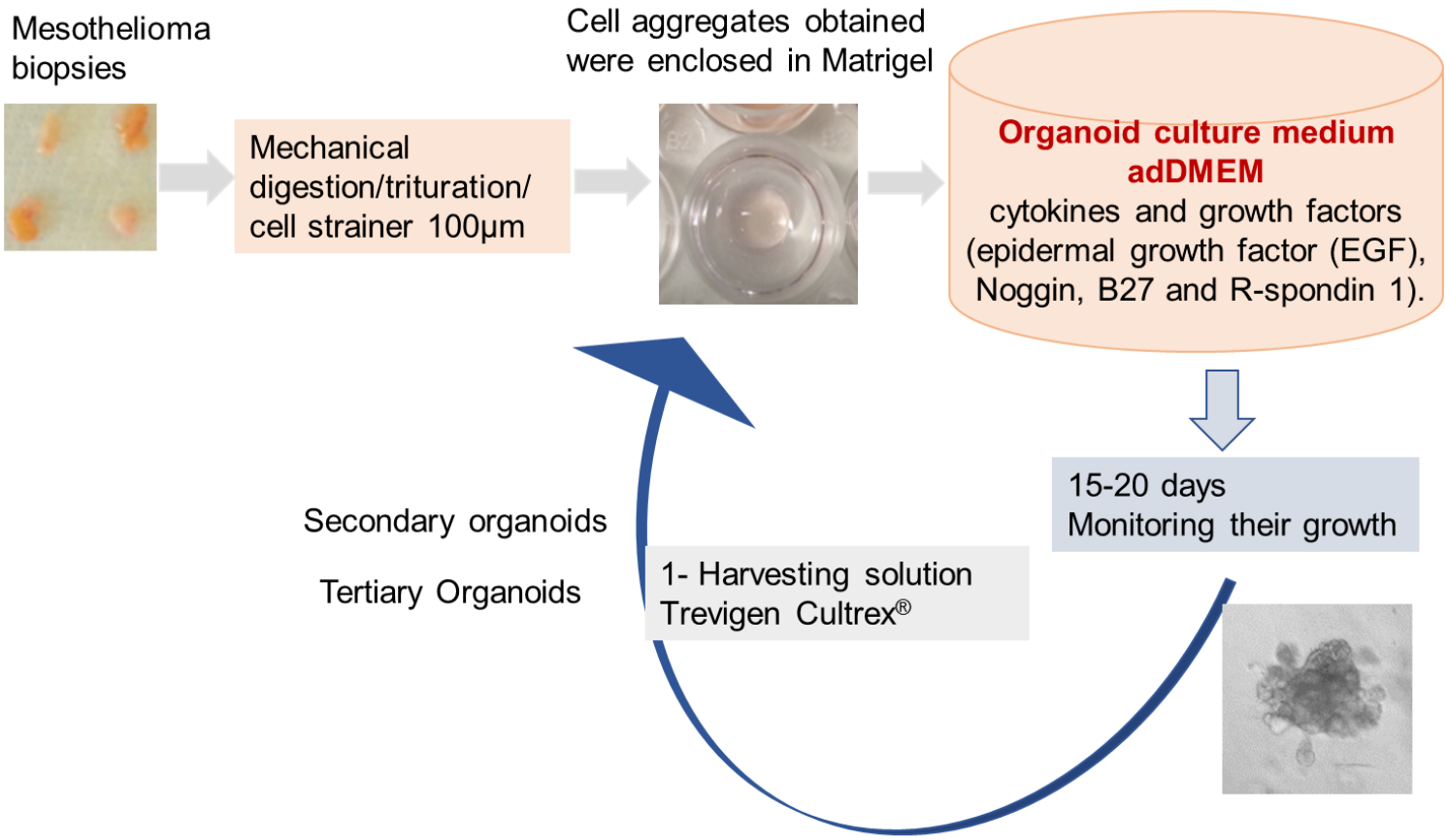

Figure 13: Representation of the protocol for Patient derived organoids generation.[200]

5. RESULTS

Patients and clinicopathologic findings

The main demographic and clinicopathologic findings of the patients included in the study are summarized in Table 3: 118 patients were male (69,4%) and patients' mean age at diagnosis was 68,5 ± 10 years (range 27 - 91, median 70). Follow-up data after surgery were obtained from all the patients. At the end of the study, 6 patients (3,53%) were alive with a median follow-up of 56 months (range 27-94 months). The mean DSS of the cohort was 16 months (range 1-94 months).

Table 3. Clinical and pathologic findings

Characteristic	Total (%)
Total number	170
Age (mean)	
<68	68 (40%)
≥68	102 (60%)
Gender	
male	118 (69.4%)
female	52 (30.6%)
Asbestos Exposure	
no	80 (47.1%)
yes	86 (50.6%)
not available data	4 (2.4%)
Histologic Subtypes	
Epithelioid	125 (73.53%)
Biphasic	23 (13.53%)
Sarcomatoid	22 (12.94%)
ECOG score	
0-2	146 (85.9%)
>2	23 (13.53%)
not available	1 (0.57%)
Clinical Stage	
I-II	104 (61.2%)
III-IV	66 (38.8%)
Treatment type	
None	40 (23.5%)
Platinum	25 (14.7%)
Platinum + Pemetrexed	105 (61.8%)
Smoking status	
Smoker	86 (50.6%)
Non Smoker	65 (38.22 %)
not available data	19 (11.18%)

%, percentage; ECOG, Eastern Cooperative Oncology Group; NA, not available data.

HMGB1 protein expression by immunohistochemistry

HMGB1 immunostaining was found in 158 cases (93%) of MPM. In all the positive samples there were tumor cells stained in the nucleus or in the cytoplasm only, mixed with tumor cells stained in both nuclei and cytoplasms (**Figure 14**). Conversely, HMGB1 immunostaining was found in the nuclei of the normal pleura (Fig. 9 *A*), and in both nuclei and cytoplasms in mesothelial cells of the reactive pleura (Fig. 9 *B*). The score of HMGB1 immunostaining in the cytoplasm of tumor cells was low in 88 cases (51,76%) (Fig. 9 C, D), and high in 82 (48,24%) (Fig. 9 E, H). The score of nuclear staining was low in 43 cases (25,29%) (Fig. 9 C, D), and high in 127 (74,71%) (Fig. 9 E, F, G, H), whereas the total HMGB1 score, was low in 69 cases (40,59%) (Fig. 9 C, D) and high in 101 (59,41%) (Fig. 9 E, F, G, H).

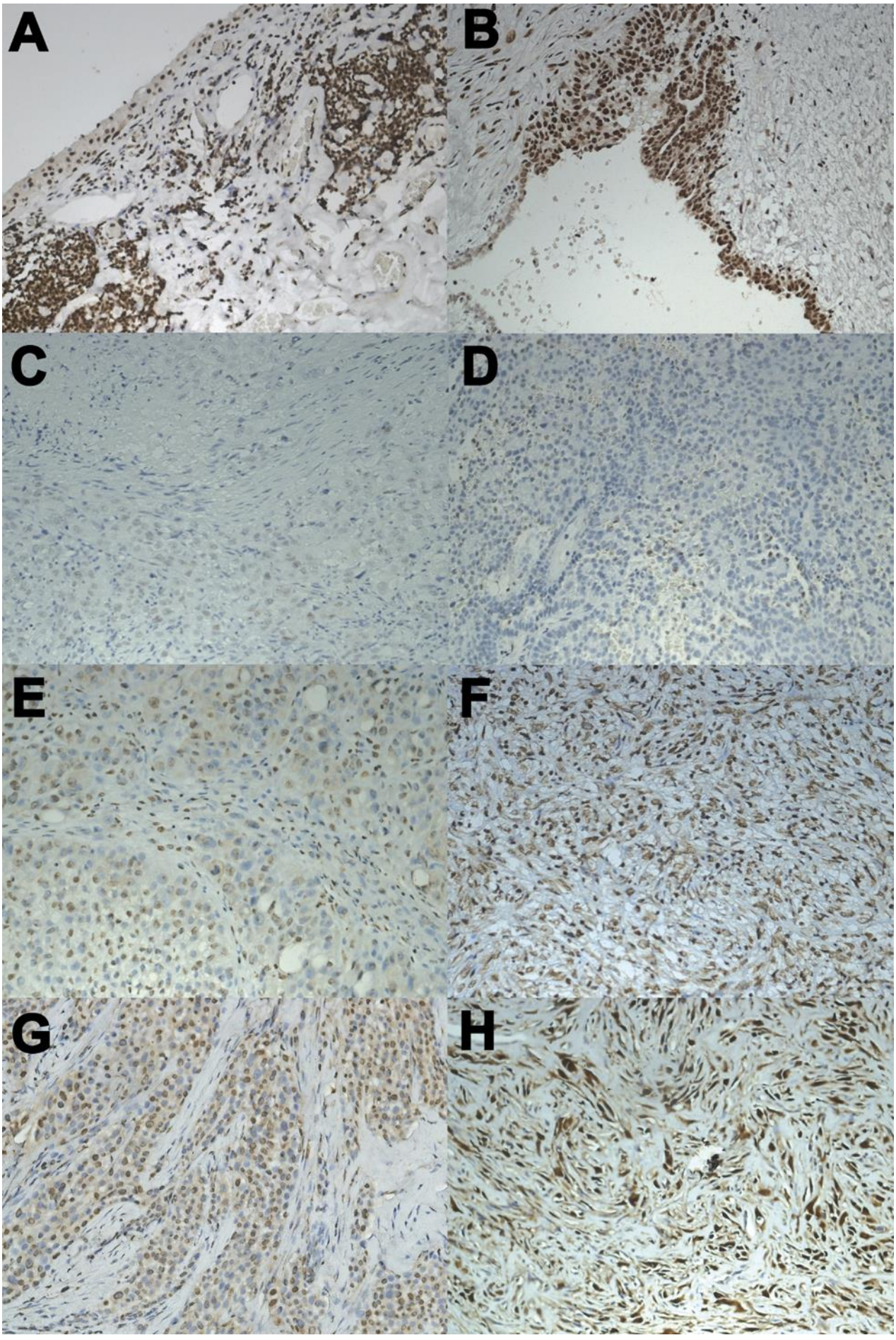
A
B
C
D
E
F
G
H

Figure 14. Representative IHC staining for HMGB1 in normal pleura (A), reactive pleura (B) and MPM samples (C, D, E, F, G, H) (original magnification 200X).[286]

Correlation between HMGB1 score by immunohistochemistry and clinicopathologic variables

The correlation between nuclear, cytoplasmic and total score of HMGB1 expression and clinicopathologic variables of MPM was examined by chi-square test. As shown in Table 2, nuclear HMGB1 expression was significantly correlated with asbestos exposure (P= 0,0001), whereas cytoplasmic HMGB1 expression showed a significant correlation only with DSS (P= 0,0295). Interestingly, total HMGB1 expression was significantly correlated with gender (P < 0,0001), tumor clinical stage (P = 0,0049), ECOG score (P = 0,0342), and DSS (P = 0,0036) (Table 4). No significant correlation between total HMGB1 expression and age, asbestos exposure, other previous malignancies, smoking status, histologic subtype and treatment was found.

Correlation between *HMGB1* gene expression and clinicopathologic variables

The *HMGB1* gene expression analysis was successfully achieved in 110 cases (67,4%); tumor tissue was exhausted in the remaining cases due to the use for standard diagnostic and immunohistochemistry procedures. The median of the relative expression level of the *HMGB1* gene (RQ value= 1,7) was used as cut off value to discriminate the patients into high-expression (RQ ≥1,7; score= 1; 55 patients; 32,35%) and low-expression groups (RQ<1,7; score= 0; 55 patients, 32,35%). Furthermore, the correlation between the gene expression levels of HMGB1 and the clinicopathologic variables of patients was investigated. As shown in Table 4, high expression levels of *HMGB1* were positively correlated with ECOG score, and treatment.

Table 4. Correlation between clinicopathologic variables and expression of HMGB1

Characteristic	HMGB1 expression					
	Total HMGB1, low	Total HMGB1, high	p value	low RQ (<1,7)	high RQ (≥1,7)	p value
Age						
<68	32	36	0,16	22	23	0,8462
≥68	37	65		33	32	
Gender						
male	102	68	<0,0001	38	37	0,8378
female	137	33		17	18	
Histologic Subtypes						
Epithelioid	47	78	0,186	43	41	0,6535
Non epithelioid	22	23		12	14	
ECOG score						
0-2	65	81	0,0342	72	42	0,0489
>2	4	19		8	13	
NA	0	1		0	1	
Clinical Stage						
I-II	51	53	0,0049	32	32	>0,999
III-IV	18	48		23	23	
Treatment type						
Untreated	15	25	0,6492	12	18	0,0016
Treated	54	76		89	37	
Smoking status						
Smoker	36	50	0,6764	27	31	0,1662
Non Smoker	24	41		26	17	
NA	9	10		2	7	
DSS						
DSS (<16)	34	72	0,0036	36	38	0,6844
DSS (≥16)	35	29		19	17	

HMGB1, High-Mobility Group Box-1; Total HMGB1, Total IHC score of HMGB1 staining; Low/High RQ, low/high HMGB1 gene expression evaluated by RT-PCR; ECOG, Eastern Cooperative Oncology Group; NA, Not available data; DSS, Disease-specific survival.

Correlation between HMGB1 score by immunohistochemistry and DSS

We investigated the relationship between the total score of HMGB1 and the DSS by means of Kaplan-Meier analysis. Patients with high total score had significantly worse DSS than patients with low total score (P = 0,0011) (Fig. 15 A). Then, we analyzed the relationship between the cytoplasmic HMGB1 score and DSS: patients with high score had worse DSS than patients with low HMGB1 score (P = 0,0462) (Fig. 15 B). Conversely, the expression levels of nuclear HMGB1 score did not show any statistically significant correlation with DSS (P = 0,5167) (Fig. 15 C). Moreover, we investigated the prognostic value of HMGB1 expression in clinicopathologic subgroups of patients with MPM, divided by age (≤68 versus >68), clinical stage (I-II versus III-IV), previous history of other malignancies (not versus yes), histologic subtype (epithelioid versus non-epithelioid), ECOG score (0-2 versus >2), and treatment (untreated versus treated with chemotherapy). High levels of total score of HMGB1 expression was correlated with worse DSS in the subgroups of patients treated by chemotherapy (*P* = 0,0097) (Fig. 15 *D*) and untreated (*P* = 0,0006) (Fig. 15 *E*), in the subgroups of patients with epithelioid (*P* = 0,0039) (Fig. 15*F*) and non-epithelioid subtypes (*P* = 0,0035) (Fig. 15 *G*), in patients older than 68 years (*P* = 0,0014) (data not shown), and in patients with no previous history of other malignancies (*P* = 0,0008).

Interestingly, high levels of cytoplasmic HMGB1 expression were associated with worse DSS in untreated patients (*P* = 0,0167) (data not shown) and in the subgroup of patients with non-epithelioid (*P* = 0,0058) mesothelioma, whereas nuclear score of HMGB1 did not show any correlation with DSS in any of the subgroups analyzed. The correlation between *HMGB1* gene expression and DSS was also investigated. The Kaplan-Meier survival curves generated for the low-expression and high-expression groups of patients indicated that there was no significant difference (*P* = 0,77) in terms of DSS between the 2 groups (Fig. 15 *H*).

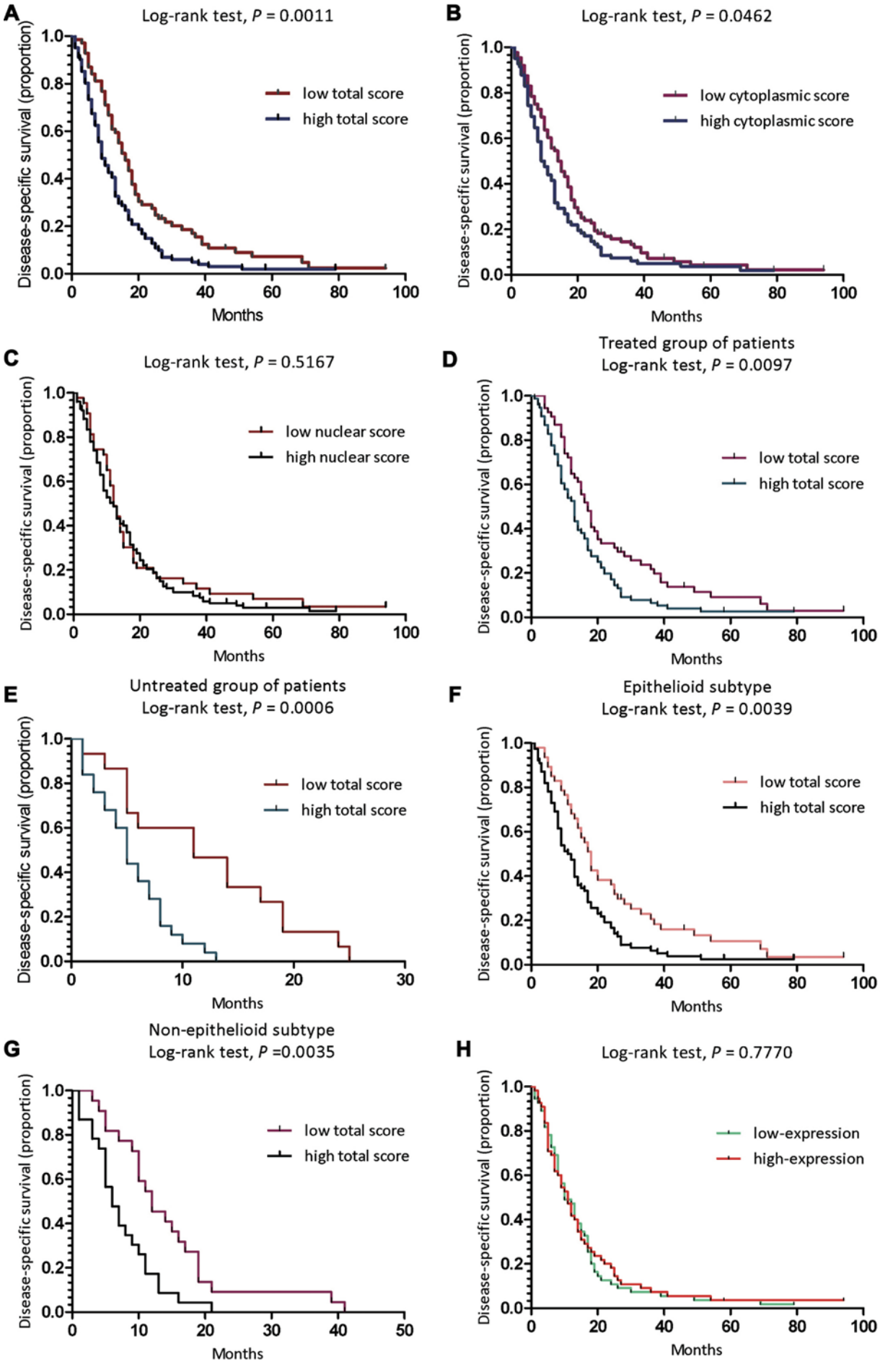
A
Log-rank test, P = 0.0011
low total score
high total score
B
Log-rank test, P = 0.0462
low cytoplasmic score
high cytoplasmic score
C
Log-rank test, P = 0.5167
low nuclear score
high nuclear score
D
Treated group of patients
Log-rank test, P = 0.0097
low total score
high total score
E
Untreated group of patients
Log-rank test, P = 0.0006
low total score
high total score
F
Epithelioid subtype
Log-rank test, P = 0.0039
low total score
high total score
G
Non-epithelioid subtype
Log-rank test, P =0.0035
low total score
high total score
H
Log-rank test, P = 0.7770
low-expression
high-expression
Disease-specific survival (proportion)
Months

Figure 15. Kaplan-Meier curves of Disease-Specific survival (DSS) for MPM patients. Patients with high total score had significantly worse DSS than patients with low total score (P = 0,0011) (A); patients with high cytoplasmic score had worse DSS than patients with low cytoplasmic score (P = 0,0462) (B), whereas the expression analysis of nuclear score did not show any statistically significant correlation with DSS (P = 0,5167) (C). Patients with high total score of HMGB1 had a significant worse DSS in the subgroups of patients treated with chemotherapy (P = 0,0097) (D) and untreated (P = 0,0006) (E) with epithelioid subtype (P = 0,0039) (F) and non-epithelioid subtypes (P = 0,0035) (G). In patients evaluated for HMGB1 gene expression, no differences in terms of DSS were identified in low-expression versus high-expression groups (P = 0,718) (H). [286]

Correlation between *HMGB1* gene expression and HMGB1 scoring by immunohistochemistry

Finally, we analyzed the statistical correlation between the *HMGB1* gene expression and IHC scoring into the cohort of 110 MPM cases, by means of Pearson test, which correlates the log fold-change values for mRNA and IHC score. No statistically significant correlation was found between the *HMGB1* gene expression and IHC scoring, evaluated in terms of total score (Fig. 16 *C*), nuclear score (Fig. 16 *B*), cytoplasmic score (Fig. 16 *A*), percentage of nuclear positivity (Fig. 16 *D*), intensity of nuclear positivity (Fig. 16 *F*), percentage of cytoplasmic positivity (Fig. 16 *E*) and intensity of cytoplasmic positivity (Fig. 16 *G*).

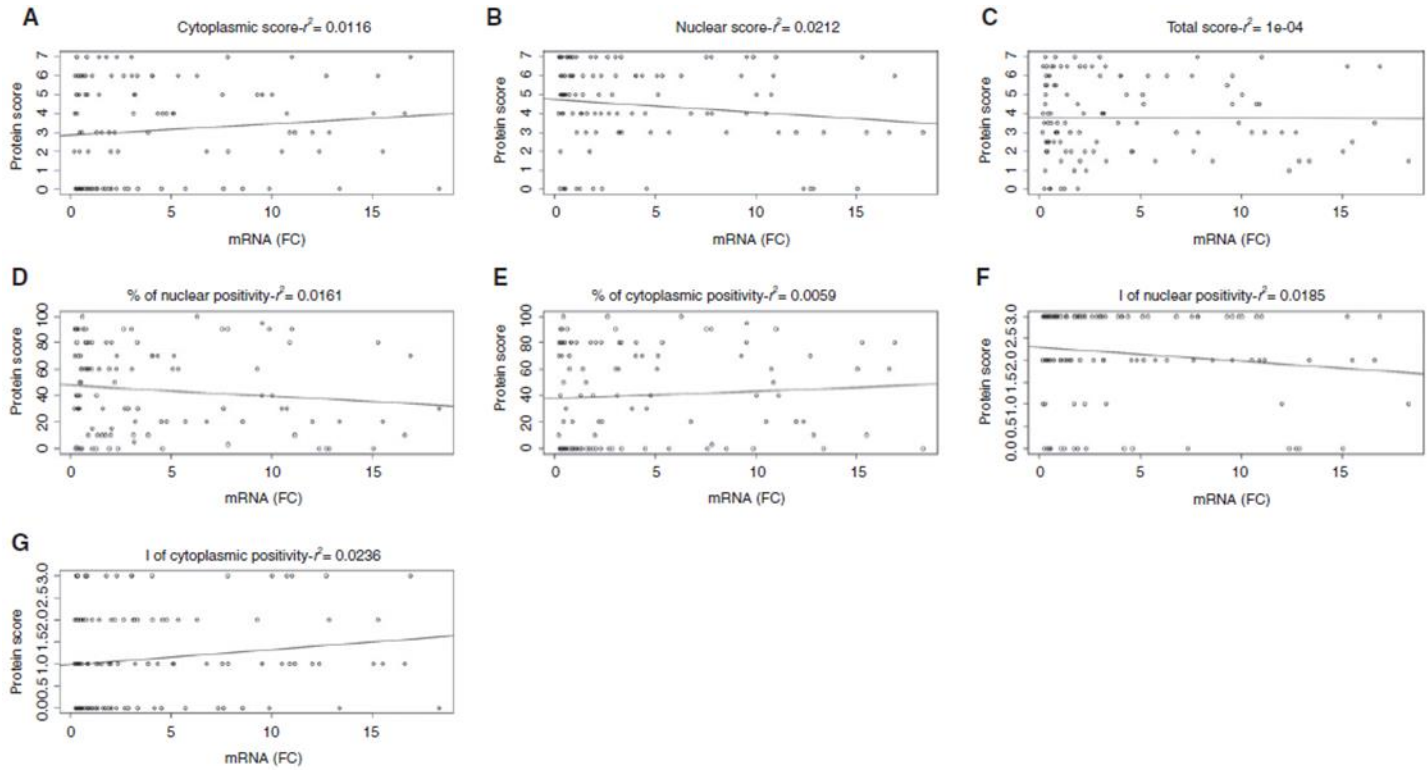

Figure 16. Pearson correlation between HMGB1 expression gene and IHC score. No statistically significant correlation was found between gene expression and IHC score, evaluated in terms of cytoplasmic score (A), nuclear score (B), total score (C), percentage of nuclear positivity (D), intensity of nuclear positivity (F), percentage of cytoplasmic positivity (E) and intensity of cytoplasmic positivity (G). [286]

Univariate and multivariate analysis

The variables putatively associated with Disease-specific survival were individually analyzed with a univariate Cox proportional hazards regression model (Table 5). Significant variables in the univariate analysis were added to a multivariate model. As shown in Table 5, clinical stage (I-II versus III-IV), histologic subtype (epithelioid versus non-epithelioid), treatment type (treated versus untreated) and interestingly, total HMGB1 score continued as significant prognostic factors.

Table 5. Univariate and multivariate analysis of Disease-Specific Survival.

Factor	Disease-Specific Survival	
	HR (95% CI)	P
Univariate analysis		
Age, mean (<68 versus ≥68)	1,02 (1,004-1,037)	0,016*
Histologic subtype (epithelioid versus non-epithelioid)	1,82 (1,28-2,59)	0,00068*
ECOG score (0-2 versus >2)	6,42 (3,85-10,69)	0,000*
Clinical Stage (I-II versus III-IV)	5,12 (3,63-7,23)	0,000*
Treatment type (treated versus untreated)	0,34 (0,234-0,496)	0,000*
HMGB1 gene expression (low versus high)	0,94 (0,65-1,38)	0,766
HMGB1 Total IHC score (low versus high)	1,69 (1,23-2,32)	0,001*
HMGB1 Cytoplasmic IHC score (low versus high)	1,37 (1,01-1,86)	0,044*
HMGB1 Nuclear IHC Score (low versus high)	1,124 (0,787-1,604)	0,519
Multivariate analysis		
Age (<68 versus ≥68)	0,97 (0,703-1,343)	0,864
Histological subtype (epithelioid versus non-epithelioid)	1,91 (1,3-2,79)	0,0009*
Clinical Stage (I-II versus III-IV)	5,42 (3,68-7,984)	0,000*
Treatment type (treated versus untreated)	0,42 (0,275-0,63)	0,00003*
HMGB1 Total IHC score (low versus high)	2,262 (1,384-3,697)	0,0011*
HMGB1 Cytoplasmic IHC score (low versus high)	0,806 (0,504-1,287)	0,366

Abbreviations: ECOG, Eastern Cooperative Oncology Group; CI, confidence interval; HR, hazard ratio; *, significant variable.

Murine mesothelioma cell lines and generation of a syngeneic system.

Characterization of murine MM cell lines.

The MM murine cell line (AB1, AB12 and AB22) were obtained from the tumor masses generated by the intraperitoneal injection of BALB/c mice with asbestos fibers and we cultured them in vitro.[14] We observed the aspect of AB1, AB12 and AB22 in microscope and detected that they have similar phenotypes to the sarcomatoid, biphasic and epithelioid cells of human mesothelioma, respectively (Figure 17a-f).

The detection of microvilli on the surface of such cells by electron microscopy (Figure 17 g-i), indicate similarities with the electron micrograph of cultured MM cells with a microvillous-rich surface; an important feature of mesothelial cells[23].

The original cell lines were re-injected into the peritoneum of BALB/c mice and the tumor masses explanted from the mice were used for isolating cell lines named AB1-B/c; AB12-B/c; AB22-B/c. Next, the cell lines were infected with a lentiviral vector in order to constitutively express the luciferase gene and were named AB1-LUC; AB12-LUC; AB22-LUC. Subsequently, the murine cell lines underwent both manipulations sequentially and were named AB1-B/c-LUC; AB12-B/c-LUC; AB22-B/c-LUC. The manipulated cell lines displayed the same features of the original strains. Therefore, they were interchangeably used in the experiments.

It has been revealed that HMGB1 is very important for MM pathogenesis and development [10,11]. Thus, we sought to determine by immunostaining the expression of HMGB1 in the murine MM cell lines and into the tumors derived from them. Interestingly, we found that HMGB1 is localized in the nucleus, but also in the cytoplasm, as expected if the protein is actively secreted (Fig. 18 a–c). In agreement with this, ELISA assays detect 20–30 fold higher levels of secreted HMGB1 in the culture medium of murine MM cells compared to that of primary mesothelial cells (Table 6). In addition, we found that HMGB1 chemoattracts all AB cell lines and promotes invasion of AB1- and AB12-B/c-LUC cells, but not of AB22-B/c-LUC cells (Fig. 19 a, b). Hence, murine MM cell lines recapitulate the features of human MM cell lines, including their response to HMGB1, supporting their migration and invasion.

Characterization of tumor masses generated by murine MM cell lines.

IP injection of murine AB cells, whether manipulated (Luciferase-expressing cells) or not, in BALB/c mice generated sizable tumour masses in approximately 2–3 weeks after injection. The tumor growth at its early stages of development (0–12 days) was followed by the increase in BLI signal only detected by IVIS. At these stages tumor masses and, for instance, lymph nodes have similar sizes and ultrasound (US) scans cannot tell them apart. However, the differences between strong vs weak BLI signals of larger tumor masses can be clarified by the parallel use of US scans with the detection of bioluminescence (IVIS) coupling BLI with US scans. The combination of the two techniques allows the evaluation of important parameters: the size and the location of masses, and reveal their relationship with other organs of the abdomen (Fig. 20). In

particular, time-wise increases of the bioluminescence signal allow following the growth of masses and assign a rough abdominal location. Strong vs. weak IVIS signals can be due to the location of tumors in the abdomen (superficial vs. deep) or to their size (large vs. small). Such quandaries can be clarified by the use of ultrasound scans that yield more precise measurements of tumor size, pinpoint their spatial location and reveal their relationship with other organs of the abdominal cavity.

Another important feature of tumour development is the neo-angiogenesis and its ability to support tumour invasiveness and growth. Figure 21.a,b shows hematoxylin-eosin staining of explanted and paraformaldehyde-fixed tumors obtained from AB1 cells. Although vascularization can be clearly observed only at the periphery of the masses, and their inner portions do not show identifiable vessels, there was no evidence of necrosis. It was shown that indeed small ectopic vases are present inside the masses (Figure 21), providing a sufficient vascularization to support tumour growth and prevent necrosis. Immunostaining with anti-CD31 antibody (which recognizes endothelial cells) showed that indeed a meshwork of capillaries is present inside the masses (Fig. 21), providing sufficient vascularization to support tumor growth. In the figure 8b we can observe the vascularization into a human MM samples stained with CD-31. The results indicate that AB cells establish aggressive tumors that display similarity of vascularization to human MM.

The H&E stain of explanted masses showed morphologic similarities with human MPM samples. Thus, murine MM cell lines accurately recapitulate the morphologic features of human MM cell lines.

Histopathological characterization of tumor masses generated by murine MM cell lines.

We report the first IHC characterization of AB murine MM lines and tumors, since none was performed either on the original asbestos-generated lesions or on the AB cell lines derived from them.

Explanted AB-derived sarcomatoid, biphasic and epithelioid tumors bear morphological similarities with samples of human biopsies of the same histological subtype (Fig. 22).

The murine MM cells and the corresponding tumors generated by them were immunostained by a panel of antibodies routinely used for the diagnosis of human malignant mesothelioma. The IHC analysis revealed that only vimentin yielded a positive signal on all cells and tumors, whereas only few AB1 cells were positive for wide spectrum cytokeratin (WSCK) and AB22 cells were positive for Wilm's Tumor antigen (WT1). Both AB cells and tumors were positive for other epithelial markers, such as E-cadherin and βcatenin, and also yielded a signal for smooth muscle actin (SMA) (Fig. 23; Table 7), whereas WSCK was expressed only in rare cells within all tumors. Interestingly, cytopellets of cultured cells and tumors derived from the same cell line display discrepancies in the expression of surface markers, as previously reported for human MM cell lines and tumors. IHC characterization of MM is still ambiguous: a high variability of diagnostic markers has been observed due to reasons pertaining to the cells or to their manipulations. Moreover, little consensus has been reached on which and how many markers should be considerate for a positive identification. These

data are the first IHC characterization of these murine MM cell lines and tumors generated from them. These results collectively indicate that murine MM tumors express a variable set of histological markers.

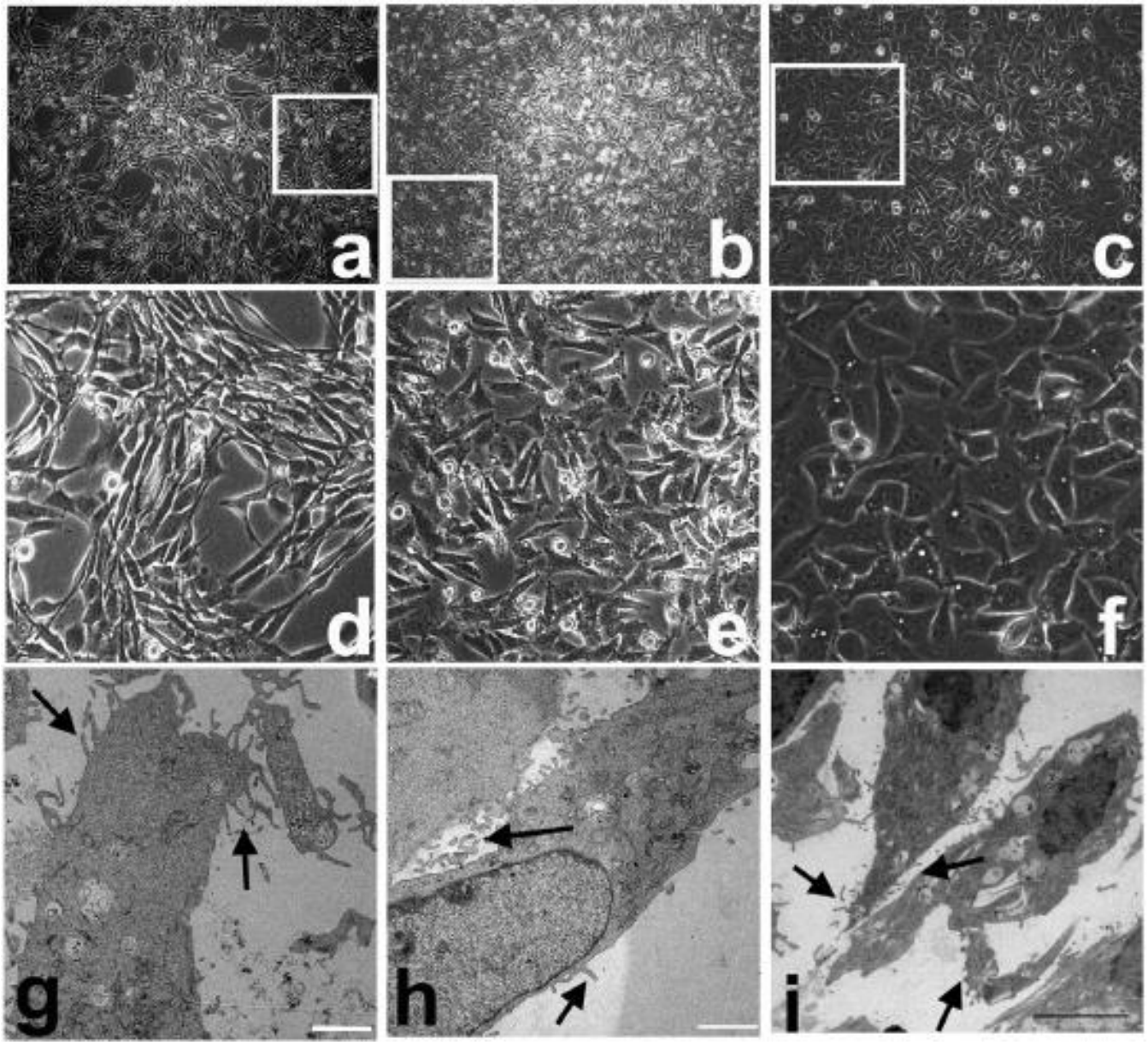

Figure 17. Morphology of murine MM cell lines. Cultured AB1, AB12 and AB22 cells, showing morphological features corresponding to sarcomatoid (AB1; (a,d)), biphasic (AB12; (b,e)) and stellate/epithelioid (AB22; (c,f)) phenotypes. Boxed areas in a, b and c are enlarged in (d–f), respectively, to better appreciate cell morphology. Transmission electron microscopy reveals the presence of microvilli (g–i), a hallmark of mesothelial cells; Bars in g and h = 2 µm; bar in i = 4 µm. [287]

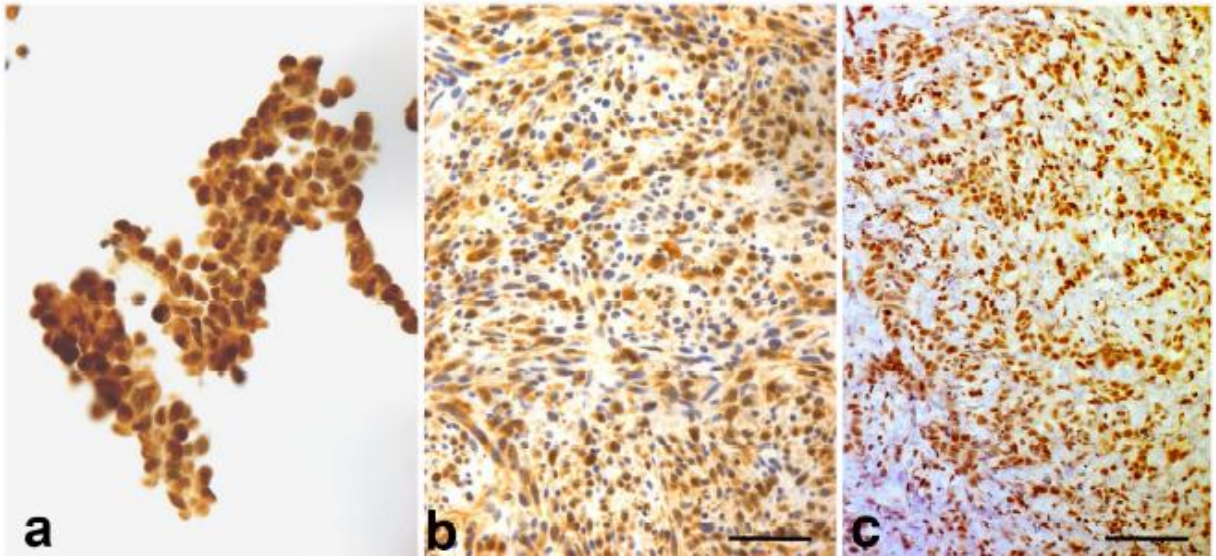

Figure 18. Murine MM cells and tumors show both nuclear and cytoplasmic localization of HMGB1. Nuclear and cytoplasmic localization of HMGB1 in cultured cells and tumor tissues. A polyclonal anti-HMGB1 antibody was used to immunostain (a) a cytopellet of cultured AB1-B/c-LUC cells, (b) a section of a tumor derived from them and (c) a section of a human MM. Bars = 100 µm. [287]

PMC	AB1	AB1-B/c-LUC	AB12	AB12-B/c-LUC	AB22	AB22-B/c-LUC
0.08	1.5	1.5	2.6	2.2	2.2	1.3

Table 6. HMGB1 is secreted by murine primary mesothelial and AB cells. HMGB1 secreted over 16 hours was measured in the culture medium by ELISA. Values are expressed as ng of HMGB1 secreted by 106 cells. PMC: Primary Mesothelial Cells.

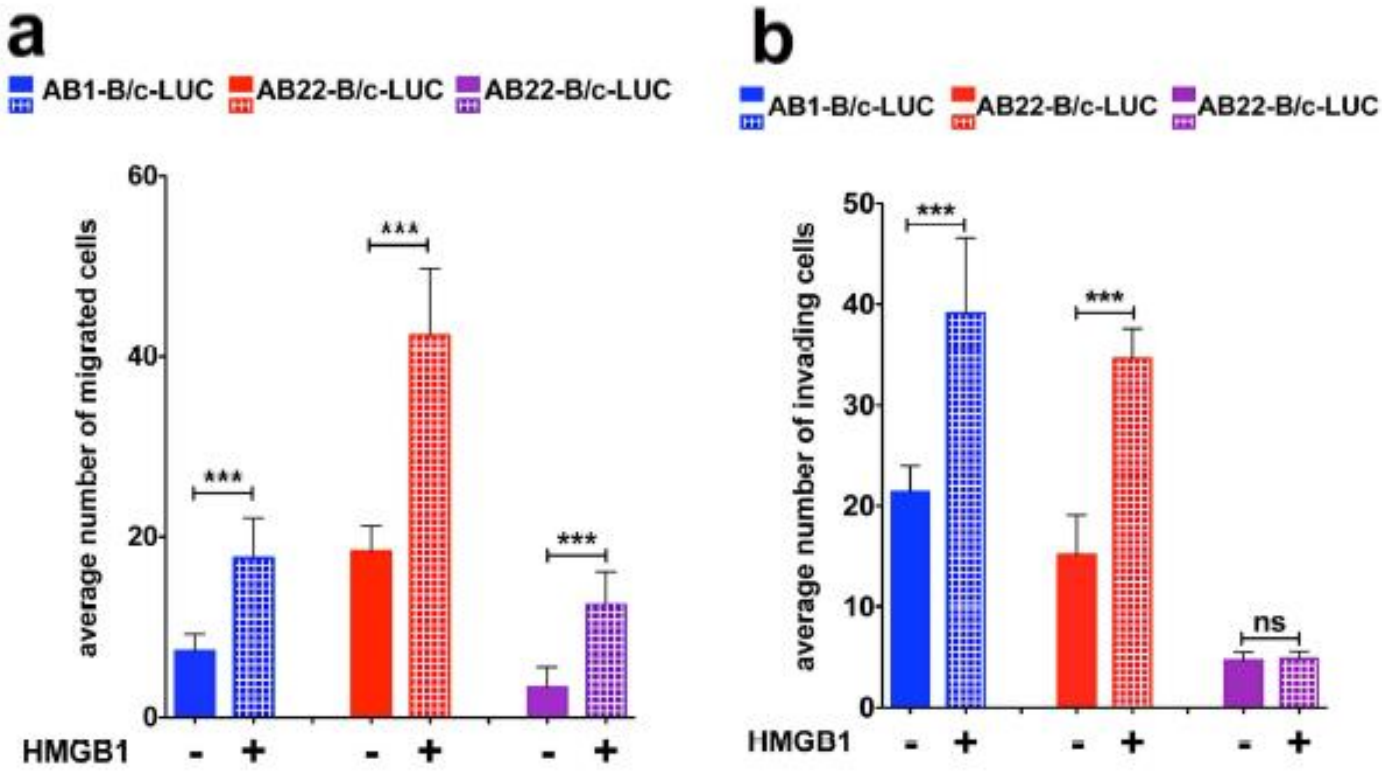

Figure 19. AB cells respond to extracellular HMGB1. (a) HMGB1 (30 ng/ml) acts as a chemoattractant for AB cell lines in Boyden chamber assays. The bars represent standard deviation (n = 3). (b) HMGB1 (30 ng/ml) increases the invasive potential of AB1-B/c-LUC and AB12-B/c-LUC cells, but not of AB22-B/c-LUC cells, in Boyden chamber invasion assays. The bars represent standard deviation (n = 3); $p < 0.0001$ (***). All experiments were repeated at least twice with similar results. [287]

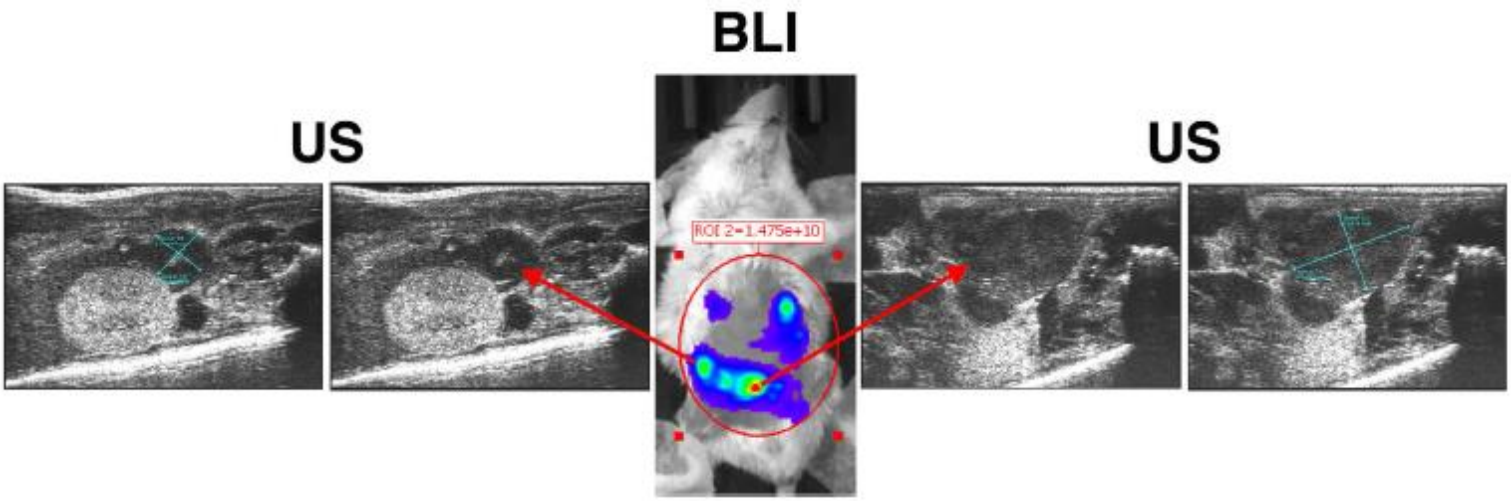

Figure 20. Tumor detection in vivo by BLI and US imaging. 15–20 days following injection of 7 × 104 AB1-B/c-LUC cells, mice developed tumor masses that were detected by BLI and US. The mass identified by US and shown in the panels on the right was estimated to measure 3.5 × 5.4 mm and yielded a higher BLI

signal, whereas the one shown in the panels on the left was estimated to measure 2.5 × 2.5 mm and had a lower BLI signal. In both cases the BLI signal is sufficiently strong, allowing their detection as individual masses. [287]

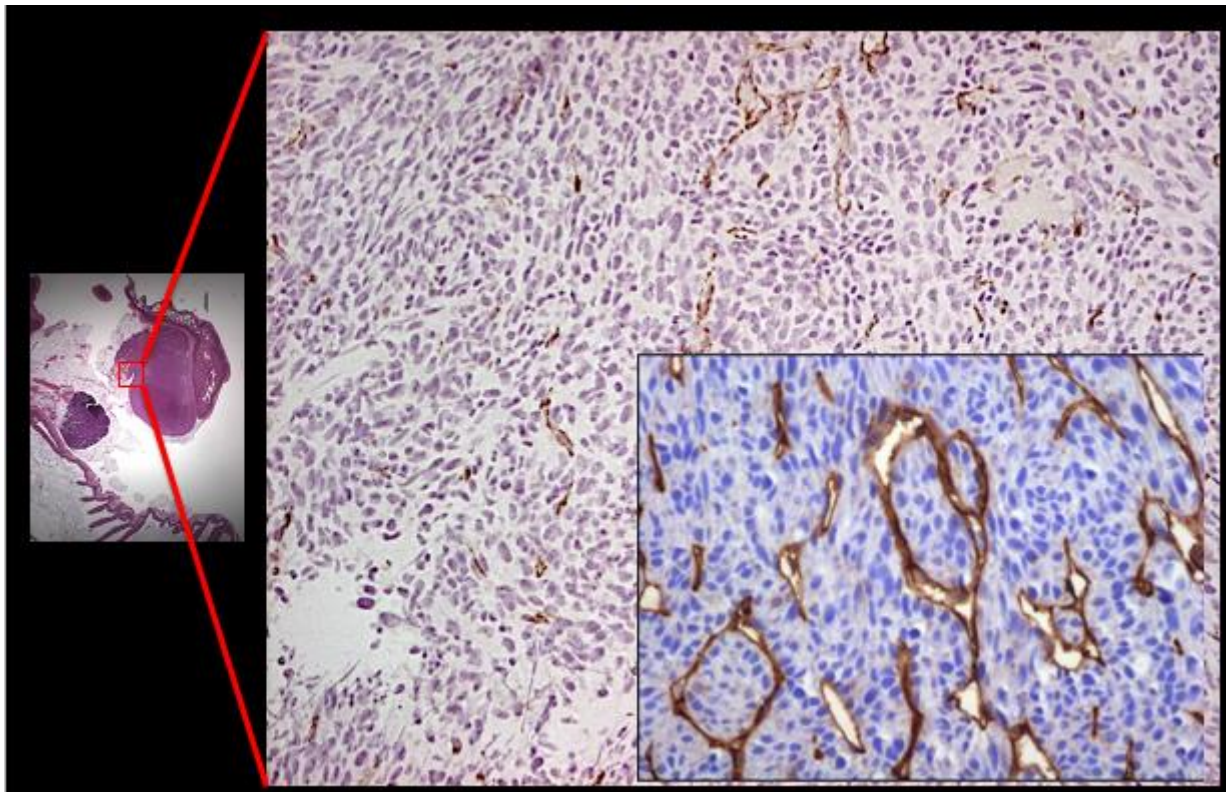

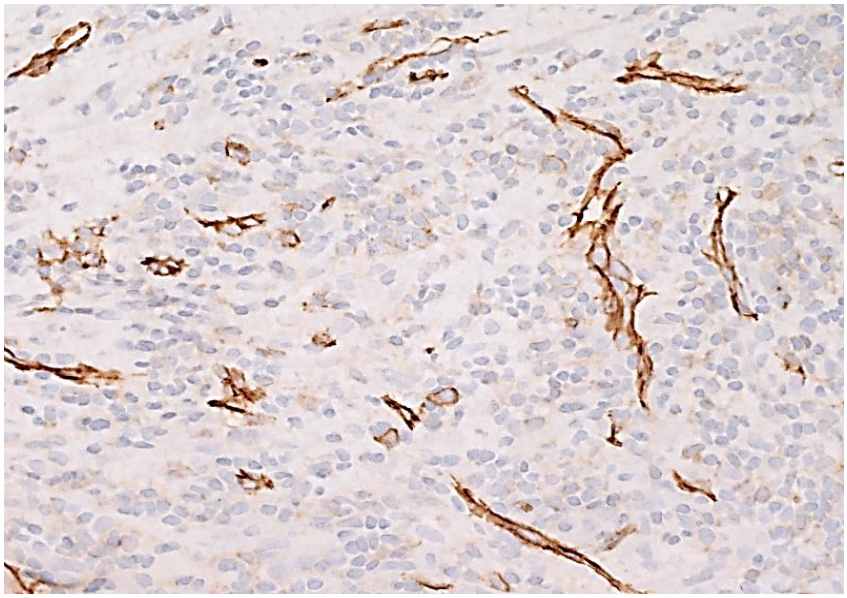

Figure 21 a: vascularization of mice tumor masses generated after IP injection of AB1 cell lines;
Figure 21 b: vascularization of human MPM

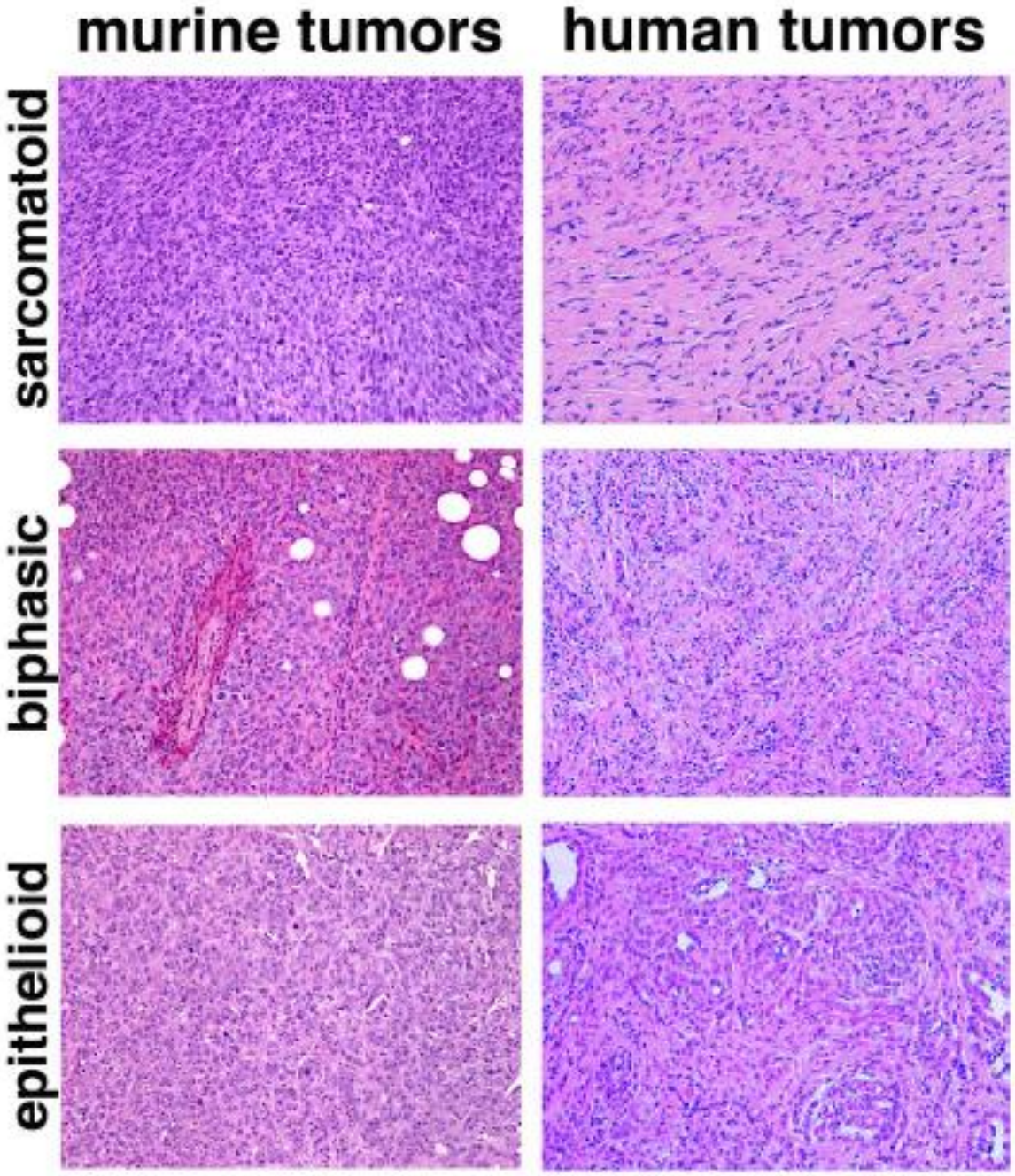

Figure 22: Murine and human tumors have similar phenotypes – Slices of explanted tumor masses generated by injection of AB1, AB12 and AB22 cells in BALB/c mice were stained with hematoxylin and eosin (H&E), as were slices from human sarcomatoid, biphasic and epithelioid mesotheliomas. The architecture of murine tumors appears similar to that of the corresponding (sarcomatoid, biphasic, epithelioid) human masses. [287]

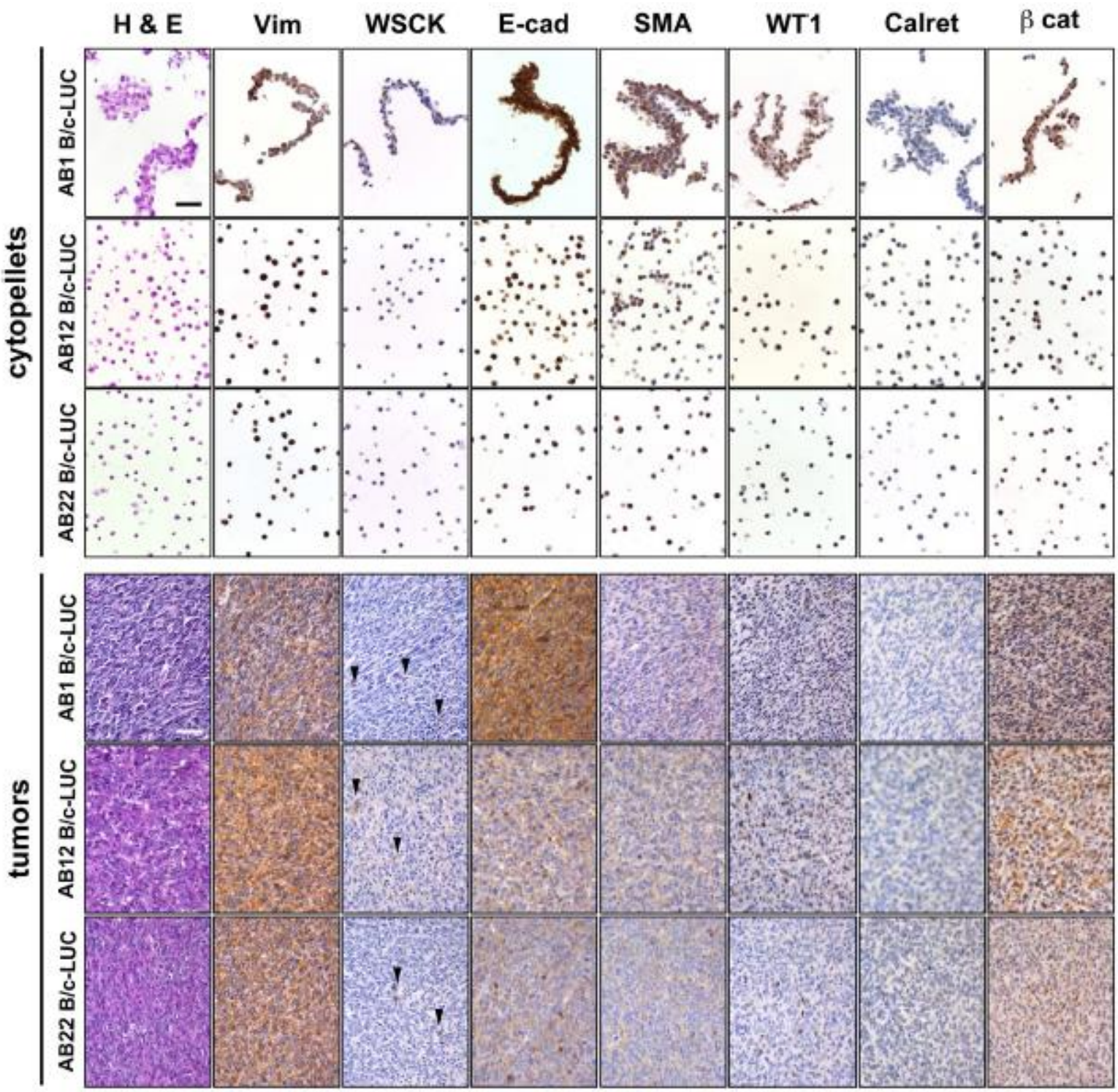

Figure 23. Immunohistochemical characterization of MM cell lines and tumors derived from them.
Following detachment from culture dishes, cells were fixed and centrifuged; the pellets were then sectioned and stained with the indicated antibodies (cytopellet). Explanted tumor masses were fixed, sectioned and stained with the same antibodies as in cytopellets. Arrows indicate positive cells. All pictures were taken with the same magnification (10X). Bars in top left panels of H&E stain of cytopellets and tumors = 50 µm. [287]

Primary Antibodies *(abbreviation)*	Cell culture			Tumors		
	AB1	AB12	AB22	AB1-B/c	AB12-B/c	AB22-B/c
Vimentin *(Vim)*	+	+	+	+	+	+
Wide Spectrum Cytokeratin *(WSCK)*	+/–	–	–	+/–	+/–	+/–
E-cadherin phosphor *(E-cad)*	+	+	+/–	+	+/–	+
Smooth Muscle Actin *(SMA)*	+	+*	+*	+/–	+/–	+/–
Wilm's Tumor Antigen 1 *(WT1)*	–	?	+	–	–	–
Calretinin *(Calret)*	–	–	–	+/–	–	–
β-catenin *(βcat)*	+	+	+	+	+	+

Table 7. Immunohistochemical characterization of MM cells. (−) = absence of staining; (+ /−) = weak staining; (+) = positive staining; (*) = some cells do not express the protein; (?) = uncertain.

Establishment of primary mesothelioma cell lines and cell spheres. The human MPM cell line, called 'MN11' was established, cultured in vitro and were subcultured for over 30 passages. Phase-contrast microscopy demonstrated epithelioid subtypes as shown in Figure 24; this cell line grew as adherent layers with no floating cells at confluence in the culture media. Phase- contrast microscopy pictures indicated that MN11 cells grew with a polygonal morphology, as shown in Figure 24. a. Following detachment from culture dishes, cells were fixed and centrifuged; the pellets were sectioned and stained by IHC with the following antibodies: Vimentin, WT-1, Calretinin, Mesothelin. IHC analysis of MN11 cytopellets indicates positivity for the diagnostic panel of mesothelioma markers such as Vimentin, WT-1 confirming their mesothelial origin (**Fig.24**).

The cell line has the ability to grow in non-adherent conditions (petri dish) generating floating spherical structures in approximately 4 days after seeding. Phase contrast microscopy demonstrated the morphology of mesothelioma spheroids. Following the collection of tumor spheroids from culture dish, spheres were fixed and centrifuged; their pellets were sectioned and characterized by H&E staining and IHC with the panel of mesothelioma antibodies. The MN11 spheres express positivity of staining for Vimentin, and WT-1, as shown in figure 25.

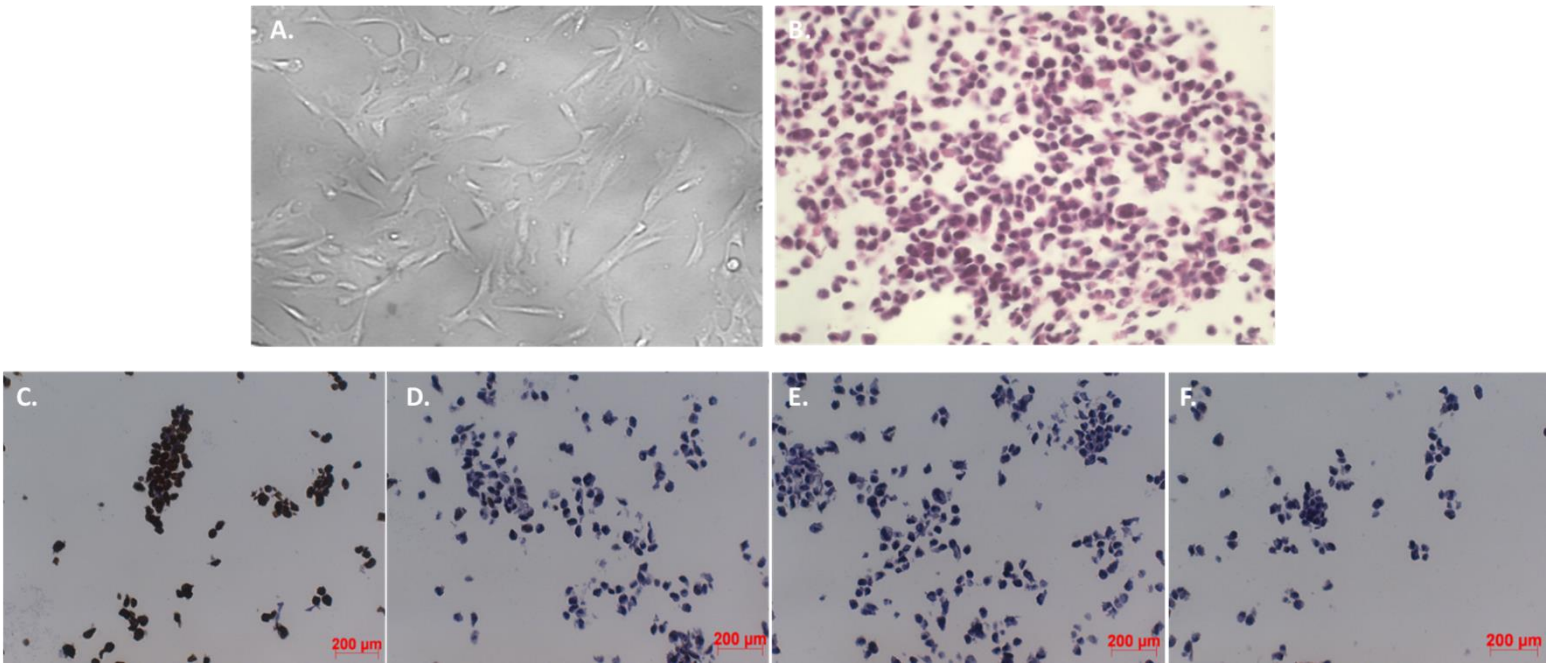

Figure 24. Phase-contrast micrographs of MPM cells in tissue culture. (A) MN11 mesothelioma cells mainly composed of polygonal epithelioid cell types can be seen. (B) Scale bar =100 µm; Representative IHC staining results of the MPM cell pellets that were formalin-fixed and paraffin-embedded. MPM1 cells stained positively for vimentin (C) and Wilms Tumor-1 (D) Scale bar= 200 µm.

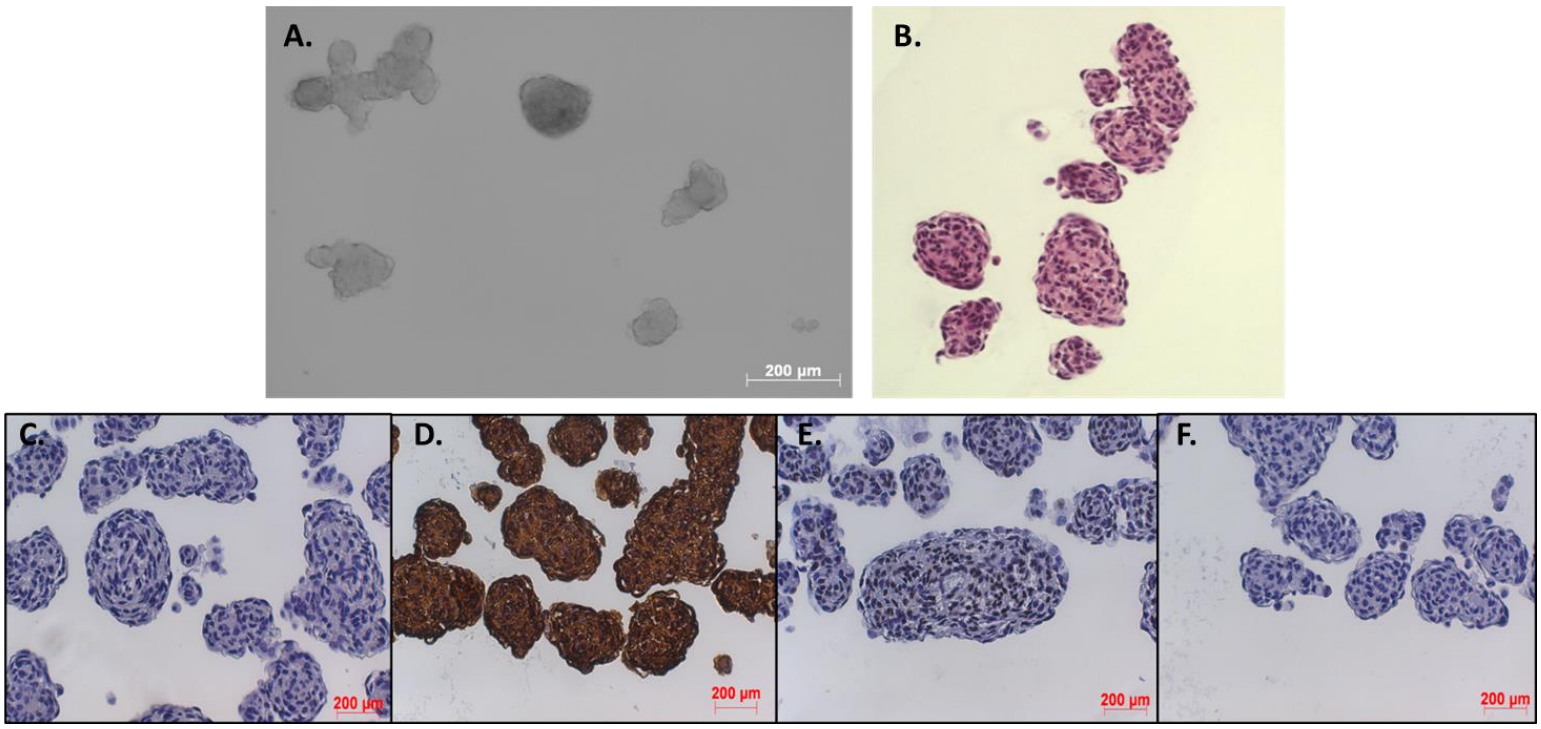

Figure 25. Phase-contrast micrographs of MPM spheres in culture. (A) MN11 mesothelioma spheres seems to be rounded, compact, but also irregular. (B) Scale bar =100 µm; Representative IHC staining results of

the MPM cell pellets that were formalin-fixed and paraffin-embedded. MPM1 cells stained positively for vimentin (D) and Wilms Tumor-1 (E). Scale bar= 200 µm.

Patient derived xenograft.

Our experience indicates that upon the tumor implantation subcutaneously in mice flanks, the formation of palpable masses (~1 cm) takes at about from 12 to 16 weeks. We were able to obtain successfully three Patient-derived xenografts (3/10 = 33%) from the human biopsies collected and used for xenograft. A pathologist confirmed that the explanted mass retains the same morphology and immuno-phenotype of original tumor (**Fig.26**): both are positive for Calretinin, CK5/6 and WT-1.

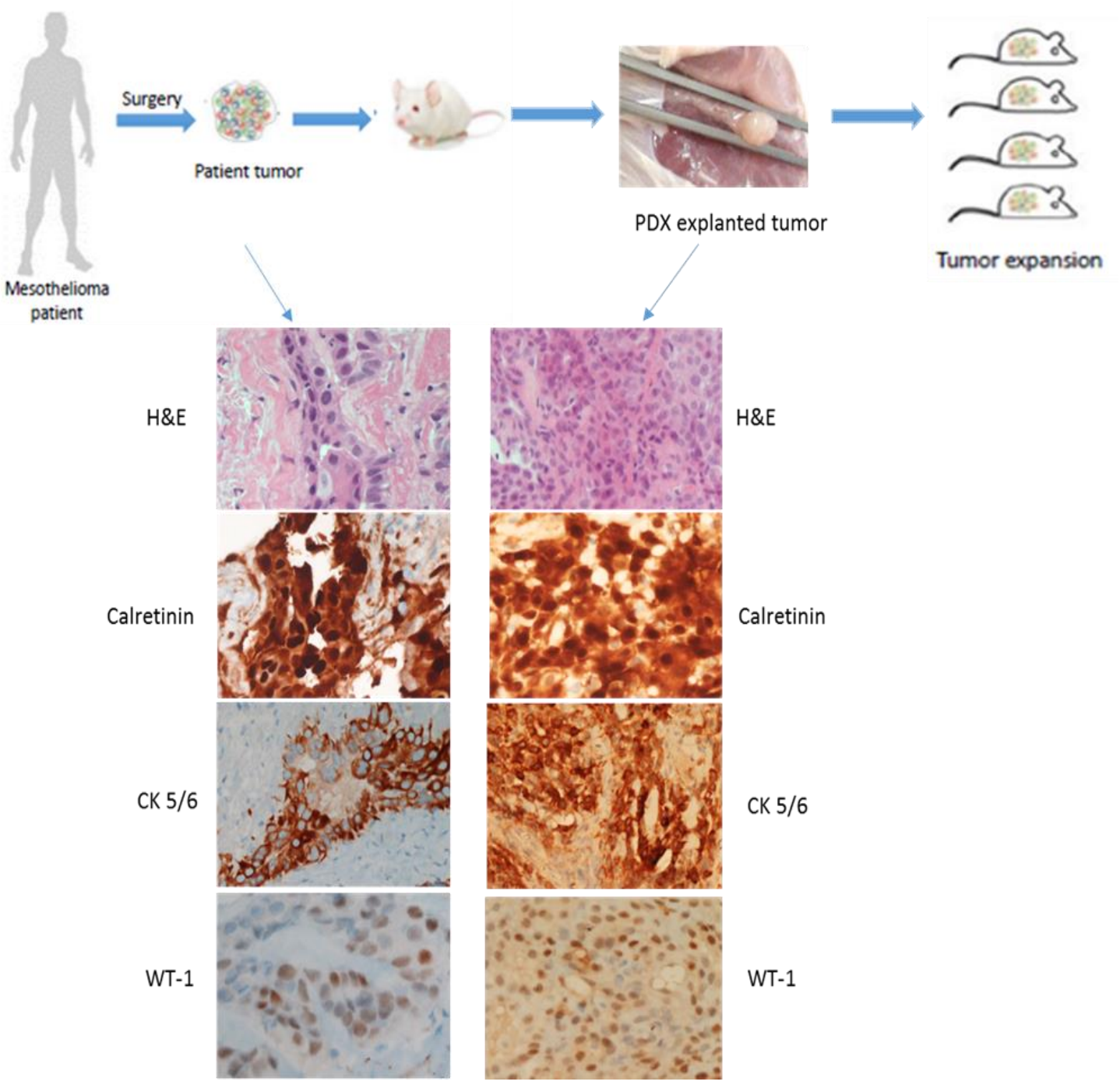

Figure 26. Schematic presentation of Patient Derived Xenograft model of MPM. Immunohistochemical characterization of the original tumor fragment/patient biopsy and of explanted tumor mass from NSG mouse.

Establishment of human mesothelioma organoids.

Organoid formation from human epithelioid mesothelioma was observed after two days post-seeding. Organoids are small in size (**Fig. 27, 28**) (starting at around 100 µm diameter and growing to 700 µm) and can be processed to form second-, third- and fourth generation organoids. Hematoxylin and eosin staining showed that human mesothelioma organoids have inside-outside polarity, and an internal matrix (**Fig. 28**); organoids were positive for mesothelioma markers such as Vimentin, WT-1 and mesothelin (**Fig. 29**). Next, we monitored the organoids growth by Axiovision, measuring their area day by day. The growth curves of tertiary organoids indicated that human organoids grow very slow (Fig.30).

In addition, we generated non-tumoral human organoids from pleural phlogosis and monitored their growth (Figure 31). Interestingly, we observed that non-tumoral organoids grow faster than the tumoral one, in the same culture conditions.

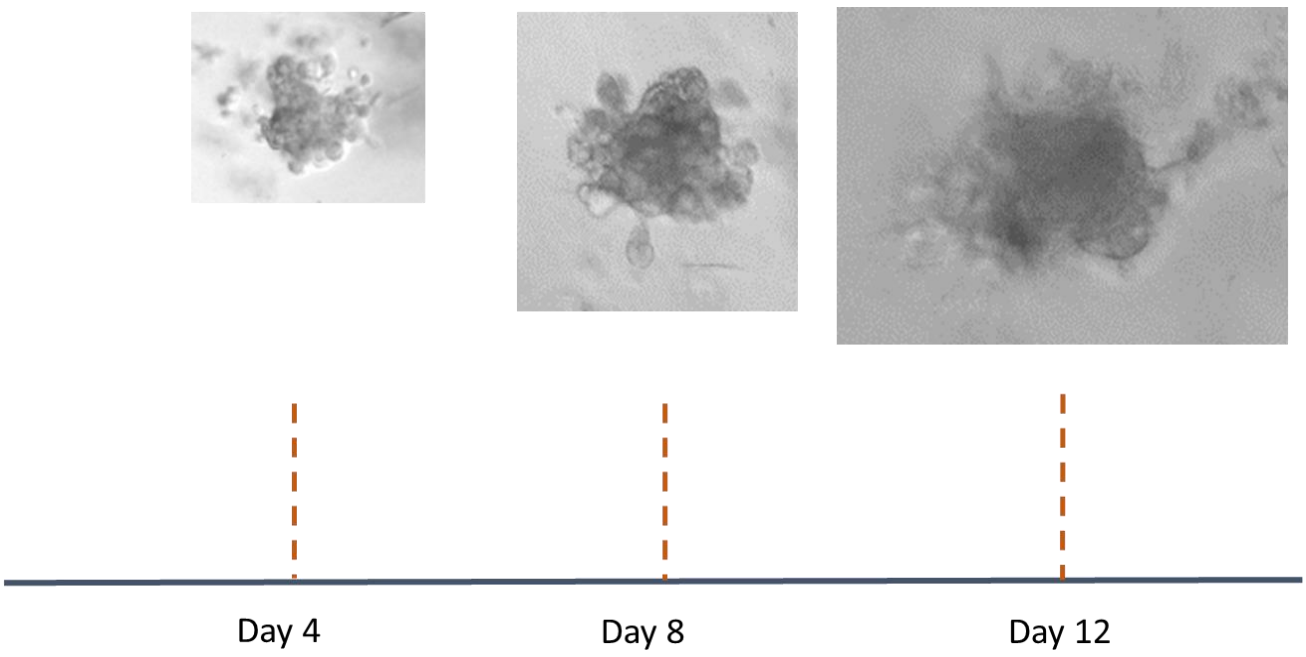

Figure 27. Phase-contrast micrograph by inverted microscope following the Organoids growth. Primary organoid generated from patient MN9.

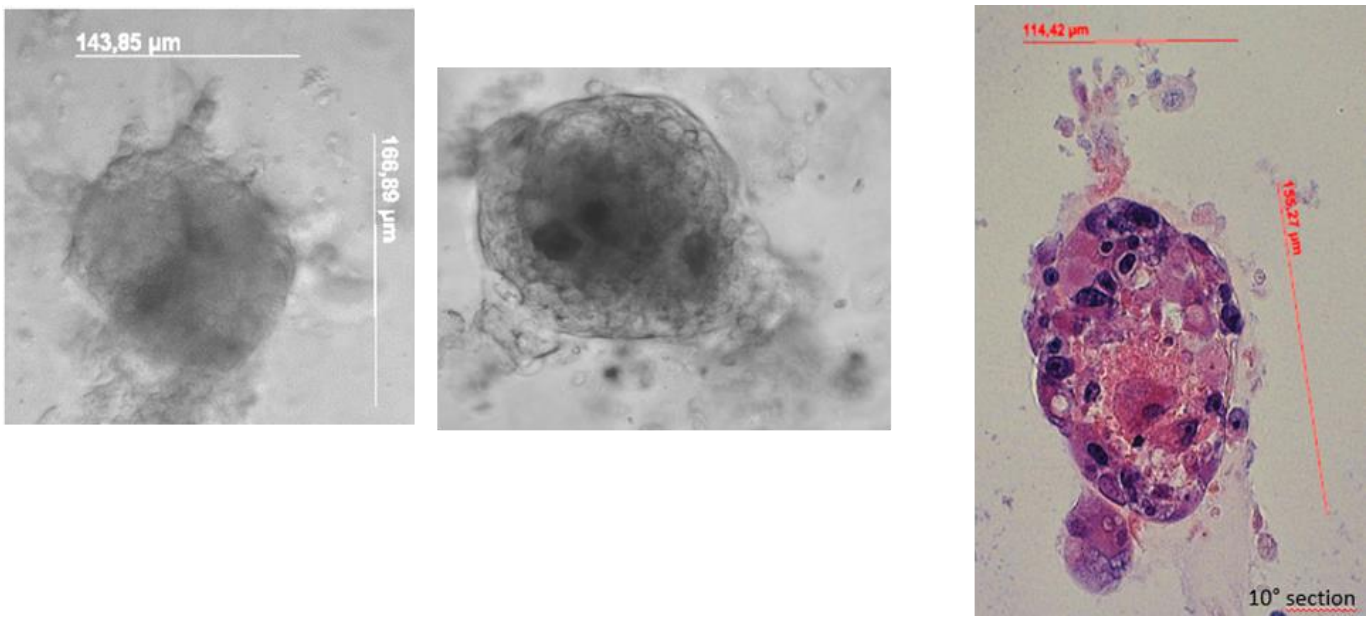

Figure 28. Organoids presentation by phase-contrast micrograph and H&E staining.

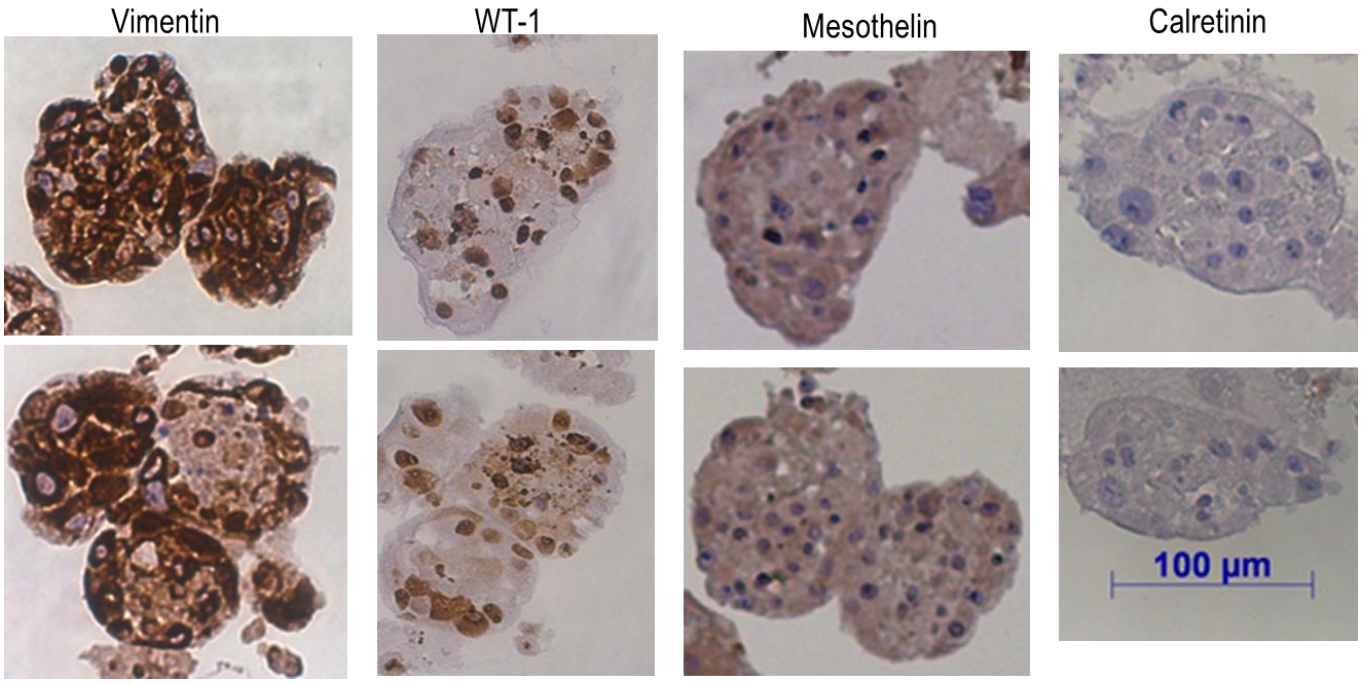

Figure 29. IHC characterization of Human Organoids, which express positivity for Vimentin, WT-1, and mesothelin.

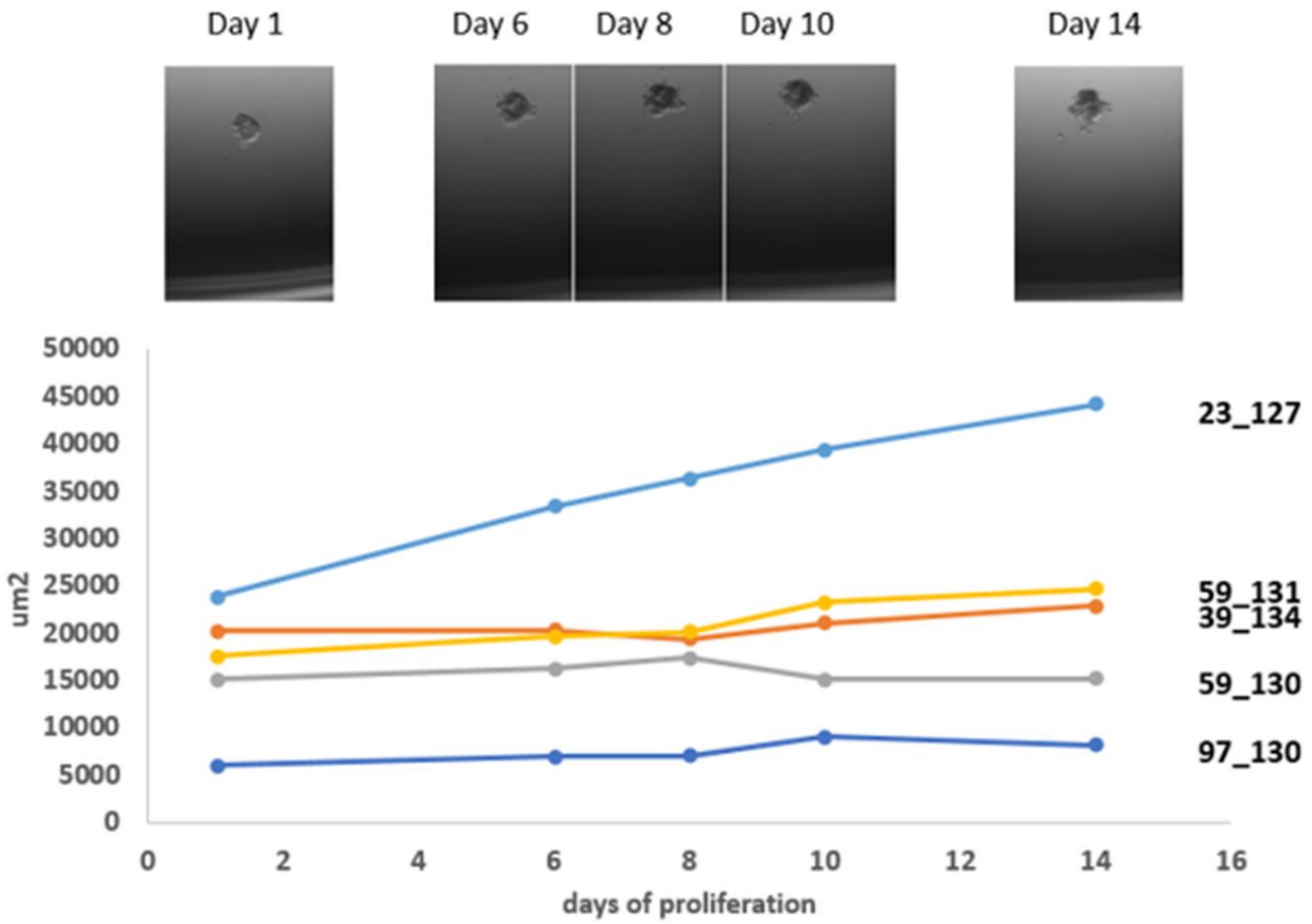

Figure 30. Monitoring the growth of tertiary organoids derived from MOSR3 patient.

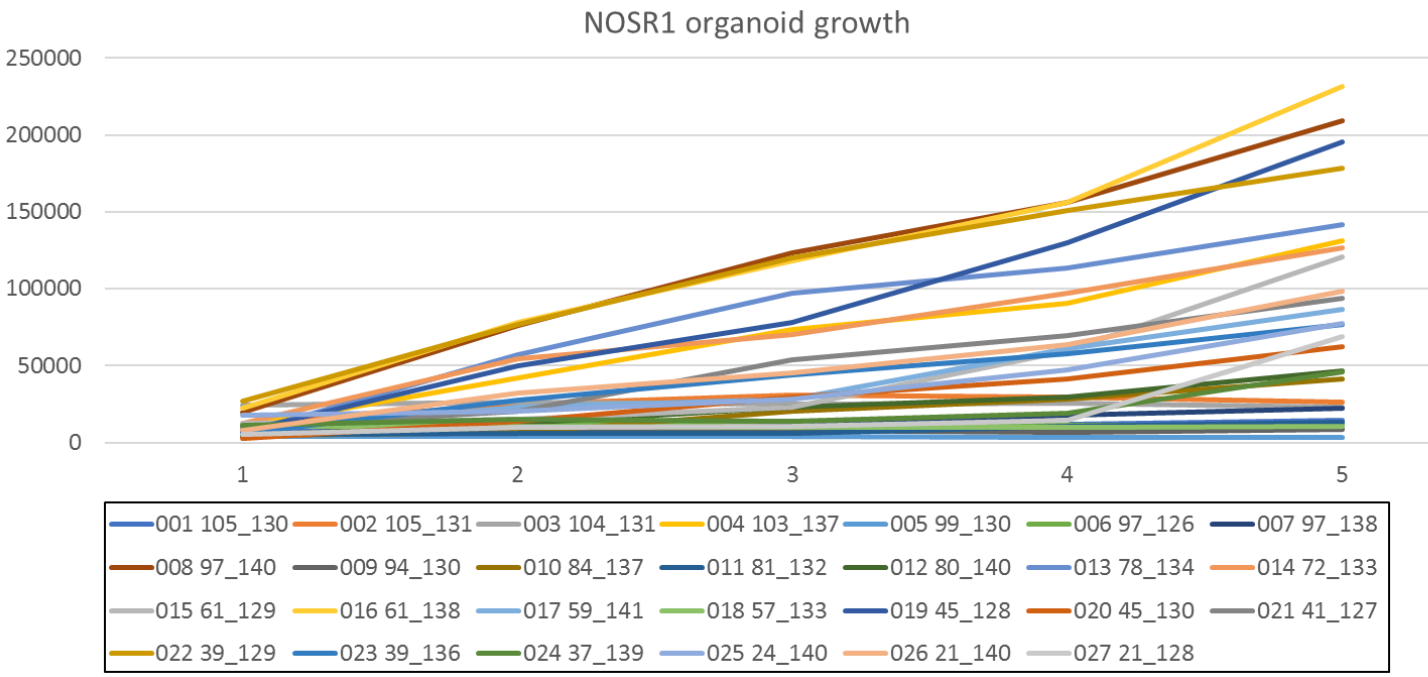
NOSR1 organoid growth
250000
200000
150000
100000
50000
0
1
2
3
4
5
001 105_130
002 105_131
003 104_131
004 103_137
005 99_130
006 97_126
007 97_138
008 97_140
009 94_130
010 84_137
011 81_132
012 80_140
013 78_134
014 72_133
015 61_129
016 61_138
017 59_141
018 57_133
019 45_128
020 45_130
021 41_127
022 39_129
023 39_136
024 37_139
025 24_140
026 21_140
027 21_128

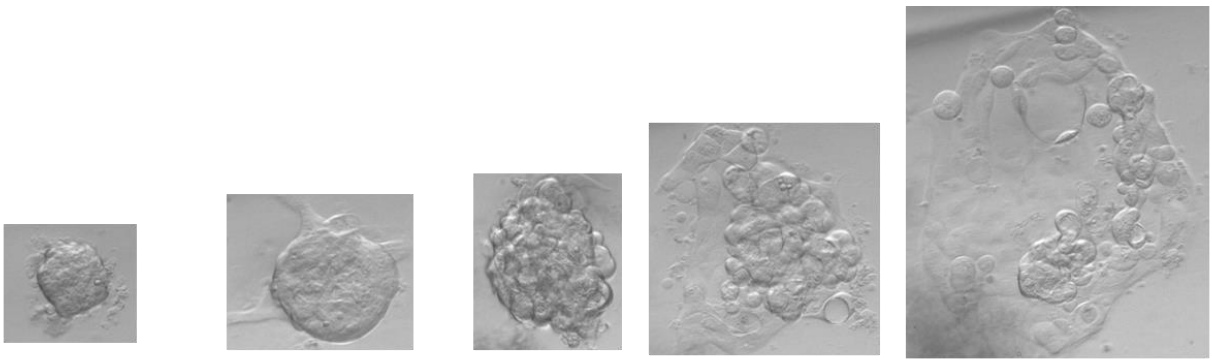

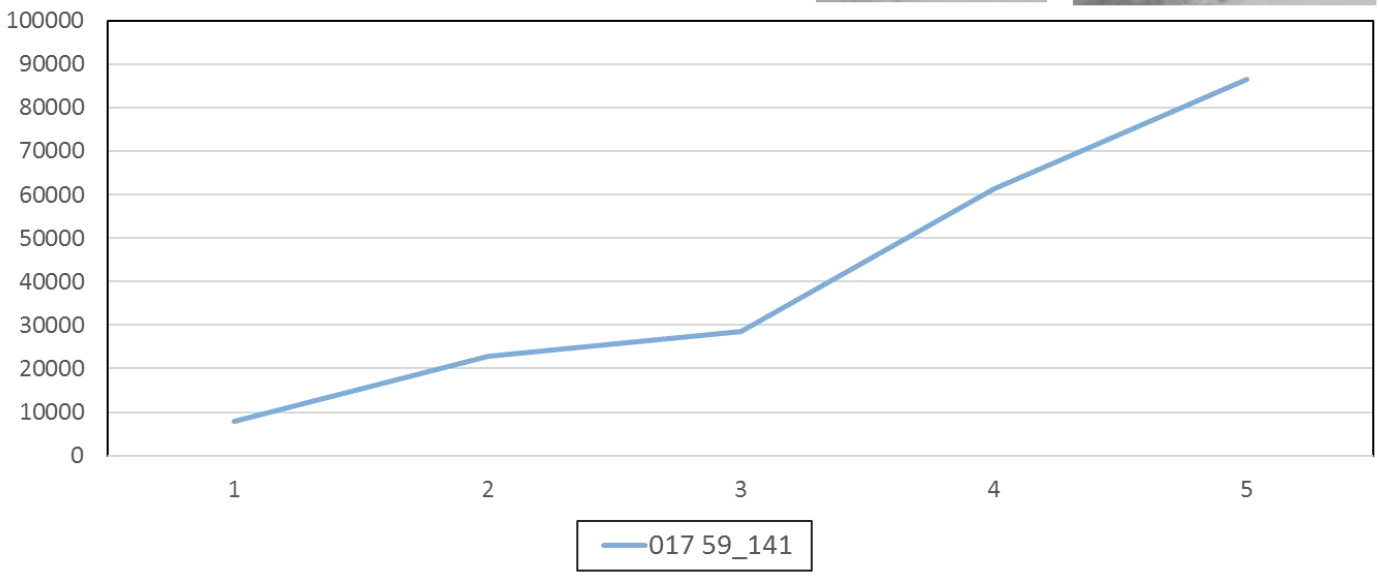
100000
90000
80000
70000
60000
50000
40000
30000
20000
10000
0
1
2
3
4
5
017 59_141

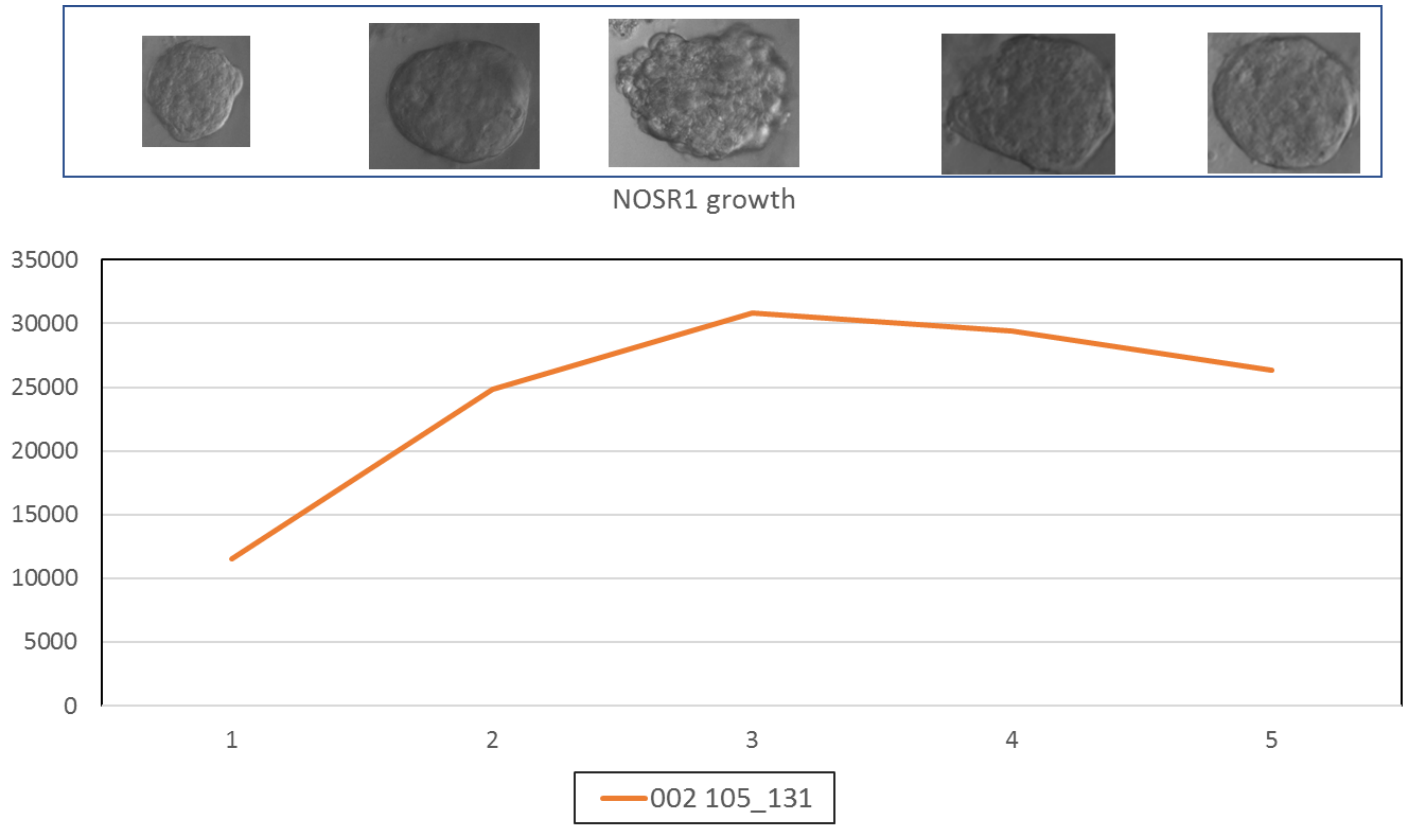

Figure 31. Monitoring NOSR1 non tumoral organoids growth. Pictures of Non-tumoral Organoids from NOSR1 (pleural phlogosis) fragment.

6. DISCUSSION

Overall, our findings indicate that expression levels of HMGB1, evaluated by immunohistochemistry, in clinical samples of MPM are significantly correlated with patients' prognosis. Malignant pleural mesothelioma (MPM), is a very aggressive tumor: the average disease-specific survival after histologic diagnosis is currently 8-12 months.[1, 260] Several prognostic factors were identified according to the Cancer and Leukaemia Group, and the European Organization for Research and Treatment of cancer. [261] However, unlike other malignant tumors, tissue biomarkers detectable by immunohistochemistry or by molecular biology techniques able to predict the prognosis of MPM are still lacking. A recent meta-analysis by Wu et al,[265] indicated that the overexpression of HMGB1, when detected by immunohistochemistry, is significantly associated with poor overall survival and progression-free survival in several types of malignant tumors. [264] In addition, Tabata et al,[277, 278] also reported that high serum levels of high mobility group box 1 (HMGB1) were related to poor prognosis, suggesting its use in clinical management of MPM. The main goals of our study were: a) to assess if the expression levels of HMGB1, evaluated by immunohistochemistry and RT-PCR in tissue samples from a large series of MPM, were related to the patients' survival and b) to evaluate if HMGB1 could be useful as a prognostic biomarker in clinical practice.

We demonstrated that high expression levels of HMGB1, evaluated by immunohistochemistry, in cancer cells of clinical samples of MPM were significantly correlated to a worse DSS. This result was obtained either when the score was calculated as total score (nuclear plus cytoplasmic) and cytoplasmic score alone, in the entire cohort and in the clinical and pathologic subgroups of patients. Conversely, the expression levels of nuclear HMGB1 score alone did not show any statistically significant correlation with DSS. HMGB1, is a nuclear protein constitutively expressed in both cancer and normal cells and acts as chromatin-binding factor that bends DNA, promoting access to several transcriptional proteins.[266] Some studies have demonstrated that HMGB1 could be actively shuttled between the nucleus and the cytoplasm of tumor cells.[267] Following various stressors (e.g., cytokine, chemokine, heat, hypoxia, H_2O_2), HMGB1 translocate from the nucleus to the cytoplasm, where it functions as a positive regulator of autophagy.[268] At the extracellular level, HMGB1 functions as a cytokine during inflammation, cell differentiation, cell migration, and seems also to play a role in tumor metastasis development.[269, 270] Since in our study the cytoplasmic but not nuclear overexpression of HMGB1 was significantly associated with poor prognosis, we can speculate that in malignant mesothelioma cells, under stress environmental stimuli, HMGB1 migrates from the nucleus to the cytoplasm of the tumor cells and after secretion into the extracellular matrix, it enhances tumor cell survival and proliferation through several cancerogenic mechanisms. [271] Furthermore, Jube et al, [170] demonstrated, by means of in vivo and in vitro experiments, that MPM cells strongly expressed HMGB1 and secreted it at high levels, establishing an autocrine circuit that promotes the HMGB1-secreting MPM cells proliferation and survival.

Our study did not show any statistically significant correlation with DSS when the detection method of RT-PCR was used. Moreover, no statistically significant correlation was found between the *HMGB1* gene expression and HMGB1 immunohistochemistry scoring. These results were similar to the findings reported by Ueda et al[272] in colorectal cancers, and could be tentatively explained by the presence of inflammatory cells, also expressing HMGB1, mixed with cancer cells in tissues used for the evaluation of *HMGB1* gene expression. Alternatively, post-transcriptional regulation of HMGB1 mRNA or post-translational modifications of the protein itself could contribute to explain this discrepancy.[273, 274, 275] Indeed, Napolitano et al reported that the different isoforms of HMGB1 (hyperacetylated and nonacetylated) are responsible for the protein release from mesothelioma cells into the extracellular compartment and therefore not detectable by immunohistochemistry.[276]

In conclusion, we have demonstrated that the expression levels of HMGB1 are inversely correlated with DSS in MPM cases, when assessed by immunohistochemistry. To the best of our knowledge, this study represents the most significant analysis in terms of the number of patients studied, and suggests the possible use of HMGB1 as new prognostic tissue biomarker in the clinical management of patients with MPM. However, since HMGB1 is expressed also in normal and reactive mesothelial cells, it cannot be used as a diagnostic biomarker, in MPM.

In our study, we have also described the generation and characterization of the *in vitro* and *in vivo* models of mesothelioma. MPM is resistant to the conventional forms of treatment, and adequate scientific and clinical assessment of this disease has been severely limited by the lack of representative cell lines and animal models and by the limited number of patients treated in a single institution. Thus, the establishment of representative in vitro cell lines and animal models is important for the development of potentially effective forms of diagnosis and therapy and for the study of basic biology. In this study, we completed the characterization of murine cell lines of mesothelioma, in order to elucidate their molecular and phenotypical features and tumor masses derived thereof in BALB/c mice. AB cell lines have been obtained by tumor masses which were developed into BALB/c mice induced by asbestos intraperitoneally injection.[210] The AB1, AB12 and AB22 cell lines are used as model systems for various in vitro and in vivo studies of mesothelioma biology. They also offer the opportunity to set up a syngeneic model system providing a full immunological tumor response. Syngeneic studies use immunocompetent wild type mice, typically inbred strains, for engraftment of a tumor cell from the same strain. Because they retain complete immune systems, these models can be particularly appropriate for studies of interplay between the tumor and immunity, and for immunologically-based targeted therapies.

Our results indicate that the MM cell lines (AB1, AB12) generated by Davis M.R. et al [210] exhibit some of the main features at the morphological level, functional and phenotypical of human MM in vitro and in vivo; whereas AB22 cells do not fully summarize epithelioid mesotheliomas. Such a model study would be used

for the pre-clinical evaluation of potential therapeutic agents because it 'mimic' the phenotypic characteristics of mesothelioma. However, this system does not allow to consider the heterogeneity of real human mesothelioma. Recently, xenografts using well-established human tumor have become popular because they accurately recapitulate the features of patient tumors and the complex factors that promote tumor progression and metastasis. Our group developed a Patient Derived Xenograft model by using tumor samples of MPM patients and directly implanted them in heterotopic sites (subcutaneously) of NSG (NOD scid gamma) mice. The direct engraftment takes approximately 2 hours and growth of palpable tumor requires an average of 14 weeks. Our experimental results indicate that we were able to establish patient derived xenograft from mesothelioma biopsies, with a success rate of 30%. Establishing a PDX Patient derived xenograft model would allow us to significantly broaden the studies on MM, ranging from sequencing to drug testing. More importantly, these studies can be carried out on the same "lesion" originally transplanted in mice (and expanded in other mice of the same strain), thus maintaining a high degree of homogeneity. Furthermore, we performed the hematoxylin and eosin staining and immunohistochemical characterization of tumor masses explanted by xenografted mice. The explanted tumor maintain the same histologic morphology and immune-phenotype of the original patient biopsy recapitulating the original tumor biology. Thus, this system results "less different" from the original lesion and therefore provides highly translational results. Different studies reported that direct xenograft tumors grow with considerable stromal elements and recapitulate the histological appearance of the original patient tumor over multiple passages in mice. [166]

In this study, the tumor take and growth were analyzed by immunohistochemistry and molecular biology experiments. Grown tumors will be then transplanted in recipient NSG mice for further studies, such as, for instance, treatment with HMGB1 inhibitors. Recent published results sustain that inhibition of HMGB1 impaired in vitro tumorigenesis of malignant mesothelioma (MM) cells and reduce tumour growth in xenografted SCID mice.[170] The treatment with BoxA (HMGB1 antagonist) will allow to determine how many and which patients are potentially responsive, providing both quantitative and qualitative pre-clinical results. The value of such a program is reflected in its inherent versatility; direct xenograft models may be used to study diverse aspects of cancer biology including drug resistance, angiogenesis, tumor microenvironment, cancer stem cells and experimental therapeutics.

Moreover, PDX models can suffer from long latency periods after engraftment and variable engraftment rates.

Recently, a new powerful model system has emerged to expand and investigate normal and cancer stem cells, i.e. three-dimensional "organoid" cultures. Organoids represent miniature tissues that recapitulate the architecture and growth pattern of the tissue from which they originate. [250, 251] Organoids can be derived from healthy or diseased tissue of each individual, propagated in vitro at will, and preserved as

frozen stocks. A number of laboratories have successfully generated various organoids. [281-285] Most recently, cancer- derived organoid models from prostate, lung and pancreatic cancers have also been established as an in vitro system to model an in vivo tumor pathophysiological state, such as tumor-associated signaling pathways and chemoresistance. [281,282] However, no reliable mesothelioma organoid models are available at the present time. In this study, we focused our attention into Patient derived organoids generation. We established a protocol to generate organoids from mesothelioma biopsies and we followed their in vitro growth. Our data indicated that we are able to generate primary, secondary and tertiary organoids. However, after the first generation, organoid growth is very slow. So far, we can go on for 3 generations, but we are not able to generate mesothelioma "organoid lines". Furthermore, we performed their morphologic and immunophenotyped characterization. The H&E staining indicated that mesothelioma organoids have a defined structure with inside/outside polarity, and an internal matrix. Maybe that is why we cannot propagate them easily. Whereas, the IHC evaluation showed positivity for Vimentin, Mesothelin and WT-1, maintaining the phenotype of a mesothelioma. In contrast to any mesothelioma cell line grown in 2D, mesothelioma derived organoids recapitulate the histological architecture and IHC expression profiles of the corresponding original tumor. Different studies also reported that tumor-organoids capture the essential uniqueness of each individual tumor –integrating its genetic, epigenetic and cellular heterogeneity– yet making it experimentally tractable in a manner that has been so far impossible to attain. [281-285] This represents a clear breakthrough compared to the use of established cancer cell lines, or to more laborious, costly and inefficient *in vivo* approaches, such as tumor xenografts. Several experiments are currently ongoing in order to perform transcriptomic analysis of organoids and their correspondent original biopsy. This type of analysis could permit us to comprehend better if the organoids recapitulate the tumor biology, molecular profile and heterogeneity.

Of critical relevance in a therapeutic perspective, tumor-organoids may represent an essential compendium to complement sequence-based therapies, as patient-derived organoids can be directly interrogated as *in vitro* proxy of the patient's tumor for sensitivity to specific drugs or combinations of drugs, to then advice the oncologist on what drug(s) to use for that specific patient.

In conclusion, our work indicates that HMGB1 detected by immunohistochemistry, may represent a useful prognostic biomarker in MPM. Moreover, we have generated and described in vitro and in vivo mesothelioma models that recapitulates the disease pathogenesis. These models could be also important to effectively treat MPM patients with a personalized medicine approach.

7. REFERENCES

1- Carbone M, Ly BH, Dodson RF, et al. Malignant mesothelioma: facts, myths, and hypotheses. J Cell Physiol. 2012;227(1):44-58.

2- Tan C, Treasure T. Mesothelioma: time to take stock. J R Soc Med. 2005 Oct;98(10):455-8

3- Bridda A, Padoan I, Mencarelli R, Frego M. Peritoneal mesothelioma: a review. MedGenMed. 2007 May 10;9(2):32.

4- WAGNER JC, SLEGGS CA, MARCHAND P. Diffuse pleural mesothelioma and asbestos exposure in the North Western Cape Province. Br J Ind Med. 1960 Oct;17:260-71.

5- Mensi C, Bonzini M, Macchione M, Sieno C, Riboldi L, Pesatori AC. Differences among peritoneal and pleural mesothelioma: data from the Lombardy Region Mesothelioma Register (Italy). Med Lav. 2011 Sep-Oct;102(5):409-16.

6- Yang H, Testa JR, Carbone M. Mesothelioma epidemiology, carcinogenesis, and pathogenesis. Curr Treat Options Oncol. 2008 Jun;9(2-3):147-57.

7- Testa JR, Cheung M, Pei J, Below JE, Tan Y, Sementino E, Cox NJ, Dogan AU, Pass HI, Trusa S, Hesdorffer M, Nasu M, Powers A, Rivera Z, Comertpay S, Tanji M, Gaudino G, Yang H, Carbone M. Germline BAP1 mutations predispose to malignant mesothelioma. Nat Genet. 2011 Aug 28;43(10):1022-5.

8- Lanphear BP, Buncher CR. Latent period for malignant mesothelioma of occupational origin. J Occup Med. 1992 Jul;34(7):718-21.

9- Vogelzang NJ, Rusthoven JJ, Symanowski J, Denham C, Kaukel E, Ruffie P, Gatzemeier U, Boyer M, Emri S, Manegold C, Niyikiza C, Paoletti P. Phase III study of pemetrexed in combination with cisplatin versus cisplatin alone in patients with malignant pleural mesothelioma. J Clin Oncol. 2003 Jul 15;21(14):2636-44.

10- Bononi A, Napolitano A, Pass HI, et al. Latest developments in our understanding of the pathogenesis of mesothelioma and the design of targeted therapies. Expert. Rev. Respir. Med. 2015; 9(5): 633–654.

11- Neumann V, Löseke S, Nowak D, Herth FJ, Tannapfel A. Malignant pleural mesothelioma: incidence, etiology, diagnosis, treatment, and occupational health. Dtsch Arztebl Int. 2013 May;110(18):319-26.

12- Henley S J, Larson T C, Wu M, Antao V C S, Lewis M, Pinheiro G A, and Eheman C. Mesothelioma incidence in 50 states and the District of Columbia, United States, 2003–2008. Int J Occup Environ Health. 2013; 19(1): 1–10.

13- Beasley MB. Immunohistochemistry of pulmonary and pleural neoplasia. Arch Pathol Lab Med. 2008 Jul;132(7):1062-72.

14- Boutin C1, Schlesser M, Frenay C, Astoul P. Malignant pleural mesothelioma. Eur Respir J. 1998 Oct;12(4):972-81.

15- Van Schil PE1, Opitz I2, Weder W2, De Laet C3, Domen A3, Lauwers P3, Hendriks JM3, Van Meerbeeck JP4. Multimodal management of malignant pleural mesothelioma: where are we today? Eur Respir J. 2014 Sep;44(3):754-64.

16- Mery É, Hommell-Fontaine J, Capovilla M3, Chevallier A4, Bibeau F5, Croce S6, Dartigues P7, Kaci R8, Lang-Averous G9, Laverriere MH10, Leroux-Broussier A11, Poizat F12, Robin N13, Valmary-Degano S14,

Verriele-Beurrier V15, Villeneuve L13, Isaac S16. Peritoneal malignant mesothelioma: review and recent data. Ann Pathol. 2014 Feb;34(1):26-33.

17- Carbone M, Kratzke RA, Testa JR. The Pathogenesis of Mesothelioma. Seminars in Oncology. 2002; Vol 29, No 1.:2-17.

18- Bononi A, Napolitano A, Pass HI, et al. Latest developments in our understanding of the pathogenesis of mesothelioma and the design of targeted therapies. Expert. Rev. Respir. Med. 2015; 9(5): 633–654.

19- Carbone M, Bedrossian CW. The pathogenesis of mesothelioma. Semin Diagn Pathol. 2006 Feb;23(1):56-60.

20- Bianchi C, Giarelli L, Grandi G, Brollo A, Ramani L, Zuch C. Latency periods in asbestos-related mesothelioma of the pleura. Eur J Cancer Prev. 1997 Apr;6(2):162-6.

21- Mossman BT, Bignon J. In reply: asbestos, carcinogenicity, and public policy. Science. 1990 May 18;248(4957):799-802

22- Marchevsky AM, Wick MR. Current controversies regarding the role of asbestos exposure in the causation of malignant mesothelioma: the need for an evidence-based approach to develop medicolegal guidelines. Ann Diagn Pathol. 2003 Oct;7(5):321-32.

23- Gibbs GW. Rapporteur's Report Session 3: exposure to grunerite (amosite) asbestos: historical perspectives of the health effects. Regul Toxicol Pharmacol. 2008 Oct;52(1 Suppl):S91.

24- Choe N, Tanaka S, Kagan E. Asbestos fibers and interleukin-1 upregulate the formation of reactive nitrogen species in rat pleural mesothelial cells. Am J Respir Cell Mol Biol. 1998 Aug;19(2):226-36.

25- Huang SX, Jaurand MC, Kamp DW, Whysner J, Hei TK. Role of mutagenicity in asbestos fiber-induced carcinogenicity and other diseases. J Toxicol Environ Health B Crit Rev. 2011;14(1-4):179-245.

26- Sekido Y. Molecular pathogenesis of malignant mesothelioma. Carcinogenesis. 2013 Jul;34(7):1413-9.

27- Yang H, Rivera Z, Jube S, et al. Programmed necrosis induced by asbestos in human mesothelial cells causes high-mobility group box 1 protein release and resultant inflammation. Proc Natl Acad Sci U S A. 2010 Jul 13;107(28):12611-6.

28- Qi F, Okimoto G, Jube S, Napolitano A, Pass HI, Laczko R, Demay RM, Khan G, Tiirikainen M, Rinaudo C, Croce A, Yang H, Gaudino G, Carbone M. Continuous exposure to chrysotile asbestos can cause transformation of human mesothelial cells via HMGB1 and TNF-α signaling. Am J Pathol. 2013 Nov;183(5):1654-66.

29- Carbone M, Emri S, Dogan AU, Steele I, Tuncer M, Pass HI, Baris YI. A mesothelioma epidemic in Cappadocia: scientific developments and unexpected social outcomes. Nat Rev Cancer. 2007 Feb;7(2):147-54.

30- Carbone M1, Baris YI, Bertino P, Brass B, Comertpay S, Dogan AU, Gaudino G, Jube S, Kanodia S, Partridge CR, Pass HI, Rivera ZS, Steele I, Tuncer M, Way S, Yang H, Miller A. Erionite exposure in North Dakota and Turkish villages with mesothelioma. Proc Natl Acad Sci U S A. 2011 Aug 16;108(33):13618-23.

31- Baumann F1, Maurizot P, Mangeas M, Ambrosi JP, Douwes J, Robineau B. Pleural mesothelioma in New Caledonia: associations with environmental risk factors. Environ Health Perspect. 2011 May;119(5):695-700.

32- Roushdy-Hammady I, Siegel J, Emri S, Testa JR, Carbone M. Genetic-susceptibility factor and malignant mesothelioma in the Cappadocian region of Turkey. Lancet. 2001 Feb 10;357(9254):444-5.

33- Dogan AU, Baris YI, Dogan M, Emri S, Steele I, Elmishad AG, Carbone M. Genetic predisposition to fiber carcinogenesis causes a mesothelioma epidemic in Turkey. Cancer Res. 2006 May 15;66(10):5063-8.

34- Saracci R, Simonato L. Familial malignant mesothelioma. Lancet. 2001 Nov 24;358(9295):1813-4.

35- Carbone M, Ferris LK, Baumann F, Napolitano A, Lum CA, Flores EG, Gaudino G, Powers A, Bryant-Greenwood P, Krausz T, Hyjek E, Tate R, Friedberg J, Weigel T, Pass HI, Yang H. BAP1 cancer syndrome: malignant mesothelioma, uveal and cutaneous melanoma, and MBAITs. J Transl Med. 2012 Aug 30;10:179.

36- Kroczynska B1, Cutrone R, Bocchetta M, Yang H, Elmishad AG, Vacek P, Ramos-Nino M, Mossman BT, Pass HI, Carbone M. Crocidolite asbestos and SV40 are cocarcinogens in human mesothelial cells and in causing mesothelioma in hamsters. Proc Natl Acad Sci U S A. 2006.

37- Robinson C, van Bruggen I, Segal A, Dunham M, Sherwood A, Koentgen F, Robinson BW, Lake RA.

A novel SV40 TAg transgenic model of asbestos-induced mesothelioma: malignant transformation is dose dependent. Cancer Res. 2006 Nov 15;66(22):10786-94.

38- Cicala C, Pompetti F, Carbone M. SV40 induces mesotheliomas in hamsters. Am J Pathol. 1993 May;142(5):1524-33.

39- Bocchetta M, Eliasz S, De Marco MA, Rudzinski J, Zhang L, Carbone M. The SV40 large T antigen-p53 complexes bind and activate the insulin-like growth factor-I promoter stimulating cell growth. Cancer Res. 2008 Feb 15;68(4):1022-9.

40- Qi F, Carbone M, Yang H, Gaudino G. Simian virus 40 transformation, malignant mesothelioma and brain tumors. Expert Rev Respir Med. 2011 Oct;5(5):683-97.

41- Cavazza A, Travis LB, Travis WD, Wolfe JT 3rd, Foo ML, Gillespie DJ, Weidner N, Colby TV. Post-irradiation malignant mesothelioma. Cancer. 1996 Apr 1;77(7):1379-85.

42- De Bruin ML, Burgers JA, Baas P, van't Veer MB, Noordijk EM, Louwman MW, Zijlstra JM, van den Berg H, Aleman BM, van Leeuwen FE. Malignant mesothelioma after radiation treatment for Hodgkin lymphoma. Blood. 2009 Apr 16;113(16):3679-81.

43- Moore AJ1, Parker RJ, Wiggins J.Malignant mesothelioma. Orphanet J Rare Dis. 2008 Dec 19;3:34. doi: 10.1186/1750-1172-3-34.

44- Salahudeen HM, Hoey ET, Robertson RJ, Darby MJ. CT appearances of pleural tumours. Clin Radiol. 2009 Sep;64(9):918-30. doi: 10.1016/j.crad.2009.03.010. Epub 2009 Jun 23.

45- Wang ZJ, Reddy GP, Gotway MB, Higgins CB, Jablons DM, Ramaswamy M, Hawkins RA, Webb WR. Malignant pleural mesothelioma: evaluation with CT, MR imaging, and PET. Radiographics. 2004 Jan-Feb;24(1):105-19.

46- Fuccio C, Spinapolice EG, Ferretti A, Castellucci P, Marzola MC, Trifirò G, Rubello D. ^{18}F-FDG-PET/CT in malignant mesothelioma. Biomed Pharmacother. 2013 Jul;67(6):539-42.

47- Nakamori T, Kosuda S, Kyoto Y, Fujikawa A, Naoi Y, Nakamori Y. Pseudomesotheliomatous lung cancer mimicking mesothelioma on ^{18}F-FDG PET/CT images: report of 2 cases. Jpn J Radiol. 2013 Aug;31(8):542-5.

48- Galateau-Salle F, Churg A, Roggli V, et al. The 2015 World Health Organization Classification of Tumors of the Pleura: Advances since the 2004 Classification. J. Thorac. Oncol. 2016;11(2):142-54.

49- Rusch VW. A proposed new international TNM staging system for malignant pleural mesothelioma. Chest. 1995;108: 1122–1128.

50- Maskell NA, Gleeson FV, Davies RJ. Standard pleural biopsy versus CT-guided cutting-needle biopsy for diagnosis of malignant disease in pleural effusions: a randomised controlled trial. Lancet. 2003 Apr 19;361(9366):1326-30.

51- Greillier L, Cavailles A, Fraticelli A, Scherpereel A, Barlesi F, Tassi G, Thomas P, Astoul P. Accuracy of pleural biopsy using thoracoscopy for the diagnosis of histologic subtype in patients with malignant pleural mesothelioma. Cancer. 2007 Nov 15;110(10):2248-52

52- Kao SC, Yan TD, Lee K, Burn J, Henderson DW, Klebe S, Kennedy C, Vardy J, Clarke S, van Zandwijk N, McCaughan BC. Accuracy of diagnostic biopsy for the histological subtype of malignant pleural mesothelioma. J Thorac Oncol. 2011 Mar;6(3):602-5.

53- Husain AN, Colby T, Ordonez N et al. Guidelines for pathologic diagnosis of malignant mesothelioma: 2012 update of the consensus statement from the International Mesothelioma Interest Group. Arch Pathol Lab Med 2013; 137: 647–667.

54- Henderson DW, Reid G, Kao SC et al. Challenges and controversies in the diagnosis of mesothelioma: Part 1. Cytology-only diagnosis, biopsies, immunohistochemistry, discrimination between mesothelioma and reactive mesothelial hyperplasia, and biomarkers. J Clin Pathol 2013; 66: 847–853.

55- Chirieac LR, Corson JM. Pathologic evaluation of malignant pleural mesothelioma. Semin Thorac Cardiovasc Surg. 2009 Summer;21(2):121-4.

56- Rusch VW. A proposed new international TNM staging system for malignant pleural mesothelioma. From the International Mesothelioma Interest Group. Chest 1995; 108: 1122–1128.

57- Scherpereel A, Astoul P, Baas P et al. Guidelines of the European Respiratory Society and the European Society of Thoracic Surgeons for the management of malignant pleural mesothelioma.

European Respiratory Society/European Society of Thoracic Surgeons Task Force. Eur Respir J. 2010 Mar;35(3):479-95.

58- Curran D, Sahmoud T, Therasse P, van Meerbeeck J, Postmus PE, Giaccone G. Prognostic factors in patients with pleural mesothelioma: The European Organization for Research and Treatment of Cancer experience. J Clin Oncol 1998;16:145–152. Eur Respir J. 2010 Mar;35(3):479-95.

59- Jaklitsch MT, Grondin SC, Sugarbaker DJ. Treatment of malignant mesothelioma. World J Surg. 2001 Feb;25(2):210-7.

60- Rusch VW. A phase II study of intrapleural immunochemotherapy, pleurectomy/decortication, radiotherapy, systemic chemotherapy, and long-term subcutaneous IL-2 in stage II-III malignant pleural mesothelioma. Eur J Cardiothorac Surg. 2007 Mar;31(3):534-5.

61- Rosenzweig KE. Current readings: improvements in intensity-modulated radiation therapy for malignant pleural mesothelioma. Semin Thorac Cardiovasc Surg. 2013 Autumn;25(3):245-50.

62- Flores RM. Surgical options in malignant pleural mesothelioma: extrapleural pneumonectomy or pleurectomy/decortication. Semin Thorac Cardiovasc Surg. 2009 Summer;21(2):149-53.

63- Kotova S, Wong RM, Cameron RB. New and emerging therapeutic options for malignant pleural mesothelioma: review of early clinical trials. Cancer Manag Res. 2015 Jan 23;7:51-63.

64- Papaspyros S, Papaspyros S. Surgical management of malignant pleural mesothelioma: impact of surgery on survival and quality of life-relation to chemotherapy, radiotherapy, and alternative therapies.ISRN Surg. 2014 Feb 3;2014:817203.

65- Rena O, Casadio C. Extrapleural pneumonectomy for early stage malignant pleural mesothelioma: a harmful procedure. Lung Cancer. 2012 Jul;77(1):151-5

66- van Zandwijk N, Clarke C, Henderson D, Musk AW, Fong K, Nowak A, Loneragan R, McCaughan B, Boyer M, Feigen M, Currow D, Schofield P, Nick Pavlakis BI, McLean J, Marshall H, Leong S, Keena V, Penman A. Guidelines for the diagnosis and treatment of malignant pleural mesothelioma. J Thorac Dis. 2013 Dec;5(6):E254-307.

67- Opitz I.Management of malignant pleural mesothelioma-The European experience. J Thorac Dis. 2014 May;6 Suppl 2:S238-52.

68- Baldini EH. Radiation therapy options for malignant pleural mesothelioma. Semin Thorac Cardiovasc Surg. 2009 Summer;21(2):159-63.

69- Van Schil PE, Opitz I, Weder W, De Laet C, Domen A, Lauwers P, Hendriks JM, Van Meerbeeck JP. Multimodal management of malignant pleural mesothelioma: where are we today? Eur Respir J. 2014 Sep;44(3):754-64.

70- Vogelzang NJ, Rusthoven JJ, Symanowski J, Denham C, Kaukel E, Ruffie P, Gatzemeier U, Boyer M, Emri S, Manegold C, Niyikiza C, Paoletti P. Phase III study of pemetrexed in combination with cisplatin versus cisplatin alone in patients with malignant pleural mesothelioma. J Clin Oncol. 2003 Jul 15;21(14):2636-44.

71- Katirtzoglou N, Gkiozos I, Makrilia N, Tsaroucha E, Rapti A, Stratakos G, Fountzilas G, Syrigos KN Carboplatin plus pemetrexed as first-line treatment of patients with malignant pleural mesothelioma: a phase II study. Clin Lung Cancer. 2010 Jan;11(1):30-5.

72- Ceresoli GL, Zucali PA, Mencoboni M, et al. Phase II study of pemetrexed and carboplatin plus bevacizumab as first-line therapy in malignant pleural mesothelioma. Br J Cancer. 2013 Aug 6;109(3):552-8.

73- Carbone M, Ferris LK, Baumann F, et al. BAP1 cancer syndrome: malignant mesothelioma, uveal and cutaneous melanoma, and MBAITs. J Transl Med. 2012; 10:179. Identification of germline mutations in the BRCA-associated protein 1 (BAP1) tumor suppressor gene as the cause of the “BAP1 cancer syndrome” that predispose to malignant mesothelioma and other cancers.

74- Wiesner T, Obenauf AC, Murali R, et al. Germline mutations in BAP1 predispose to melanocytic tumors. Nature genetics. 2011; 43(10):1018–1021

75- Piris A, Mihm MC Jr, Hoang MP. BAP1 and BRAFV600E expression in benign and malignant melanocytic proliferations. Hum Pathol. 2015; 46(2):239–245

76- Carbone M, Yang H, Pass HI, Krausz T, Testa JR, Gaudino G. BAP1 and cancer. Nature reviews. Cancer. 2013; 13(3):153–159.

77- Nasu M, Emi M, Pastorino S, et al. High Incidence of Somatic BAP1 Alterations in Sporadic Malignant Mesothelioma. J Thorac Oncol. 2015; 10(4):565–576. [PubMed: 25658628] * BAP1 is mutated in about 60% of sporadic malignant mesotheliomas making it the most commonly mutated gene in this malignancy.

78- Lo Iacono M, Monica V, Righi L, et al. Targeted next-generation sequencing of cancer genes in advanced stage malignant pleural mesothelioma: a retrospective study. J Thorac Oncol. 2015; 10(3):492–499.

79- Jensen DE, Proctor M, Marquis ST, et al. BAP1: a novel ubiquitin hydrolase which binds to the BRCA1 RING finger and enhances BRCA1-mediated cell growth suppression. Oncogene. 1998; 16(9):1097–1112.

80- Scheuermann JC, de Ayala Alonso AG, Oktaba K, et al. Histone H2A deubiquitinase activity of the Polycomb repressive complex PR-DUB. Nature. 2010; 465(7295):243–247.

81- Bolden JE, Peart MJ, Johnstone RW. Anticancer activities of histone deacetylase inhibitors. Nat Rev Drug Discov. 2006; 5(9):769–784. [PubMed: 16955068]

82- Cao XX, Mohuiddin I, Ece F, McConkey DJ, Smythe WR. Histone deacetylase inhibitor downregulation of bcl-xl gene expression leads to apoptotic cell death in mesothelioma. Am J Respir Cell Mol Biol. 2001; 25(5):562–568.

83- Neuzil J, Swettenham E, Gellert N. Sensitization of mesothelioma to TRAIL apoptosis by inhibition of histone deacetylase: role of Bcl-xL down-regulation. Biochem Biophys Res Commun. 2004; 314(1):186–191.

84- Nguyen DM, Schrump WD, Chen GA, et al. Abrogation of p21 expression by flavopiridol enhances depsipeptide-mediated apoptosis in malignant pleural mesothelioma cells. Clin Cancer Res. 2004; 10(5):1813–1825. [PubMed: 15014036]

85- Symanowski J, Vogelzang N, Zawel L, Atadja P, Pass H, Sharma S. A histone deacetylase inhibitor LBH589 downregulates XIAP in mesothelioma cell lines which is likely responsible for increased apoptosis with TRAIL. Journal of thoracic oncology : official publication of the International Association for the Study of Lung Cancer. 2009; 4(2):149–160.

86- Vandermeers F, Hubert P, Delvenne P, et al. Valproate, in combination with pemetrexed and cisplatin, provides additional efficacy to the treatment of malignant mesothelioma. Clin Cancer Res. 2009; 15(8):2818–2828. [PubMed: 19351772]

87- Krug LM, Kindler HL, Calvert H, et al. Vorinostat in patients with advanced malignant pleural mesothelioma who have progressed on previous chemotherapy (VANTAGE-014): a phase 3, double-blind, randomised, placebo-controlled trial. Lancet Oncol. 2015; 16(4):447–456. [PubMed: 25800891] * Negative results of the VANTAGE-014 study raise awareness about the relevance and predictively of preclinical outcomes.

88- Altomare DA, Vaslet CA, Skele KL, et al. A mouse model recapitulating molecular features of human mesothelioma. Cancer research. 2005; 65(18):8090–8095. [PubMed: 16166281

89- Bianchi AB, Mitsunaga SI, Cheng JQ, et al. High frequency of inactivating mutations in the neurofibromatosis type 2 gene (NF2) in primary malignant mesotheliomas. Proc Natl Acad Sci U S A. 1995; 92(24):10854–10858. [PubMed: 7479897]

90- Lopez-Lago MA, Okada T, Murillo MM, Socci N, Giancotti FG. Loss of the tumor suppressor gene NF2, encoding merlin, constitutively activates integrin-dependent mTORC1 signaling. Molecular and cellular biology. 2009; 29(15):4235–4249. [PubMed: 19451229]

91- Ou SH, Moon J, Garland LL, et al. SWOG S0722: phase II study of mTOR inhibitor everolimus (RAD001) in advanced malignant pleural mesothelioma (MPM). Journal of thoracic oncology : official publication of the International Association for the Study of Lung Cancer. 2015; 10(2):387–391.

92- Carracedo A, Ma L, Teruya-Feldstein J, et al. Inhibition of mTORC1 leads to MAPK pathway activation through a PI3K–dependent feedback loop in human cancer. J Clin Invest. 2008; 118(9):3065–3074. [PubMed: 18725988]

93- Kanteti R, Dhanasingh I, Kawada I, et al. MET and PI3K/mTOR as a potential combinatorial therapeutic target in malignant pleural mesothelioma. PLoS One. 2014; 9(9):e105919. [PubMed: 25221930]

94- Hirao T, Bueno R, Chen CJ, Gordon GJ, Heilig E, Kelsey KT. Alterations of the p16(INK4) locus in human malignant mesothelial tumors. Carcinogenesis. 2002; 23(7):1127–1130. [PubMed: 12117769]

95- Sekido Y, Pass HI, Bader S, et al. Neurofibromatosis type 2 (NF2) gene is somatically mutated in mesothelioma but not in lung cancer. Cancer research. 1995; 55(6):1227–1231. [PubMed: 7882313

96- Musti M, Kettunen E, Dragonieri S, et al. Cytogenetic and molecular genetic changes in malignant mesothelioma. Cancer Genet Cytogenet. 2006; 170(1):9–15. [PubMed: 16965949]

97- Altomare DA, Menges CW, Xu J, et al. Losses of both products of the Cdkn2a/Arf locus contribute to asbestos-induced mesothelioma development and cooperate to accelerate tumorigenesis. PloS one. 2011; 6(4):e18828. [PubMed: 21526190]

98- Tada Y, Shimada H, Hiroshima K, Tagawa M. A potential therapeutic strategy for malignant mesothelioma with gene medicine. Biomed Res Int. 2013; 2013:572609. [PubMed: 23484132]

99- Frizelle SP, Grim J, Zhou J, et al. Re-expression of p16INK4a in mesothelioma cells results in cell cycle arrest, cell death, tumor suppression and tumor regression. Oncogene. 1998; 16(24):3087–3095. [PubMed: 9671387]

100- Frizelle SP, Kratzke MG, Carreon RR, et al. Inhibition of both mesothelioma cell growth and Cdk4 activity following treatment with a TATp16INK4a peptide. Anticancer research. 2008; 28(1A):1–7. [PubMed: 18383817]

101- Brevet M, Shimizu S, Bott MJ, et al. Coactivation of receptor tyrosine kinases in malignant mesothelioma as a rationale for combination targeted therapy. Journal of thoracic oncology : official publication of the International Association for the Study of Lung Cancer. 2011; 6(5):864–874.

102- Zhang J, Yang PL, Gray NS. Targeting cancer with small molecule kinase inhibitors. Nature reviews. Cancer. 2009; 9(1):28–39. [PubMed: 19104514]

103- Yano S, Li Q, Wang W, et al. Antiangiogenic therapies for malignant pleural mesothelioma. Front Biosci (Landmark Ed). 2011; 16:740–748. [PubMed: 21196199]

104- Strizzi L, Catalano A, Vianale G, et al. Vascular endothelial growth factor is an autocrine growth factor in human malignant mesothelioma. J Pathol. 2001; 193(4):468–475. [PubMed: 11276005]

105- Muhsin M, Graham J, Kirkpatrick P. Bevacizumab. Nat Rev Drug Discov. 2004; 3(12):995–996. [PubMed: 15645606]

106- Ceresoli GL, Zucali PA, Mencoboni M, et al. Phase II study of pemetrexed and carboplatin plus bevacizumab as first-line therapy in malignant pleural mesothelioma. British journal of cancer. 2013; 109(3):552–558. [PubMed: 23860535]

107- Dowell JE, Dunphy FR, Taub RN, et al. A multicenter phase II study of cisplatin, pemetrexed, and bevacizumab in patients with advanced malignant mesothelioma. Lung Cancer. 2012; 77(3):567–571. [PubMed: 22770372]

108- Kindler HL, Karrison TG, Gandara DR, et al. Multicenter, double-blind, placebo-controlled, randomized phase II trial of gemcitabine/cisplatin plus bevacizumab or placebo in patients with malignant mesothelioma. J Clin Oncol. 2012; 30(20):2509–2515. [PubMed: 22665541]

109- Garland LL, Rankin C, Gandara DR, et al. Phase II study of erlotinib in patients with malignant pleural mesothelioma: a Southwest Oncology Group Study. J Clin Oncol. 2007; 25(17):2406–2413. [PubMed: 17557954]

110- Govindan R, Kratzke RA, Herndon JE 2nd, et al. Gefitinib in patients with malignant mesothelioma: a phase II study by the Cancer and Leukemia Group B. Clin Cancer Res. 2005; 11(6):2300–2304. [PubMed: 15788680]

111- Jackman DM, Kindler HL, Yeap BY, et al. Erlotinib plus bevacizumab in previously treated patients with malignant pleural mesothelioma. Cancer. 2008; 113(4):808–814. [PubMed: 18543326]

112- Strizzi L, Vianale G, Catalano A, Muraro R, Mutti L, Procopio A. Basic fibroblast growth factor in mesothelioma pleural effusions: correlation with patient survival and angiogenesis. Int J Oncol. 2001; 18(5):1093–1098. [PubMed: 11295061]

113- Schelch K, Hoda MA, Klikovits T, et al. Fibroblast growth factor receptor inhibition is active against mesothelioma and synergizes with radio- and chemotherapy. Am J Respir Crit Care Med. 2014; 190(7):763–772. [PubMed: 25188816]

114- Stapelberg M, Gellert N, Swettenham E, et al. Alpha-tocopheryl succinate inhibits malignant mesothelioma by disrupting the fibroblast growth factor autocrine loop: mechanism and the role of oxidative stress. The Journal of biological chemistry. 2005; 280(27):25369–25376. [PubMed: 15878867]

115- Matsumoto K, Nakamura T. NK4 (HGF-antagonist/angiogenesis inhibitor) in cancer biology and therapeutics. Cancer Sci. 2003; 94(4):321–327. [PubMed: 12824898]

116- Leon LG, Gemelli M, Sciarrillo R, Avan A, Funel N, Giovannetti E. Synergistic activity of the c-Met and tubulin inhibitor tivantinib (ARQ197) with pemetrexed in mesothelioma cells. Curr Drug Targets. 2014; 15(14):1331–1340. [PubMed: 25483224]

117- Robinson C, Callow M, Stevenson S, et al. Serologic responses in patients with malignant

mesothelioma: evidence for both public and private specificities. Am J Respir Cell Mol Biol 2000,22: 550-556.

118- Boutin C, Viallat JR, Van Zandwijk N, et al. Activity of intrapleural recombinant gamma-interferon in malignant mesothelioma. Cancer 67: 2033-2037, 1991.

119- Goey S, Eggermont A, Punt C, et al. Intrapleural administration of interleukin 2 in pleural

mesothelioma: a phase I-II study. Br J Cancer 1995 72: 1283-1288.

120- Parra HS, Tixi L, Latteri F, et al. Combined regimen of cisplatin, doxorubicin, and alpha-2b

interferon in the treatment of advanced malignant pleural mesothelioma: a Phase II multicenter trial of the Italian Group on Rare Tumors (GITR) and the Italian Lung Cancer Task Force (FONICAP) Cancer 2001 92: 650-656.

121- Hanahan D, Weinberg RA. Hallmarks of cancer: the next generation. Cell. 2011; 144(5):646–674. [PubMed: 21376230]

122- Pardoll DM. The blockade of immune checkpoints in cancer immunotherapy. Nat Rev Cancer. 2012; 12(4):252–264. [PubMed: 22437870]

123- Mansfield AS, Roden AC, Peikert T, et al. B7-H1 expression in malignant pleural mesothelioma is associated with sarcomatoid histology and poor prognosis. Journal of thoracic oncology : official publication of the International Association for the Study of Lung Cancer. 2014; 9(7):1036–1040.

124- Cedres S, Ponce-Aix S, Zugazagoitia J, et al. Analysis of expression of programmed cell death 1 ligand 1 (PD-L1) in malignant pleural mesothelioma (MPM). PloS one. 2015; 10(3):e0121071. [PubMed: 25774992]

125- Calabro L, Morra A, Fonsatti E, et al. Tremelimumab for patients with chemotherapy-resistant advanced malignant mesothelioma: an open-label, single-arm, phase 2 trial. Lancet Oncol. 2013; 14(11):1104–1111. [PubMed: 24035405]

126- Calabro L, Morra A, Fonsatti E, et al. Efficacy and safety of an intensified schedule of tremelimumab for chemotherapy-resistant malignant mesothelioma: an open-label, single-arm, phase 2 study. Lancet Respir Med. 2015; 3(4):301–309. [PubMed: 25819643] ** The CTLA-4 inhibitor, tremelimumab, showed clinical and immunological activity in patients with advanced malignant mesothelioma, and a good safety profile.

127- Lotze MT, Tracey KJ. High-mobility group box 1 protein (HMGB1): nuclear weapon in the immune arsenal. Nat Rev Immunol. 2005 Apr;5(4):331-42.

128- Müller S, Scaffidi P, Degryse B, Bonaldi T, Ronfani L, Agresti A, Beltrame M, Bianchi ME. New EMBO members' review: the double life of HMGB1 chromatin protein: architectural factor and extracellular signal. EMBO J. 2001 Aug 15;20(16):4337-40.

129- Goodwin GH, Johns EW. The isolation and purification of the high mobility group (HMG) nonhistone chromosomal proteins. Methods Cell Biol. 1977;16:257-67.

130-Lotze MT, Tracey KJ. High-mobility group box 1 protein (HMGB1): nuclear weapon in the immune

arsenal. Nat Rev Immunol 2005;5:331–342. [PubMed: 15803152]

131-Dong XD, Ito N, Lotze MT, Demarco RA, Popovic P, Shand SH, Watkins S, Winikoff S, Brown CK,

Bartlett DL, Zeh HJ 3rd. High Mobility Group Box I (HMGB1) Release From Tumor Cells After

Treatment: Implications for Development of Targeted Chemoimmunotherapy. J Immunother (1997)

2007;30:596–606.

132- Scaffidi P, Misteli T, Bianchi ME. Release of chromatin protein HMGB1 by necrotic cells triggers

inflammation. Nature 2002;418:191–195. [PubMed: 12110890]

133- Land W, Schneeberger H, Schleibner S, Illner WD, Abendroth D, Rutili G, Arfors KE, Messmer K.The beneficial effect of human recombinant superoxide dismutase on acute and chronic rejection

events in recipients of cadaveric renal transplants. Transplantation 1994;57:211–217. [PubMed:

8310510]

134. Matzinger P. Tolerance, danger, and the extended family. Annu Rev Immunol 1994;12:991–1045.

[PubMed: 8011301]

135- Wang H, Yang H, Tracey KJ. Extracellular role of HMGB1 in inflammation and sepsis. J Intern Med. 2004 Mar;255(3):320-31.

136- Enokido Y1, Yoshitake A, Ito H, Okazawa H. Age-dependent change of HMGB1 and DNA double-strand break accumulation in mouse brain. Biochem Biophys Res Commun. 2008 Nov 7;376(1):128-33.

137- Ellerman JE, Brown CK, de Vera M, Zeh HJ, Billiar T, Rubartelli A, Lotze MT. Masquerader: high mobility group box-1 and cancer. Clin Cancer Res. 2007 May 15;13(10):2836-48.

138- Lotze MT, DeMarco RA. Dealing with death: HMGB1 as a novel target for cancer therapy Curr Opin Investig Drugs. 2003 Dec;4(12):1405-9.

139- Lange SS1, Vasquez KM. HMGB1: the jack-of-all-trades protein is a master DNA repair mechanic. Mol Carcinog. 2009 Jul;48(7):571-80.

140- Jantzen HM1, Admon A, Bell SP, Tjian R. Nucleolar transcription factor hUBF contains a DNA-binding motif with homology to HMG proteins. Nature. 1990 Apr 26;344(6269):830-6.

141- Travers AA. Priming the nucleosome: a role for HMGB proteins? EMBO Rep. 2003; 4:131–6.

142- Stros M1, Muselíková-Polanská E, Pospísilová S, Strauss F. High-affinity binding of tumor-suppressor protein p53 and HMGB1 to hemicatenated DNA loops. Biochemistry. 2004 Jun 8;43(22):7215-25.

143- Uramoto H1, Izumi H, Nagatani G, Ohmori H, Nagasue N, Ise T, Yoshida T, Yasumoto K, Kohno K. Physical interaction of tumour suppressor p53/p73 with CCAAT-binding transcription factor 2 (CTF2) and differential regulation of human high-mobility group 1 (HMG1) gene expression. Biochem J. 2003 Apr 15;371(Pt 2):301-10.

144- Jiao Y1, Wang HC, Fan SJ. Growth suppression and radiosensitivity increase by HMGB1 in breast cancer. Acta Pharmacol Sin. 2007 Dec;28(12):1957-67.

145- Agresti A1, Lupo R, Bianchi ME, Müller S. HMGB1 interacts differentially with members of the Rel family of transcription factors. Biochem Biophys Res Commun. 2003 Mar 7;302(2):421-6

146- Banerjee S1, Kundu TK. The acidic C-terminal domain and A-box of HMGB-1 regulates p53-mediated transcription. Nucleic Acids Res. 2003 Jun 15;31(12):3236-47.

147- Lange SS, Vasquez KM. HMGB1: the jack-of-all-trades protein is a master DNA repair mechanic. Mol Carcinog. 2009; 48:571–80. [PubMed: 19360789]

148- Einck L, Soares N, Bustin M. Localization of HMG chromosomal proteins in the nucleus and cytoplasm by microinjection of functional antibody fragments into living fibroblasts. Exp Cell Res. 1984; 152(2):287–301

149- Kuehl L, Salmond B, Tran L. Concentrations of high-mobility-group proteins in the nucleus and cytoplasm of several rat tissues. J Cell Biol. 1984; 99(2):648–654.

150- Tang D, Kang R, Livesey KM, Cheh CW, Farkas A, Loughran P, Hoppe G, Bianchi ME, Tracey KJ, Zeh HJ 3rd, Lotze MT. Endogenous HMGB1 regulates autophagy. J Cell Biol. 2010c; 190(5):881–892.

151-Dintilhac A, Bernues J. HMGB1 interacts with many apparently unrelated proteins by recognizing short amino acid sequences. J Biol Chem. 2002; 277(9):7021–7028. [PubMed: 11748221]

152- Lee H, Shin N, Song M, Kang UB, Yeom J, Lee C, Ahn YH, Yoo JS, Paik YK, Kim H. Analysis of nuclear high mobility group box 1 (HMGB1)-binding proteins in colon cancer cells: clustering with proteins involved in secretion and extranuclear function. J Proteome Res. 2010a; 9(9):4661–4670.

153- Qin S, Wang H, Yuan R, Li H, Ochani M, Ochani K, et al. Role of HMGB1 in apoptosis-mediated sepsis lethality. J Exp Med. 2006; 203:1637–42.

154- Lotze MT, Tracey KJ. High-mobility group box 1 protein (HMGB1): nuclear weapon in the immune arsenal. Nat Rev Immunol. 2005; 5:331–42. [PubMed: 15803152]

155- Tang D, Kang R, Coyne CB, Zeh HJ, Lotze MT. PAMPs and DAMPs: signals that spur autophagy and immunity. Immunol Rev. 2012; 249:158–75. [PubMed: 22889221]

156-Tang D, Billiar TA, Lotze MT. A Janus Tale of Two Active HMGB1 Redox States. Mol Med. 2012; 18:1360–1362. [PubMed: 23073660]

157- Zimmermann K, Volkel D, Pable S, Lindner T, Kramberger F, Bahrami S, Scheiflinger F. Native versus recombinant high-mobility group B1 proteins: functional activity in vitro. Inflammation. 2004; 28(4):221–229.

158- Chen GY, Tang J, Zheng P, Liu Y. CD24 and Siglec-10 selectively repress tissue damage-induced

immune responses. Science. 2009; 323:1722–5. [PubMed: 19264983]

159- Chiba S, Baghdadi M, Akiba H, Yoshiyama H, Kinoshita I, Dosaka-Akita H, et al. Tumorinfiltrating

DCs suppress nucleic acid-mediated innate immune responses through interactions

between the receptor TIM-3 and the alarmin HMGB1. Nat Immunol. 2012; 13:832–42. [PubMed:

22842346]

160- Hori O, Brett J, Slattery T, Cao R, Zhang J, Chen JX, et al. The receptor for advanced glycation

end products (RAGE) is a cellular binding site for amphoterin. Mediation of neurite outgrowth and

co-expression of rage and amphoterin in the developing nervous system. J Biol Chem. 1995;

270:25752–61. [PubMed: 7592757]

161- Tian J, Avalos AM, Mao SY, Chen B, Senthil K, Wu H, et al. Toll-like receptor 9-dependent

activation by DNA-containing immune complexes is mediated by HMGB1 and RAGE. Nat Immunol. 2007; 8:487–96. [PubMed: 17417641]

162- Orlova VV, Choi EY, Xie C, Chavakis E, Bierhaus A, Ihanus E, et al. A novel pathway of HMGB1-mediated inflammatory cell recruitment that requires Mac-1-integrin. Embo J. 2007; 26:1129–39. [PubMed: 17268551]

163- Yang H, Hreggvidsdottir HS, Palmblad K, Wang H, Ochani M, Li J, et al. A critical cysteine is required for HMGB1 binding to Toll-like receptor 4 and activation of macrophage cytokine release. Proc Natl Acad Sci U S A. 2010; 107:11942–7. [PubMed: 20547845]

164- Tsung A, Sahai R, Tanaka H, Nakao A, Fink MP, Lotze MT, et al. The nuclear factor HMGB1 mediates hepatic injury after murine liver ischemia-reperfusion. J Exp Med. 2005; 201:1135–43. [PubMed: 15795240]

165- Tang D, Kang R, Zeh HJ, Lotze MT. High-mobility group box 1, oxidative stress, and disease. Antioxid Redox Signal. 2011; 14:1315–35. [PubMed: 20969478]

166- Tang D, Shi Y, Kang R, Li T, Xiao W, Wang H, et al. Hydrogen peroxide stimulates macrophages and monocytes to actively release HMGB1. J Leukoc Biol. 2007; 81:741–7. [PubMed: 17135572]

167- Venereau E, Casalgrandi M, Schiraldi M, Antoine DJ, Cattaneo A, De Marchis F, et al. Mutually exclusive redox forms of HMGB1 promote cell recruitment or proinflammatory cytokine release. J Exp Med. 2012; 209:1519–28. [PubMed: 22869893]

168- Schiraldi M, Raucci A, Munoz LM, Livoti E, Celona B, Venereau E, et al. HMGB1 promotes recruitment of inflammatory cells to damaged tissues by forming a complex with CXCL12 and signaling via CXCR4. J Exp Med. 2012; 209:551–63. [PubMed: 22370717]

169-Tang D, Kang R, Cheh CW, Livesey KM, Liang X, Schapiro NE, et al. HMGB1 release and redox regulates autophagy and apoptosis in cancer cells. Oncogene. 2010; 29:5299–310. [PubMed: 20622903]

170- Jube S, Rivera ZS, Bianchi ME, Powers A, Wang E, Pagano I, et al. Cancer cell secretion of the DAMP protein HMGB1 supports progression in malignant mesothelioma. Cancer Res. 2012; 72:3290–301. [PubMed: 22552293]

171- . Kang R, Tang D, Schapiro NE, Loux T, Livesey KM, Billiar TR, et al. The HMGB1/RAGE inflammatory pathway promotes pancreatic tumor growth by regulating mitochondrial bioenergetics. Oncogene. 2013

172-. Tang D, Kang R, Livesey KM, Kroemer G, Billiar TR, Van Houten B, et al. High-mobility group box 1 is essential for mitochondrial quality control. Cell Metabolism. 2011; 13:701–11. [PubMed: 21641551]

173- Gebhardt C, Riehl A, Durchdewald M, Nemeth J, Furstenberger G, Muller-Decker K, et al. RAGE signaling sustains inflammation and promotes tumor development. J Exp Med. 2008; 205:275–85. [PubMed: 18208974]

174- Mittal D, Saccheri F, Venereau E, Pusterla T, Bianchi ME, Rescigno M. TLR4-mediated skin carcinogenesis is dependent on immune and radioresistant cells. Embo J. 2010; 29:2242–52. [PubMed: 20526283]

175- 39. Kuniyasu H, Oue N, Wakikawa A, Shigeishi H, Matsutani N, Kuraoka K, et al. Expression of receptors for advanced glycation end-products (RAGE) is closely associated with the invasive and metastatic activity of gastric cancer. J Pathol. 2002; 196:163–70. [PubMed: 11793367]

176-. Sasahira T, Akama Y, Fujii K, Kuniyasu H. Expression of receptor for advanced glycation end products and HMGB1/amphoterin in colorectal adenomas. Virchows Arch. 2005; 446:411–5. [PubMed: 15789216]

177- Taguchi A, Blood DC, del Toro G, Canet A, Lee DC, Qu W, et al. Blockade of RAGE-amphoterin signalling suppresses tumour growth and metastases. Nature. 2000; 405:354–60. [PubMed: 10830965]

178- Huttunen HJ, Fages C, Kuja-Panula J, Ridley AJ, Rauvala H. Receptor for advanced glycation end products-binding COOH-terminal motif of amphoterin inhibits invasive migration and metastasis. Cancer Res. 2002; 62:4805–11. [PubMed: 12183440]

179- Campana L, Bosurgi L, Rovere-Querini P. HMGB1: a two-headed signal regulating tumor progression and immunity. Current opinion in immunology. 2008; 20:518–23. [PubMed: 18599281]

180- Kusume A, Sasahira T, Luo Y, Isobe M, Nakagawa N, Tatsumoto N, et al. Suppression of dendritic cells by HMGB1 is associated with lymph node metastasis of human colon cancer. Pathobiology. 2009; 76:155–62. [PubMed: 19571604]

181- Liu Z, Falo LD Jr, You Z. Knockdown of HMGB1 in tumor cells attenuates their ability to induce regulatory T cells and uncovers naturally acquired CD8 T cell-dependent antitumor immunity. J Immunol. 2011; 187:118–25. [PubMed: 21642542]

182- Jiao Y, Wang HC, Fan SJ. Growth suppression and radiosensitivity increase by HMGB1 in breast cancer. Acta Pharmacol Sin. 2007; 28:1957–67. [PubMed: 18031610]

183- Zhao Z, Oh S, Li D, Ni D, Pirooz SD, Lee JH, et al. A Dual Role for UVRAG in Maintaining Chromosomal Stability Independent of Autophagy. Dev Cell. 2012

184- Degenhardt K, Mathew R, Beaudoin B, Bray K, Anderson D, Chen G, et al. Autophagy promotes tumor cell survival and restricts necrosis, inflammation, and tumorigenesis. Cancer Cell. 2006; 10:51–64. [PubMed: 16843265]

185- Mathew R, Kongara S, Beaudoin B, Karp CM, Bray K, Degenhardt K, et al. Autophagy suppresses tumor progression by limiting chromosomal instability. Genes Dev. 2007; 21:1367–81. [PubMed: 17510285]

186- Takahashi Y, Hori T, Cooper TK, Liao J, Desai N, Serfass JM, et al. Bif-1 haploinsufficiency promotes chromosomal instability and accelerates Myc-driven lymphomagenesis via suppression of mitophagy. Blood. 2013

187- Suzuki Y, Mimura K, Yoshimoto Y, Watanabe M, Ohkubo Y, Izawa S, et al. Immunogenic tumor cell death induced by chemoradiotherapy in patients with esophageal squamous cell carcinoma. Cancer Res. 2012; 72:3967–76. [PubMed: 22700877]

188- Fucikova J, Kralikova P, Fialova A, Brtnicky T, Rob L, Bartunkova J, et al. Human tumor cells killed by anthracyclines induce a tumor-specific immune response. Cancer Res. 2011; 71:4821–33. [PubMed: 21602432]

189- Apetoh L, Ghiringhelli F, Tesniere A, Obeid M, Ortiz C, Criollo A, et al. Toll-like receptor 4- dependent contribution of the immune system to anticancer chemotherapy and radiotherapy. Nat Med. 2007; 13:1050–9. [PubMed: 17704786]

190- Luo Y, Chihara Y, Fujimoto K, Sasahira T, Kuwada M, Fujiwara R, et al. High mobility group box 1 released from necrotic cells enhances regrowth and metastasis of cancer cells that have survived chemotherapy. Eur J Cancer. 2012

191- Kang R, Tang D, Schapiro NE, Livesey KM, Farkas A, Loughran P, et al. The receptor for advanced glycation end products (RAGE) sustains autophagy and limits apoptosis, promoting pancreatic tumor cell survival. Cell Death Differ. 2010; 17:666–76. [PubMed: 19834494]

192- Huang J, Ni J, Liu K, Yu Y, Xie M, Kang R, et al. HMGB1 promotes drug resistance in osteosarcoma. Cancer Res. 2012; 72:230–8. [PubMed: 22102692]

193- Livesey KM, Kang R, Vernon P, Buchser W, Loughran P, Watkins SC, et al. p53/HMGB1 complexes regulate autophagy and apoptosis. Cancer Res. 2012; 72:1996–2005. [PubMed: 22345153]

194- Rowell JP, Simpson KL, Stott K, Watson M, Thomas JO. HMGB1-Facilitated p53 DNA Binding Occurs via HMG-Box/p53 Transactivation Domain Interaction, Regulated by the Acidic Tail. Structure. 2012; 20:2014–24. [PubMed: 23063560]

195- Liu L, Yang M, Kang R, Wang Z, Zhao Y, Yu Y, et al. HMGB1-induced autophagy promotes chemotherapy resistance in leukemia cells. Leukemia. 2011; 25:23–31. [PubMed: 20927132]

196- Ohndorf UM, Rould MA, He Q, Pabo CO, Lippard SJ. Basis for recognition of cisplatin-modified

DNA by high-mobility-group proteins. Nature. 1999; 399:708–12. [PubMed: 10385126]

197- Liang X, Chavez AR, Schapiro NE, Loughran P, Thorne SH, Amoscato AA, et al. Ethyl pyruvate administration inhibits hepatic tumor growth. J Leukoc Biol. 2009; 86:599–607. [PubMed: 19584311].

198- Carbone M, Yang H. Molecular pathways: targeting mechanisms of asbestos and erionite carcinogenesis in mesothelioma. Clin Cancer Res. 2012; 18(3):598–604. [PubMed: 22065079]

199- Matsuzaki H1, Maeda M, Lee S, Nishimura Y, Kumagai-Takei N, Hayashi H, Yamamoto S, Hatayama T, Kojima Y, Tabata R, Kishimoto T, Hiratsuka J, Otsuki T. Asbestos-induced cellular and molecular alteration of immunocompetent cells and their relationship with chronic inflammation and carcinogenesis. J Biomed Biotechnol. 2012.

200- Rui Kang, Ruochan Chen, Qiuhong Zhang, Wen Hou, Sha Wu,1 Lizhi Cao,2 Jin Huang,3 Yan Yu,2 Xue-gong Fan,4 Zhengwen Yan,1,5 Xiaofang Sun,6 Haichao Wang,7 Qingde Wang,1 Allan Tsung,1 Timothy R. Billiar,1 Herbert J. Zeh, III,1 Michael T. Lotze,1 and Daolin Tang. HMGB1 in Health and Disease. Mol Aspects Med.; 2014; 0:1-116.

201-Jensen DE, Proctor M, Marquis ST, et al. BAP1: a novel ubiquitin hydrolase which binds to the BRCA1 RING finger and enhances BRCA1-mediated cell growth suppression. Oncogene. 1998; 16(9):1097–1112. [PubMed: 9528852]

202- Ventii KH, Devi NS, Friedrich KL, et al. BRCA1-associated protein-1 is a tumor suppressor that requires deubiquitinating activity and nuclear localization. Cancer research. 2008; 68(17):6953–6962. [PubMed: 18757409]

203- Misaghi S, Ottosen S, Izrael-Tomasevic A, et al. Association of C-terminal ubiquitin hydrolase BRCA1-associated protein 1 with cell cycle regulator host cell factor 1. Molecular and cellular biology. 2009; 29(8):2181–2192. [PubMed: 19188440]

204- Machida YJ, Machida Y, Vashisht AA, Wohlschlegel JA, Dutta A. The deubiquitinating enzyme BAP1 regulates cell growth via interaction with HCF-1. J Biol Chem. 2009; 284(49):34179–34188. [PubMed: 19815555]

205- Eletr ZM, Wilkinson KD. An emerging model for BAP1's role in regulating cell cycle progression. Cell Biochem Biophys. 2011; 60(1–2):3–11. [PubMed: 21484256]

206- Sporn MB, Liby KT (2005) Cancer chemoprevention: scientific promise, clinical uncertainty. Nat Clin Pract Oncol 2(10): 518-525.

207- Finn OJ (2012) Immuno-oncology: understanding the function and dysfunction of the immune system in cancer. Ann Oncol 23(suppl 8).

208- Lollini PL, Cavallo F, Nanni P, Guido F (2006) Vaccines for tumour prevention. Nat Rev Cancer 6: 204-216.

209- Murphy JF (2015) Frontiers in Cancer Immunotherapy. In: Nima Rezaei (Ed.), Cancer Immunology: Bench to Bedside Immunotherapy of Cancers, Springer, USA, p. 1-22.

210- M. R. Davis, L. S. Manning, D. Whitaker, M. J. Garlepp, B. W. S. Robinson. Establishment of a murine model of malignant mesothelioma. Experimental cancer. 1992.

211- Richmond A, Su Y (2008) Mouse xenograft models vs GEM models for human cancer therapeutics. Dis Model Mech. 1(2-3): 78-82.

212- Kelland LR (2004) "Of mice and men": values and liabilities of the athymic nude mouse model in anticancer drug development. Eur J Cancer 40(6): 827-836.

213- Sausville EA, Newell DR (2004) Preclinical models in cancer drug discovery and development. Eur J Cancer 40: 783-784.

214- Anderson MJ, Shafer-Weaver K, Greenberg NM, Hurwitz AA (2007) Tolerization of tumor-specific T cells despite efficient initial priming in a primary murine model of prostate cancer. J Immunol 178(3): 1268-1276.

215- Gavalas NG, Karadimou A, Dimopoulos MA, Bamias A (2010) Immune response in ovarian cancer: how is the immune system involved in prognosis and therapy: potential for treatment utilization. Clin Dev Immunol.

216- Rangarajan A, Weinberg RA. Opinion: Comparative biology of mouse versus human cells: modelling human cancer in mice. Nat Rev Cancer. 2003; 3:952–959.

217- Bosma GC, Custer RP, Bosma MJ. A severe combined immunodeficiency mutation in the mouse.

Nature. 1983; 301:527–530. [PubMed: 6823332]

218- Ito M, et al. NOD/SCID/gamma(c)(null) mouse: an excellent recipient mouse model for engraftment of human cells. Blood. 2002; 100:3175–3182. [PubMed: 12384415]

219- Lin, Hui Xue, Yuwei Wang, Rebecca Wu, Akira Watahiki, Xin Dong, Hongwei Cheng, Alexander W Wyatt, Colin C Collins, Peter W Gout, Yuzhuo Wang. Next generation patient-derived prostate cancer xenograft models.

220- Quintana E, et al. Efficient tumour formation by single human melanoma cells. Nature. 2008; 456:593–598.

221- Zhou BB, et al. Tumour-initiating cells: challenges and opportunities for anticancer drug discovery.

Nat Rev Drug Discov. 2009; 8(10):806–23. [PubMed: 19794444]

222- Cancer multidrug resistance. Nat Biotechnol. 2000; 18(Suppl):IT18–20. [PubMed: 11221708]

223- Gillet JP, et al. Redefining the relevance of established cancer cell lines to the study of mechanisms

of clinical anti-cancer drug resistance. Proc Natl Acad Sci U S A. 2011; 108(46):18708–13.

[PubMed: 22068913]

224- Gazdar AF, Gao B, Minna JD. Lung cancer cell lines: Useless artifacts or invaluable tools for

medical science? Lung Cancer. 2010; 68(3):309–18. [PubMed: 20079948]

225- Kirk R. Genetics: Personalized medicine and tumour heterogeneity. Nat Rev Clin Oncol. 2012; 9(5):

250. [PubMed: 22430855]

226- Lima SC, Hernandez-Vargas H, Herceg Z. Epigenetic signatures in cancer: Implications for the

control of cancer in the clinic. Curr Opin Mol Ther. 2010; 12(3):316–24. [PubMed: 20521220]

227- Toyota M, Issa JP. Epigenetic changes in solid and hematopoietic tumors. Semin Oncol. 2005;

32(5):521–30. [PubMed: 16210093]

228. Schilsky RL. Personalized medicine in oncology: the future is now. Nat Rev Drug Discov. 2010;

9(5):363–6. [PubMed: 20431568]

229. Mitsiades CS, et al. Future directions of next-generation novel therapies, combination approaches,

and the development of personalized medicine in myeloma. J Clin Oncol. 2011; 29(14):1916–23.

[PubMed: 21482978]

230. Trusheim MR, et al. Quantifying factors for the success of stratified medicine. Nat Rev Drug

Discov. 2011; 10(11):817–33. [PubMed: 22037040]

231. Chopra DP, Yeh K, Brockman RW. Isolation and characterization of epithelial cell types from the

normal rat colon. Cancer Res. 1981; 41(1):168–75. [PubMed: 7448757]

232. McCallum HM, Lowther GW. Long-term culture of primary breast cancer in defined medium.

Breast Cancer Res Treat. 1996; 39(3):247–59. [PubMed: 8877005]

233. Castell JV, Gomez-Lechon MJ. Liver cell culture techniques. Methods Mol Biol. 2009; 481:35–46.

[PubMed: 19096795]

234. Burdall SE, et al. Breast cancer cell lines: friend or foe? Breast Cancer Res. 2003; 5(2):89–95.

[PubMed: 12631387]

235. Gazdar AF, et al. Characterization of paired tumor and non-tumor cell lines established from

patients with breast cancer. Int J Cancer. 1998; 78(6):766–74. [PubMed: 9833771]

236. Wurdak H, et al. An RNAi screen identifies TRRAP as a regulator of brain tumor- initiating cell

differentiation. Cell Stem Cell. 2010; 6(1):37–47. [PubMed: 20085741]

237. Dhanabal M, et al. Endostatin induces endothelial cell apoptosis. J Biol Chem. 1999; 274(17):

11721–6. [PubMed: 10206987]

238- Lee, G. Y., Kenny, P. A., Lee, E. H. & Bissell, M. J. Three-dimensional culture models of normal and malignant breast epithelial cells. Nat. Methods 4, 359–365 (2007).

239- Thoma, C. R., Zimmermann, M., Agarkova, I., Kelm, J. M. & Krek, W. 3D cell culture systems modeling tumor growth determinants in cancer target discovery. Adv. Drug Deliv. Rev. 69-70, 29–41 (2014).

240- Kimlin, L. C., Casagrande, G. & Virador, V. M. In vitro three-dimensional (3D) models in cancer research: an update. Mol. Carcinog. 52, 167–182 (2013).

241- Baker, B. M. & Chen, C. S. Deconstructing the third dimension: how 3D culture microenvironments alter cellular cues. J. Cell. Sci. 125, 3015–3024 (2012).

242- Wartenberg, M. et al. Regulation of the multidrug resistance transporter P-glycoprotein in multicellular tumor spheroids by hypoxia-inducible factor (HIF-1) and reactive oxygen species. FASEB J. 17, 503–505 (2003).

243- Minchinton, A. I. & Tannock, I. F. Drug penetration in solid tumours. Nat. Rev. Cancer. 6, 583–592 (2006).

244- Weiswald, L. B., Bellet, D. & Dangles-Marie, V. Spherical cancer models in tumor biology. Neoplasia 17, 1–15 (2015).

245- Yamada, K. M. & Cukierman, E. Modeling tissue morphogenesis and cancer in 3D. Cell 130, 601–610 (2007).

246- Friedrich, J., Seidel, C., Ebner, R. & Kunz-Schughart, L. A. Spheroid-based drug screen: considerations and practical approach. Nat. Protoc. 4, 309–324 (2009).

247- Jaganathan, H. et al. Three-dimensional in vitro co-culture model of breast tumor using magnetic levitation. Sci. Rep. 4, 6468 (2014).

248- Hay, M., Thomas, D.W., Craighead, J.L., Economides, C., and Rosenthal, J. (2014). Clinical development success rates for investigational drugs. Nat. Biotechnol. 32, 40–51.

249- Clevers, H. (2016). Modeling development and disease with organoids. Cell 165, 1586–1597.

250- Sato, T., Vries, R.G., Snippert, H.J., van de Wetering, M., Barker, N., Stange, D.E., van Es, J.H., Abo, A., Kujala, P., Peters, P.J., et al. (2009). Single Lgr5 stem cells build crypt-villus structures in vitro without a mesenchymal niche. Nature 459, 262–265.

251- Sato, T., Stange, D.E., Ferrante, M., Vries, R.G., Van Es, J.H., Van den Brink, S., Van Houdt, W.J., Pronk, A., Van Gorp, J., Siersema, P.D., et al. (2011).

252- Drost, J., van Jaarsveld, R.H., Ponsioen, B., Zimberlin, C., van Boxtel, R., Buijs, A., Sachs, N., Overmeer, R.M., Offerhaus, G.J., Begthel, H., et al. (2015). Sequential cancer mutations in cultured human intestinal stem cells. Nature 521, 43–47.

253- Nadauld, L.D., Garcia, S., Natsoulis, G., Bell, J.M., Miotke, L., Hopmans, E.S., Xu, H., Pai, R.K., Palm, C., Regan, J.F., et al. (2014). Metastatic tumor evolution and organoid modeling implicate TGFBR2 as a cancer driver in diffuse gastric cancer. Genome Biol. 15, 428.

254- van de Wetering, M., Francies, H.E., Francis, J.M., Bounova, G., Iorio, F., Pronk, A., van Houdt, W., van Gorp, J., and Clevers, H. (2015). Prospective derivation of a 'Living Organoid Biobank' of colorectal cancer patients. Cell 161, 933–945.

255- Travis W, Brambilla E, Burke A, Marx A, and Nicholson A. WHO Classification of Tumours of the Lung, Pleura, Thymus and Heart. Lyon, France: International Agency for Research on Cancer; 2015.

256- Brierley JD, Gospodarowicz MK, and Wittekind C. TNM Classification of Malignant Tumours, 8th ed. Oxford, UK: Wiley-Blackwell; 2016.

257- Soumaoro LT, Uetake H, Higuchi T, Takagi Y, Enomoto M, Sugihara K. Cyclooxygenase-2 expression: a significant prognostic indicator for patients with colorectal cancer. Clin Cancer Res 2004;10:8465–8471.

258- Koo CL, Kok LF, Lee MY, et al. Scoring mechanisms of p16INK4a immunohistochemistry based on either independent nucleic stain or mixed cytoplasmic with nucleic expression can significantly signal to distinguish between endocervical and endometrial adenocarcinomas in a tissue microarray study. J Transl Med 2009;7:25.

259- Robinson BM. Malignant pleural mesothelioma: an epidemiological perspective. Ann. Cardiothorac. Surg. 2012; 1(4):491-496.

260- Vogelzang NJ, Rusthoven JJ, Symanowski J, et al. Phase III study of pemetrexed in combination with cisplatin versus cisplatin alone in patients with malignant pleural mesothelioma. J Clin Oncol 2003;21:2636–2644.

261- Moore AJ, Parker RJ and Wiggins J. Malignant mesothelioma. Orphanet J Rare Dis 2008;3:34.

262- Hollevoet K, Reitsma JB, Creaney J, et al. Serum mesothelin for diagnosing malignant pleural mesothelioma: an individual patient data meta-analysis. J Clin Oncol 2012;30:1541–1549.

263- Pass HI, Lott D, Lonardo F, et al. Asbestos exposure, pleural mesothelioma, and serum osteopontin levels. N Engl J Med 2005; 353: 1564-1573.

264- Pass HI, Levin SM, Harbut MR, et al. Fibulin-3 as a Blood and effusion biomarker for pleural Mesothelioma. N Engl J Med 2012;367:1417-1427.

265- Wu T, Zhang W, Yang G, et al. HMGB1 overexpression as a prognostic factor for survival in cancer: a meta-analysis and systematic review. Oncotarget 2016;7:50417-50427.

266- Kang R, Zhang Q, Zeh HJ, Lotze MT, Tang D. HMGB1 in cancer: good, bad, or both? Clin Cancer Res 2013;19: 4046-4057.

267- Gardella S, Andrei C, Ferrera D, et al. The nuclear protein HMGB1 is secreted by monocytes via a non-classical, vesicle-mediated secretory pathway. EMBO Rep 2002;3:995-1001.

268- Tang D, Kang R, Livesey KM, et al. Endogenous HMGB1 regulates autophagy. J Cell Biol 2010;190:881-892.

269- Muller S, Ronfani L, Bianchi ME. Regulated expression and subcellular localization of HMGB1, a chromatin protein with a cytokine function. J Intern Med 2004;255:332-343.

270- Ellerman JE, Brown CK, de Vera M, et al. Masquerader: high mobility group box-1 and cancer. Clin Cancer Res 2007;13:2836-2848.

271- Tang D, Kang R, Zeh HJ, Lotze MT. High-mobility group box 1 and cancer. Biochim Biophys Acta 2010;1799:131-140.

272- Ueda M, Takahashi Y, Shinden Y, et al. Prognostic Significance of High Mobility Group Box 1 (HMGB1) Expression in Patients with Colorectal Cancer. Anticancer Res 2014;34: 5357-5362.

273- Liu K, Huang J, Xie M, et al. MIR34A regulates autophagy and apoptosis by targeting HMGB1 in the retinoblastoma cell. Autophagy 2014; 10:442-452.

274- Zhang C, Ge S, Hu C, Yang N, Zhang J. MiRNA-218, a new regulator of HMGB1, suppresses cell migration and invasion in non-small cell lung cancer. Acta Biochim Biophys Sin 2013;45:1055–1061.

275- Andersson U, Antoine DJ, Tracey KJ. The functions of HMGB1 depend on molecular localization and post-translational modifications. J Intern Med 2014;276: 420–424.

276- Napolitano A, Antoine DJ, Pellegrini L, et al. HMGB1 and its hyperacetylated isoform are sensitive and specific serum biomarkers to detect asbestos exposure and to identify mesothelioma patients. Clin Cancer Res 2016;22: 3087-96.

277- Tabata C, Kanemura S, Tabata R, et al. Serum HMGB1 as a diagnostic marker for malignant peritoneal mesothelioma. J Clin Gastroenterol 2013;47:684–688.

278- Tabata C, Shibata E, Tabata R, et al. Serum HMGB1 as a prognostic marker for malignant pleural mesothelioma. BMC Cancer 2013;13:205.

279- Kim MP, Evans DB, Wang H, Abbrusseze JL, Fleming JB, and Gallick GE. Orthotopic and heterotopic generation of murine pancreatic cancer xenografts. Nat Protoc. 2009; 4(11): 1670–1680.

280- Drost J, Karthaus WR, Gao D, Driehuis E, Sawyers CL, Chen Y, and Clevers H. Organoid culture systems for prostate epithelial tissue and prostate cancer tissue. Nat Protoc. 2016 Feb; 11(2): 347–358.

281- Koehler, K. R., Mikosz, A. M., Molosh, A. I., Patel, D. & Hashino, E. Generation of inner ear sensory epithelia from pluripotent stem cells in 3D culture. Nature 500, 217–221, doi: 10.1038/nature12298 (2013).

282- Chua, C. W. et al. Single luminal epithelial progenitors can generate prostate organoids in culture. Nature cell biology 16, 951–961, 951–954, doi: 10.1038/ncb3047 (2014).

283- Karthaus, W. R. et al. Identification of multipotent luminal progenitor cells in human prostate organoid cultures. Cell 159, 163–175, doi: 10.1016/j.cell.2014.08.017 (2014).

284- Gao, D. et al. Organoid cultures derived from patients with advanced prostate cancer. Cell 159, 176–187, doi: 10.1016/j. cell.2014.08.016 (2014).

285- Crystal, A. S. et al. Patient-derived models of acquired resistance can identify effective drug combinations for cancer. Science (New York, NY) 346, 1480–1486, doi: 10.1126/science.1254721 (2014).

286- Rrapaj E, Trisolini E, Bertero L et al. Expression analysis of HMGB1 in histological samples of malignant pleural mesothelioma. Histopathology. 2018. DOI: 10.1111/his.13470

287- Mezzapelle R, Rrapaj E, Gatti E et al. Human malignant mesothelioma is recapitulated in immunocompetent BALB/c mice injected with murine AB cells. Scientific Reports. 2016. 6:22850 | DOI: 10.1038/srep22850.

,